UNIVERSIDAD POLITÉCNICA DE MADRID

ESCUELA TÉCNICA SUPERIOR
DE INGENIEROS DE TELECOMUNICACIÓN

THESIS DOCTORAL

COLOR UNIFORMITY IN SPOTLIGTHS - VISUAL PERCEPTION AND SYSTEM DESIGN

Anne Teupner
Master of Engineering

2015

UNIVERSIDAD POLITÉCNICA DE MADRID

Instituto de Energía Solar
Departamento de Electrónica Física
Escuela Técnica Superior de Ingenieros de Telecomunicación

THESIS DOCTORAL

COLOR UNIFORMITY IN SPOTLIGTHS - VISUAL PERCEPTION AND SYSTEM DESIGN

AUTOR: Anne Teupner
DIRECTOR: Pablo Benítez Giménez
Ingeniero en Telecomunicación
CO-DIRECTOR: Krister Bergenek
Master of Engineering

2015

Tribunal nombrado por el Magfco. Y Excmo. Sr. Rector de la Universidad Politécnica de Madrid.

PRESIDENTE:

VOCALES:

SECRETARIO:

SUPLENTES:

Realizado el actor de defensa y lecture de la Tesis en Madrid,
el día _____ de _____ de 2015.

Calificación:

EL PRESIDENTE LOS VOCALES

EL SECRETARIO

Acknowledgment

First, this thesis would not be realized without Pablo Benítez and Juan Carlos Miñano. I thank them for their support, their confidence in my work over a long distance, and guidance through the work and thesis.
The advanced optical group at Cedint was great for their support, unhesitating interest and sharing of knowledge. Especially, Marina Buljan, Milena Nicolić, João Mendes Lopes, Pablo Zamora, Dejan Grabovičkić, and Eduardo Montoya were provided helpful assistance. Everyone at Cedint to make the pleasant stays possible and for comfortable working place. And all people who took part in the first human factor experiment and principally enabled the investigations in Madrid, Spain.

Especially, I thank Krister Bergenek for his advices, he saw through all the work, structural criticisms during the whole time, his reviews of all written works, continuous exchange and collaboration. Further thanks to Ralph Wirth for offering the topic, Dennis Sprenger, Andreas Dobner, Meik Weckbecker, Anouar Khemiri and Stephan Finger for their direct support for constructions, simulations, and software development. Thanks to all employees of the research center in Regensburg, Germany who took part in the human factor experiments and comfortable working place.

Furthermore, I would like to thank LPI for providing models of secondary optics, especially thanks to Aleksandra Cvetković and Ruben Mohedano.

And last but not least, many thanks to my family and to Hannes for all their support and their belief in my actions.

Abstract

Illumination with light-emitting diodes (LED) is more and more replacing traditional light sources. They provide advantages in efficiency, energy consumption, design, size and light quality. For more than 50 years, researchers have been working on LED improvements. Their main relevance for illumination is rapidly increasing.
This thesis is focused on one important field of application which are spotlights. They are used to focus light on defined areas, outstanding objects in professional conditions. This high performance illumination required a defined light quality including tunable correlated color temperatures (CCT), high color rendering index (CRI), high efficiencies and bright, vivid colors.
Several differently colored chips (red, blue, phosphor converted) in the LED package are combined to meet spectral power distribution with high CRI, tunable white and several light colors and secondary optics are used to collimate the light into the desired narrow spots with defined angle of emission. The combination of multi-color LED source and optical elements may cause chromatic inhomogeneities in spatial and angular light distribution which needs to solved at the optical design. However, there is no need for perfect uniformity in the spot light due to threshold in visual perception of human eye. Therefore, a mathematical description of color uniformity level with regard to visual perception is required.

This thesis is organized seven seven chapters. After an initial one presenting the motivation that has guided the research of this thesis, Chapter 2 introduces the scientific basics of color uniformity in spot lights including: the applied color space CIELAB, the visual color perception, the spotlight design fundamentals with regards to light engines and nonimaging optics, and the state of the art for the evaluation of color uniformity in the far field of spotlights.
Chapter 3 develops different methods for mathematical description of spatial color

distribution in a defined area, which are the maximum color difference, the average color deviation, the gradient of spatial color distribution as well as the radial and axial smoothness. Each function refers to different visual influencing factors, and they need different handling of data be taken into account, along with weighting functions which pre- and post-process the simulated or measured data for noise reduction, luminance cutoff, the implementation of luminance weighting, contrast sensitivity function, and cumulative distribution function.

In chapter 4, the merit function U_{sl} for the estimation of the perceived color uniformity in spotlights is derived. It was based on the results of two sets of human factor experiments performed to evaluate the visual perception of typical spotlight patterns by subjects. The first human factor experiment resulted in the perceived rank order of the spotlights. The perceived rank order was used to correlate the mathematical descriptions of basic functions and weighted function concerning the spatial color distribution, which lead to the U_{sl} function. The second human factor experiment tested the perception of spotlights under varied environmental conditions, with to objective to provide an absolute scale for U_{sl}, so the subjective personal opinion of individuals could be replaced by a standardized merit function.

The validation of the U_{sl} function is presented concerning the application range and conditions as well as limitations and restrictions in carried out in chapter 5. Measured and simulated data of various optical several systems were compared. Fields of applications are discussed as well as validations and restrictions of the function.

Chapter 6 presents spotlight system design and their optimization. An evaluation shows the analysis of reflector-based and TIR lens systems. The simulated optical systems are compared in color uniformity U_{sl} , sensitivity to colored shadows, efficiency, and peak luminous intensity. It has been found that no single system which performed best in all categories, and that excellent color uniformity could be reached by two different system assemblies.

Finally, chapter 7 summarizes the conclusions of the present thesis and an outlook for further investigation topics.

Resumen

La iluminación con diodos emisores de luz (LED) está reemplazando cada vez en mayor medida a las fuentes de luz tradicionales. La iluminación LED ofrece ventajas en eficiencia, consumo de energía, diseño, tamaño y calidad de la luz. Durante más de 50 años, los investigadores han estado trabajando en mejoras LED. Su principal relevancia para la iluminación está aumentando rápidamente.
Esta tesis se centra en un campo de aplicación importante, como son los focos. Se utilizan para enfocar la luz en áreas definidas, en objetos sobresalientes en condiciones profesionales. Esta iluminación de alto rendimiento requiere una calidad de luz definida, que incluya temperaturas ajustables de color correlacionadas (CCT), de alto índice de reproducción cromática (CRI), altas eficiencias, y colores vivos y brillantes.
En el paquete LED varios chips de diferentes colores (rojo, azul, fósforo convertido) se combinan para cumplir con la distribución de energía espectral con alto CRI. Para colimar la luz en los puntos concretos deseados con un ángulo de emisión determinado, se utilizan blancos sintonizables y diversos colores de luz y ópticas secundarias. La combinación de una fuente LED de varios colores con elementos ópticos puede causar falta de homogeneidad cromática en la distribución espacial y angular de la luz, que debe resolverse en el diseño óptico. Sin embargo, no hay necesidad de uniformidad perfecta en el punto de luz debido al umbral en la percepción visual del ojo humano. Por lo tanto, se requiere una descripción matemática del nivel de uniformidad del color con respecto a la percepción visual.

Esta tesis está organizada en siete capítulos. Después de un capítulo inicial que presenta la motivación que ha guiado la investigación de esta tesis, en el capítulo 2 se presentan los fundamentos científicos de la uniformidad del color en luces concentradas, como son: el espacio de color aplicado CIELAB, la percepción visual del color, los fundamentos de diseño de focos respecto a los motores de luz y

ópticas no formadoras de imágenes, y los últimos avances en la evaluación de la uniformidad del color en el campo de los focos.
El capítulo 3 desarrolla diferentes métodos para la descripción matemática de la distribución espacial del color en un área definida, como son la diferencia de color máxima, la desviación media del color, el gradiente de la distribución espacial de color, así como la suavidad radial y axial. Cada función se refiere a los diferentes factores que influyen en la visión, los cuales necesitan un tratamiento distinto que el de los datos que se tendrán en cuenta, además de funciones de ponderación que pre- y post-procesan los datos simulados o medidos para la reducción del ruido, la luminancia de corte, la aplicación de la ponderación de luminancia, la función de sensibilidad de contraste, y la función de distribución acumulativa.
En el capítulo 4, se obtiene la función de mérito U_{sl} para la estimación de la uniformidad del color percibida en focos. Se basó en los resultados de dos conjuntos de experimentos con factor humano realizados para evaluar la percepción visual de los sujetos de los patrones de focos típicos. El primer experimento con factor humano dio lugar al orden de importancia percibida de los focos. El orden de rango percibido se utilizó para correlacionar las descripciones matemáticas de las funciones básicas y la función ponderada sobre la distribución espacial del color, que condujo a la función U_{sl}. El segundo experimento con factor humano probó la percepción de los focos bajo condiciones ambientales diversas, con el objetivo de proporcionar una escala absoluta para U_{sl}, para poder así sustituir la opinión subjetiva personal de los individuos por una función de mérito estandarizada.
La validación de la función U_{sl} se presenta en relación con el alcance de la aplicación y condiciones, así como las limitaciones y restricciones que se realizan en el capítulo 5. Se compararon los datos medidos y simulados de varios sistemas ópticos. Se discuten los campos de aplicación , así como validaciones y restricciones de la función.
El capítulo 6 presenta el diseño del sistema de focos y su optimización. Una evaluación muestra el análisis de sistemas basados en el reflector y la lente TIR. Los sistemas ópticos simulados se comparan en la uniformidad del color U_{sl}, sensibilidad a las sombras coloreadas, eficiencia e intensidad luminosa máxima. Se ha comprobado que no hay un sistema único que obtenga los mejores resultados en todas las categorías, y que una excelente uniformidad de color se pudo alcanzar por la conjunción de dos sistemas diferentes.
Finalmente, el capítulo 7 presenta el resumen de esta tesis y la perspectiva para

investigar otros aspectos.

Contents

1 Motivation

An enormous number of lighting techniques are available for various functions and applications. One of the leading technologies and a rapidly expanding field is the solid state lighting technique (SSL) and its concepts for luminaires with light emitting diodes (LED). In 2015, more than 50 % of new installes lamps include SSL technology. Till 2020, up to 90 % of new installed lamps and luminoaires contain LEDs as light source [Kunzer, 2014]. For more than 50 years, researchers have been developing diodes and techniques for increased light output, efficiency, functionality and simulation methods for LEDs. Now, they have a huge relevance for illumination in all kind of utilization from professional lighting to consumer products.
There are different types of illumination for linear, area, and spot lighting. Spotlights are defined by a narrow beam with a defined angle, and high luminance flux to emphasis outstanding objects, important information or illuminate design highlights. Spotlights are mainly used in hospitality, shops lighting, and hotels but also for residential purpose. In this context, a high quality and special settings are required to guide the attention of the audience towards the object and to get a comfortable feeling. Therefore, high color rendering index (CRI), tunable white light, vivid bright colors and high efficient implementations are necessary. Spotlights are created by combining light source for emitting white light with a secondary optics to collimate the light into defined angular distribution.
LEDs are used as light sources because of high efficiency, enabling integration, new designs, and diversity in light properties. White light can be generated either by combining several colored LED chips with each other (RGB) or by phosphor conversion of blue LED chips or by a combination of both. Both methods create angularly and spatial separated emitted colors, respectively. Furthermore, the assembly, arrangement, number and size of the LED chips influence the color blending. The narrow beam is collimated by secondary optics. Commonly, TIR

lenses and reflectors are applied. Imaging properties and geometric boundaries can enhance the separated colors and force the appearance of colors and patterns in the far field. There are various combinations of light engine and secondary optics with very different far field appearances. The design of the light engine and the optical system are responsible for the light distribution and the color uniformity in the light beam.
Excellent color uniformity in spotlights can be reached by scattering layers, mixing chambers, or additional elements but often these methods increase angular distribution and decrease the efficiency. But perfect color uniformity is not necessary because of thresholds in the visual perception. An adjusted weighting between color uniformity in the far field and reduced performance in other properties is necessary. The perception of color is highly individual and therefore it is difficult to determine values of specification over a wide far field appearance. Two very different far fields are shown in Figure 1.1.

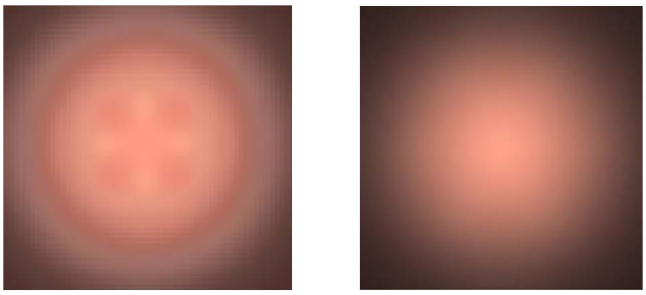

Figure 1.1: Two examples of far fields of spotlights

These two examples illustrate the wide range of potential color uniformity in light spots. One spotlight shows clear red dots in the center and a red ring at the edge. The other spotlight shows a very uniform spatial color distribution. The first example (left) is not acceptable due to insufficient color uniformity, the second example (right) shows an excellent color uniformity which is not requested in most cases. In the design phase of spotlights, they are evaluated by individuals with regard to their personal subjective opinion. There is no standardized evaluation method to quantify the color uniformity of the spotlights accurately. Depending on experience, visual acuity and individual preferences, the evaluation leads to divergent judgments. Additionally, many visual influencing factors have an effect on the judgment.
An objective evaluation of these spotlights is required independent of arbitrary

individual judgments. In this context, it is indispensable to acquire knowledge about requirements of color uniformity in spotlights in combination with visual color perception. An objective mathematical description based on mean color perception by a plurality of subjects, is necessary. Such a description can be applied on measurements and optical simulation to quantify the color uniformity in the far field of spotlights. Then, it is not necessary anymore to build prototypes and test the uniformity in laboratories.

The discrepancy between individual visual perception (judgment) and a consistent mathematical description based on human factor studies is addressed in this thesis. This thesis attempt is to close gap between simulations of theoretical calculations and the visual perception in application of the spotlights as well as the relation to optical systems which are in charge of color uniformity. The research in this thesis is divided consecutively into the following steps:

1) Project definition
2) Human factor experiments: visual perception of color uniformity in spot lights
3) Derivation of merit function U_{sl} for color uniformity
4) Optical system design and optimization considering color uniformity
5) Conclusion

The five steps represent seven chapters of the present thesis including the introduction in Chapter 1. Chapter 2 presents the scientific basics of color uniformity in spot lights. The applied color space CIELAB is illustrated. The visual color perception is explained in its main features. The spotlight design with regard to light engine and secondary optics are presented as well as the state of the art for the evaluation of color uniformity in the far field of spotlights. Chapter 3 presents different methods for mathematical description of spatial color distribution in a defined area. Several formulas are discussed with regard to visual influencing factors, and weighting functions for pre- and post-processing of data are presented. In Chapter 4, the human factor experiments are described. The first human factors experiments lead to a perceived rank order of color spotlights and the merit function is derived. The second human factor experiment leads to a classification with regard to color uniformity levels from excellent to insufficient. The next Chapter 5

is about the merit function. A comparison between measured and simulated optical system is performed. Fields of applications are discussed as well as the validity and restrictions of the function. Chapter 6 presents spotlight system design and their optimization. An evaluation shows the performance of reflector and TIR lens systems considering also color uniformty. Finally, Chapter 7 gives a conclusion about the present thesis' output and an outlook for further investigation topics.

2 Basics for Color Uniformity in Spotlights

Chapter 2 gives a summary about the scientific basics for color uniformity in spot lights. Fundamental colorimetry and the application of color space $CIELAB$ are explained. The visual color perception is presented with regard to visual influencing factors of chromatic vision. The state of the art of spotlights design with its optical systems, color mixing elements, and far field appearances are described. Additionally, existing methods for the evaluation of color uniformity in far fields are reviewed.

2.1 CIE Classification

The International Commission on Illumination (CIE) is an organization that defines standards for all fields of illumination, light, and colors in research and art. The CIE establishes colorimetric specifications and definitions of color spaces which are applied throughout the science.

2.1.1 Colorimetry

The fundamentals of Colorimetry are described in Schanda [2007] which was the basis for the main part of this section.

The visible spectrum, from 380 nm to 780 nm, is detected by the human eye and visually processed in the brain. The proper spectral power distributions are perceived and assigned to colors. The basis for colorimetry is the trichromatic vision of the eye. Based on three cone types in the human eye, a color is defined by the

values of three independent color channels [Wyszecki and Stiles, 1967]. Trichromatic vision and experimental color matching data [Guild, 1931; Wright, 1929] lead to the definition of a standard observer and derivation of color matching functions (CMF) $\overline{r}(\lambda)$, $\overline{g}(\lambda)$ and $\overline{b}(\lambda)$. Due to calculations of a visualized color space, the real but partly negative functions are transformed to imaginary primaries of $\overline{x}(\lambda)$, $\overline{y}(\lambda)$, and $\overline{z}(\lambda)$ CMFs and they represent the chromatic response of the standard observer to chromatic stimuli. They are shown in Figure 2.1.

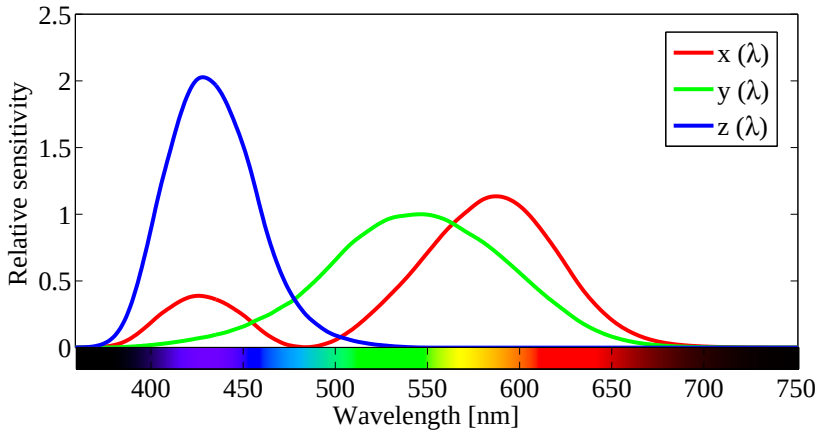

Figure 2.1: CIE 1931 standard observer color matching function

The tristimulus values are defined by CMFs. They describe the ratio of three primary colors to match color stimuli in visual perception. They are defined as:

$$X = \int_{380}^{780} I(\lambda) \cdot \overline{x}(\lambda)\, d\lambda \tag{2.1}$$

$$Y = \int_{380}^{780} I(\lambda) \cdot \overline{y}(\lambda) d\lambda \tag{2.2}$$

$$Z = \int_{380}^{780} I(\lambda) \cdot \overline{z}(\lambda) d\lambda \tag{2.3}$$

and $I(\lambda)$ is the spectral power distribution of the color. To visualize the color, the tristimulus values are converted into chromaticity coordinates and represented in

the $CIExyY$ chromaticity diagram. The Y value represents the luminance of a color.

$$x = \frac{X}{X+Y+Z} \tag{2.4}$$

$$y = \frac{Y}{X+Y+Z} \tag{2.5}$$

$$z = \frac{Z}{X+Y+Z} = 1 - x - y \tag{2.6}$$

For color visualization, the x and y coordinates are plotted in a chromaticity diagram. Figure (2.2) illustrates the $CIExyY$ chromaticity diagram. It is a common way to describe a color with the coordinates x and y. Whereupon the third quantity for a complete description of the color is provided by Y. [Wyszecki and Stiles, 1967]

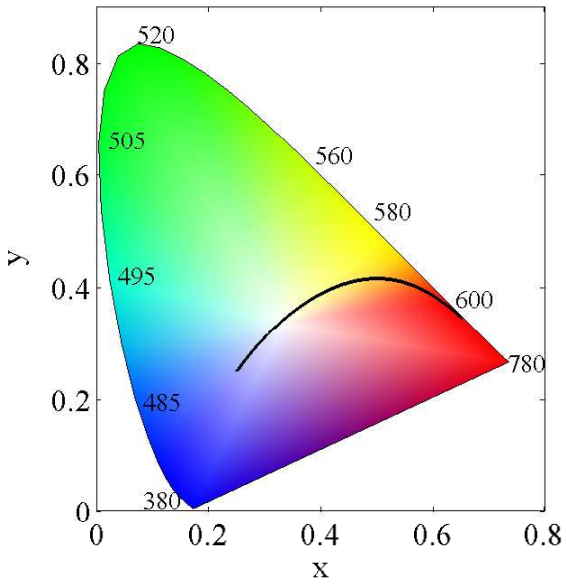

Figure 2.2: CIExyY color space chromaticity diagram, including monochromatic wavelength from 380 nm to 780 nm and Planckian locus (black body locus)

The Planckian locus corresponds to the color coordinates of black bodies emitting at different temperatures. If a given light source has its color coordinates close to the Planckian locus, the temperature associated of the closest point of the locus is taken as the Correlated Color Temperature (CCT) of that light source. Since

the spectrum of that light source may differ significantly from that of the black body, the measure of the difference is quantified using the Color Rendering Index (CRI). Color rendering describes the appearance of object colors under specific illumination in comparison to a reference illumination. The CRI is the degree of conformity of the perceived colors under the defined illumination by a test light source and the reference illumination.

In this color space system every color impression is created by three defined values e.g. XYZ or xyY values. These values do not contain any information about the spectral power distribution of the color. Hence, two colors with same the visual impression and color values can consist of different spectral power distributions. This effect is called "metamerism" and two colors which appear the same but are based on two different spectral power distributions are called "metamers".
The CIExy chromaticity diagram is widely-used because it enables the monochromatic light at the boarder which is relevant for LED. The Planckian locus is included, that represent the color of an incandescent black body radiator. The application of the CIExyY is allowed under specific conditions. Testing conditions should be considered, because changes in visual fields affect the visual processing (see next section 2.2.2 on page 15). In addition, the CIE recommends a luminance above 200 cd/m^2 in order to avoid scotopic vision (vision in the darkness) and to be sure that rod vision is absent [CIE, 2004]. In fact, it is commonly known that the CMFs are not as accurate as requested in any case. They are still applied because they are very similar to current measurements, their wide distribution in the industry, and sufficient precision for main applications.

Based on the CIExyY color space, many experiments were performed in order to prove the thesis that equal distances in the color space are perceived as the same color difference by human vision. The experiments of MacAdam proved a strong non-uniformity over the complete color space, illustrated by ellipses with various size and orientation [MacAdam, 1942]. Therefore, several further developments of the CIExyY color space were made to reach a more uniform color space.

2.1.2 CIELAB Color Space

The CIE 1976 $(L^*a^*b^*)$ color space (CIELAB) is based on the CIE tristimulus values X, Y, and Z [CIE, 1976]. The CIELAB parameters are: L^*, the normalized luminance; a^* and b^*, the green-red and blue-yellow axis, respectively.

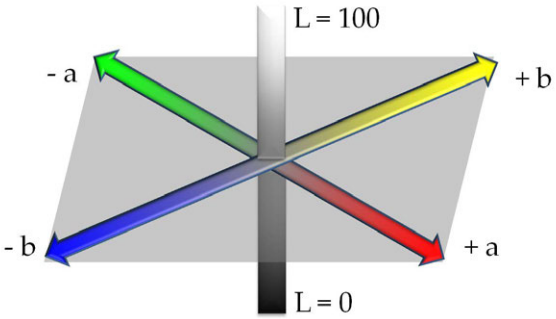

Figure 2.3: CIELAB color space and its three axis L^* - luminance, a^* - green-red, and b^* - blue-yellow

The two color axes are based on the opponent color theory [Hurvich and Jameson, 1957]. The CIELAB color space is designed to represent human vision and offers perceptual uniformity. It is the most complete color space with regard to its gamut and perceivable colors. The calculation of the L^*, a^*, and b^* values is based on the tristimulus values calculated in equation 2.1, 2.2 and 2.3 [Schanda, 2007].

$$L^* = 116 \cdot f\left(\frac{Y}{Y_n}\right) - 16 \tag{2.7}$$

$$a^* = 500 \cdot \left(f\left(\frac{X}{X_n}\right) - f\left(\frac{Y}{Y_n}\right)\right) \tag{2.8}$$

$$b^* = 200 \cdot \left(f\left(\frac{Y}{Y_n}\right) - f\left(\frac{Z}{Z_n}\right)\right) \tag{2.9}$$

where

$$f(I) = \begin{cases} I^{1/3} & \text{if } I > (24/116)^3 \\ (841/108)I + 16/116 & \text{otherwise} \end{cases} \tag{2.10}$$

The parameters X_n, Y_n, and Z_n are the tristimulus values of the reference white color. For large differences between reference white and test point, whereas the reference white would be clearly brighter, $I^{1/3}$ is replaced. The CIELAB color space is a

device-independent color space because it defines its own normalized illumination. It is applied for surface colors mainly in printing industry, for reproduction and image processing.

Additionally, the concepts of "hue" and "chroma" (also colorfulness, saturation, or color intensity) are introduced when a point ($a^a st$, $b^a st$) is expressed in polar coordinates, so hue is the azimuth angle and chroma is the radial distance to the origin. This two concepts can be used in a qualitative way, too. Here, hue in a pattern refers to the different colors named as red, blue, red-blue, yellow-blue, and rgb with the number of colors. Chroma refers to low, medium or high saturation. The concept of hue and chroma is presented in Figure 2.4.

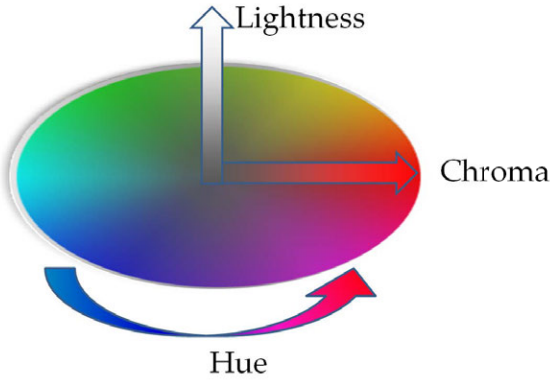

Figure 2.4: CIELAB color space with indication of hue and chroma

A color difference in the CIELAB color space can be described as:

$$\Delta E^*_{Lab} = \sqrt{\left(L^*_1 - L^*_2\right)^2 + \left(a^*_1 - a^*_2\right)^2 + \left(b^*_1 - b^*_2\right)^2} \tag{2.11}$$

It is a challenge to define a threshold ΔE values describing the perceived color differences. The effects of viewing conditions, settings and practice of the subject affect the visually perceived color differences. Furthermore, the threshold depends mainly on the exposure duration. The longer two colors are presented, the lower differences can be recognized. Another important factor is the test plate itself. If standard plates or standardized patterns are used, it is possible to distinguish between very small color differences. The CIELAB was developed based on the definition that the just noticeable difference is $\Delta E \approx 1$. With suitable settings and trained persons smaller color differences can be perceived. [Lindsey et al., 2010;

Wang et al., 2012]

2.2 Visual Perception

The visual perception is influenced by many factors. Now, the process of color perception is presented. The influencing factors for chromatic vision that can be environmental and individual conditions are illustrated.

2.2.1 Color Perception

The human eye is a highly sensitive sensor. It consists of a complex structure to receive and handle the light in order to produce a perception of color. Therefore, the visual system is a multi-functional structure. The receptors convert the light into electrical signals which are processed by neurons in the visual region of the brain, the visual cortex, and finally the stimuli are transformed into perceivable colors. [Wyszecki and Stiles, 1967]
The receptors for light in the eye are cones and rods. The cones are responsible for color perceptions and the rods for achromatic vision. Cones are active during photopic vision. Light stimuli are received by the cones for color vision mainly in the fovea with its diameter of about 1°. The eye holds more than $4 \cdot 10^6$ cones with a varying distribution over the retina. Rods are active during scotopic vision. They perceive only the luminance level and are distributed mainly over the peripheral retina. The activities of rods and cones depend on the luminance level whereupon the transition is smoothed. The cones need at least 0.1 cd/m^2 to get active, below only the rods absorb light. [Grand and Hage, 1980]
The cones are sensitive to photons of different wavelengths due to biochemical processes. There are three types of cones, each sensitive to another spectral wavelength range as presented in Figure 2.5 [Stockman and Sharpe, 2000].

- Short-wavelength cones (S): maximum at 419.0 nm
- Middle-wavelength cones (M): maximum at 530.8 nm

- Long-wavelength cones (L): maximum at 558.4 nm

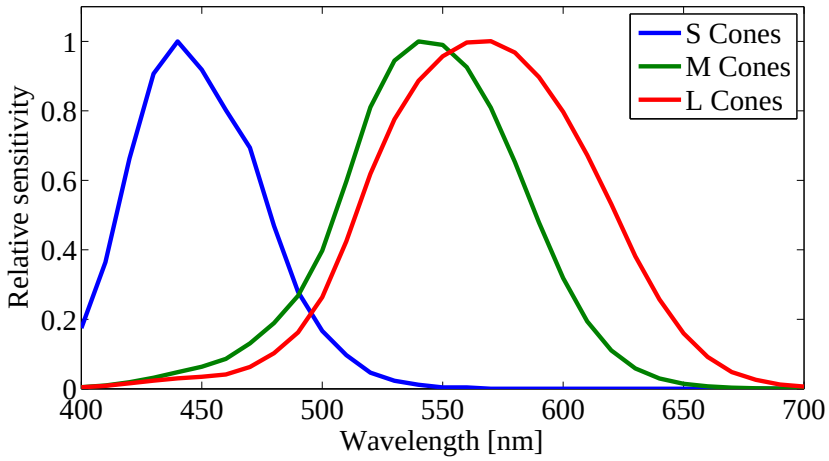

Figure 2.5: Spectral sensitivity of cone types

The quantitative distribution L:M:S of the cones is not specified and is very individual. Most cones are of L type and least cones are of S type. They have different distribution in every human eye. The performance of the individual human eye depends very strongly on the arrangement and distribution of the cones. The sensitivity of the cones weighted by their quantity in an human eye is presented in Figure 2.6. [Roorda and Williams, 1999]

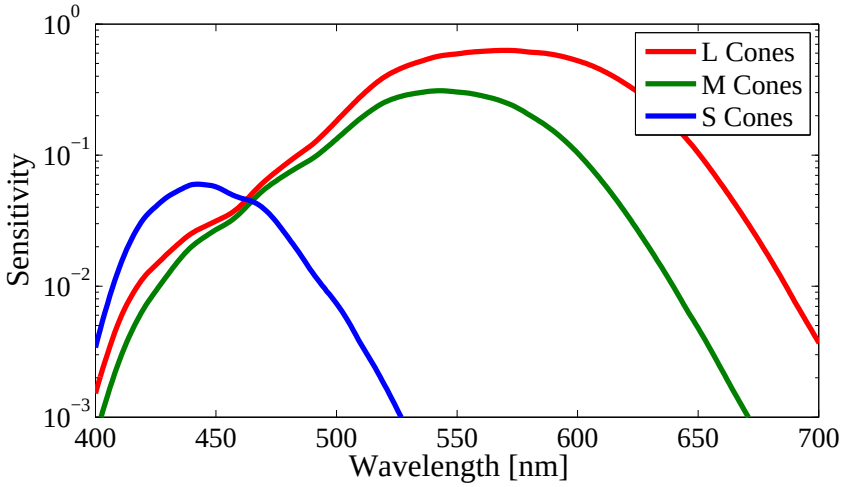

Figure 2.6: Spectral sensitivity of cone types weighted by quantity of each type

The three different cone types are essential for color perception. They are the basis for the two stage zone model theory which is the common theory for the

visual color processing [Hurvich and Jameson, 1957]. The two stage model theory states that the visual process is divided into two subsequent stages. The first stage processes after the trichromatic theory related to the photoreceptors. The second stage is related to the color opponent process of vision. Color vision is coded in initial stages, two color-opponent mechanisms and one achromatic mechanism. Therefore, the three cone types are linearly connected in different combinations to generate the luminance channel as well as the two color channels green-red (g-r) and blue-yellow (b-y). The color opponent channels are based on unique color impressions. They are arranged in opposite pairs because there is no color impression of reddish green or yellowish blue (opponent colors). The combination of the three cones from the first stage to the second stage is illustrated in Figure 2.7

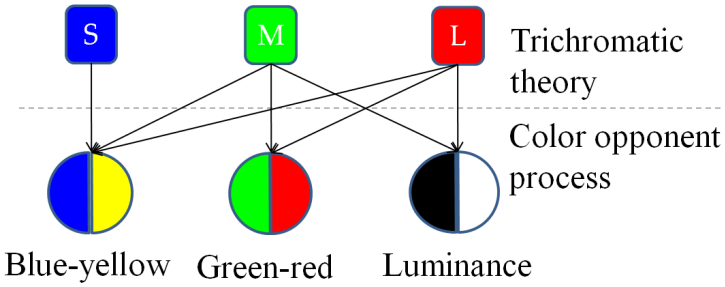

Figure 2.7: Two stage zone model theory of human color vision: Processing of the L, M, and S cones of trichromatic vision in the first stage to the color opponent processing of the second stage

The output of the L and M cones produce the luminance channel which is achromatic. The S cones just care for a weak input of luminance under special conditions [Webster, 1996, p. 595]. All three cone types contribute to the two chromatic channels. The g-r channel is the combination of $L - M + S$, whereas S cones count just a little. The S cones contribute most to the b-y that combines $L + M - S$ [Boynton and Kambe, 1980]. The chromatic channels $L - M + S$ and $S - L + M$ are low-pass functions with a lower spatial resolution and lower frequency cutoff in comparison to achromatic channel. As one result, the chromatic channels are sensitive to the absolute chromaticity and not brightness perception (see Figure 2.9 on page 18).

The processing of the three cone types is essential for color vision but the complex process is not completely understood yet. The discrimination of chromatic stimuli may require a model involving interactions between the two color opponent mecha-

nisms and mechanisms of higher order. The color perception is not just an image in the eye but a huge amount of data processing in the complex visual system and processing of multi-stage color opponent mechanisms in the visual cortex. However, the concept of the trichromatic perception at the cones of the retina together with the color opponent theory at higher processing levels is proven by neurophysiologic research. [Bouman, 2013; Bollmann and Mertsching, 1996]
Dedicated psychological color experiments have identified that signals in the second stage vary with chromatic and luminance of the stimuli. Recent studies lead to the proposal of several theoretical models. The color-opponent and luminance signals are separated into different neural pathways at a higher stage of the visual system in the visual cortex. For further processing, they are independent of each other. Therefore, color perception must be allocated by higher mechanisms to combine color-opponent signals. At these processing levels, the luminance stimuli have no effect on chromatic signals for color perception and identification. [Nagy, 1999; Monaci et al., 2004]
The visual processing to decode electromagnetic waves into color perception induces a high complexity. There are various psychological and physiological effects which influence the perception of colors further.

2.2.2 Influence Factors of Chromatic Vision

There are many factors influencing the color vision with regard to ability for perception, discrimination and estimation. The most relevant effects and factors for color perception and further considerations of this work are summarized below and explained in following paragraphs.

a) Visual field and stimulus size
b) Surrounding field
c) Adaptation
d) Luminance level
e) Contrast
f) Exposure duration
g) Pattern recognition

h) Color memory

Depending on the visual stimulus, test environment and individual constitution, the effects occur in various characteristics and quantities.

a) Visual field and stimulus size

The visual perception over the complete visual field is shifting. The visual field itself has a high impact on the visual color perception because the cones are unequally disturbed over the retina. Cones differ in quantity and placement. They are concentrated in the fovea centralis and their density decreases towards the periphery. The peripheral color vision is fundamentally different compared to the vision within the fovea. [Abramov et al., 1991]
A peripheral stimulus that strikes the retina has to be larger than a foveal stimulus. Otherwise it would not be perceived as colored stimulus [Smith and Pokorny, 2003]. Furthermore, the acuity gets worse if the stimulus strikes only the periphery. Nevertheless, color stimuli can be detected reliable upto 50° [Hansen et al., 2009]. The perception improves considerably if the stimulus is not just a small area but an expanded field. Consequently, the threshold for stimuli with larger field becomes smaller. Color discrimination of a large stimulus field is clearly better than the discrimination of fields covering only the fovea region [Brown, 1952]. On these grounds, the CIE defines two standard observers. Own CMFs and application conditions are used for 2° and 10° standard observer. [Schanda, 2007]

b) Surrounding field

The surrounding field is bordering the direct visual stimulus. It causes a large influence on the perception, especially at small visual stimulus fields. For larger fields, there is an increasing independence of the surrounding field because the stimulus covers a larger retinal area and become more separate.
The surrounding appearance has an impact on thresholds for color differences. The influence is small for surroundings with similar color and chromatic properties to the test stimulus. The threshold for colors increases in differing surroundings. The visual field and surrounding is not particular relevant during color discrimination of nearly white light and the eye remains at constant adaptation level.
The full field stimulus represents most real-world conditions because the eye is in permanent motion to cover a wide field and to perceive the complete environment.

A large test stimuli and similar light properties (spectral power distribution) in the whole environment minimize the influence of the surrounding field. [Brown, 1952; Uchikawa et al., 1989; Brainard and Wandell, 1992; Brown and MacLeod, 1997]

c) Adaptation

The ability of the eye to adapt to widely different situations is highly developed. It is a dynamic mechanism to respond to changed viewing conditions. The adaptation state can be regulated by the luminance level (light-dark adaptation) or the average color of the stimuli (chromatic adaptation or rather color constancy). The light dark adaptation depends on change of luminance level. The adaptation from dark to light is performed faster than the dark adaption. For the light adaption, a luminance level of 3 cd/m^2 - 30 cd/m^2 are necessary in the whole environment. At lower luminance levels, the color perception is not consistent [Stockman et al., 1993; Yebra et al., 2001; Abrams et al., 2007; Fotios and Houser, 2009].

The chromatic adaptation is present during photopic vision. It describes the perception of colored objects independent of surrounding illumination. By chromatic adaptation, the color impression of an object is preserved. [Krauskopf and Gegenfurtner, 1992; Webster and Mollon, 1994]

The color perception depends on the level of adaptation of the eye within the photopic vision. There are some effects which influences the perceived color. One effect is the Bezold-Brücke shift. It states that a variation of luminance level modifies the perceived hues of monochromatic light. Increased luminance levels shifts the perception of red and yellowish-green towards yellow and violet, respectively. At very low luminance, level the color perception shifts to blue because rods become active [Le Grand, 1968]. Another effect is the Helmholz-Kohlrausch effect. Saturated colors appear brighter than their measurements state. Additionally, the Abney effect is existing. It describes the hue shift when light becomes more desaturated [Kurtenbach et al., 1984].

The level of color adaptation has a huge impact on the size of color discrimination thresholds. Observers which are adapted to the test light have fewer difficulties to distinguish between different colors [Loomis and Berger, 1979]. The threshold of color discrimination increases, if the adaptation state changes and removes from the test light stimulus [Krauskopf and Gegenfurtner, 1992]. In addition, the adaptation to color temperature in the range of 2870 K to 6500 K has little impact on the color difference threshold [Pointer, 1973].

d) Luminance level

In the context of adaptation, the influence of luminance to the ability of color discrimination has to be considered. A standard observer has a constant sensitivity to color differences over a large luminance range. There is no influence of luminance on the perception of color in a luminance range of about 50 cd/m^2 - 550 cd/m^2. But experiments showed that thresholds for color discrimination are smallest in a luminance range of 80 cd/m^2 - 300 cd/m^2. The threshold increases considerably below these luminance levels. [Brown and MacAdam, 1949; Brown, 1951; Smith and Pokorny, 2003]

Recent investigations showed that color perception is not completely independent of the illumination level and the background luminance. It is incorrect to ignore the influence of luminance. The relation between color discrimination and luminance level is logarithmic and thus, at higher luminance levels the improvement of color discrimination is not fundamental any more [Pridmore and Melgosa, 2005]. The ability to differ between colors is modified by the adaptation state and luminance level. Both influencing factors should be considered. Therefore, a constant luminance and background light should be provided in order to avoid effects of modified discrimination thresholds through different luminance levels. [Jennings and Barbur, 2010; Clery et al., 2013]

e) Contrast

The contrast in the perceived stimulus between colors and luminance is affecting the color perception. The contrast sensitivity is the ability to distinguish between different levels of luminance and color. Visual perception is not only influenced by environmental parameters but also by characteristic of the human eye. The color and pattern perception depends on the cone characteristics based on the distribution of S-, M-, and L-cones in the retina. There are three different contrast sensitivity functions (CSF) according to the three visual channels. The achromatic CSF belongs to the luminance channel and the chromatic CSFs belong to green-red and blue-yellow chromatic channels.

The sensitivity of the eye in dependence of the spatial frequency is shown in Figure 2.8 for the achromatic contrast and green-red contrast. It illustrates that the sensitivity of the visual perception depends on the spatial frequency of the color and pattern combination. For luminance contrast, the sensitivity is highest at about

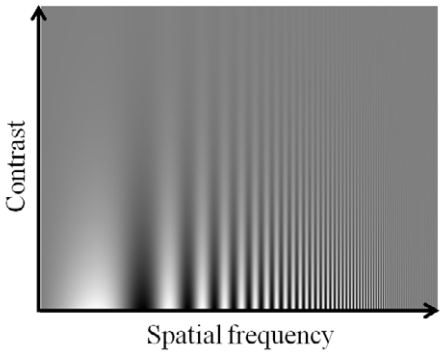

Figure 2.8: Achromatic and chromatic (green-red) contrast sensitivity function

$15 - 35$ *cycle/degree*. The sensitivity decreases for lower and higher frequencies with a cutoff frequency at about $3 - 10$ *cycle/degree* [Green, 1968]. The sensitivity for chromatic channels is highest at about $0.1 - 1$*cycles/degree*. It decreases for higher frequencies but remains constant for lower frequencies. The functions of the three CSFs are presented in Figure 2.9. They are based on formulas in Johnson et al. [2010].

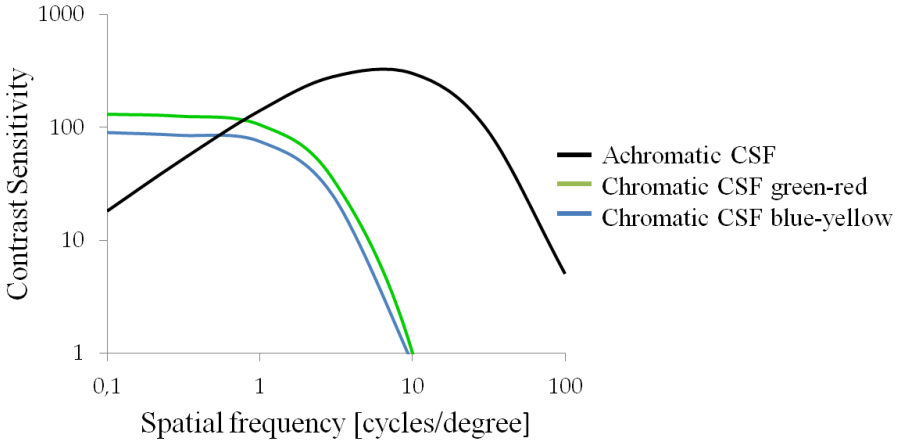

Figure 2.9: Contrast sensitivity functions for achromatic and chromatic channels of the human eye

The performance of color contrast sensitivity differs from achromatic contrast vision. Furthermore, the perception of green-red and blue-yellow is slightly different because of the three cone types and the color opponent processing. The color contrast sensitivity is a bit higher for green-red test pairs than for blue-yellow ones. In contrast to the luminance differences, there is no decrease at lower frequencies. The chromatic sensitivity threshold is at a lower frequency. There is no color

discrimination possible above $10 - 15$ *cycles/degree* [Mullen, 1985; Rovamo et al., 1999]. For lower frequencies the color contrast vision works more accurate than the achromatic contrast vision. During the shift to higher frequencies, the luminance contrast sensitivity improves compared to color contrast. At very high frequencies there is no perception of color nor of contrast possible.
The ability of the eye to detect contrasts depends mainly of the topography of the cones in the retina. The perception of higher contrast frequencies of color is not possible because the L and M cones are arranged in groups, hence the resolution is reduced. However, luminance contrast detection is improved due to this cone pattern in the human eye [Barlett et al., 1965; Roorda and Williams, 1999; Bouma, 1971; Rovamo et al., 1999; Watson and Ahumada, 2005; Schanda, 2007]

f) Exposure duration
The ability to discriminate colors depends on the exposure duration and it has an influence on the threshold of color differences. On the one hand, very short exposure duration times do not enable accurate perception and leads to perception deficits. On the other hand, longer durations can cause adaptation effects of the observer vision which influence its capability, and often the attention is reduced. [Hita et al., 1982]

g) Pattern recognition
Another consideration is the combination of color and pattern. The recognition of patterns is improved when colors are involved in the pattern [Wurm et al., 1993]. Experimental results confirm the possibility to search for colors and objects simultaneous, if the observer can distinguish between figure and background [D'Zmura and Lennie, 1986]. Therefore, the attention of the observer is important, because during the visual process familiar objects are recognized before unknown objects. It is suggested that adaptive mechanisms are responsible for the ability of object and pattern recognition due to discrimination of colors. These mechanisms seem to detect chromatic patterns through mediation of mechanisms regulated by color direction in the visual cortex [Monaci et al., 2004].
One important aspect is the appearance of patterns. In the environment many symmetrical objects are present. Symmetrical patterns, especially mirror symmetry, are quickly detectable and proceeded. The recognition of symmetries is an automatic process and it is used constantly during visual perception. [Carmody et al., 1977;

Wagemans, 1995; Bloj et al., 1999; Norcia et al., 2002; Ghose and Palmer, 2010]

h) Color memory

Color memory is the ability to remember a previously seen color. A color seen successively within a temporal interval can be reproduced by memory. The ability depends on individual skills and viewing conditions. Color matching experiments in successive sequences shows generally larger divergences in precision compared to simultaneous test [Pérez-Carpinell et al., 1998]. In this connection, the delay time has a significant influence. The experiments show a clear shift in chroma. Lighter chroma is remembered lighter just as darker chroma is remembered darker but this effect depends on the reference color. The memory of decreased contrast seems to be easier than to remember an increased contrast [Amano et al., 2002]. In the same way, changes in similar colors are more difficult to remember than changes between several color categories [Uchikawa and Shinoda, 1996]. Colors belonging to different color categories but with same color difference as before are easier to distinguish in memory.

The best visual conditions for color perception tasks include photopic vision to achieve generally color vision. A large visual field improves the recognition for color differences. The adaptation level of the eye should be equal to the test light in luminance and chromaticity to avoid bias. It is necessary to differentiate between the contrast of luminance and the color contrast because they act on noticeable different visual functions. It is also advised to keep the surrounding field similar by similar spectral power distributions to avoid adaptation changes. There should be well defined exposure duration to get noticeable but not excited stimuli. At least, the color memory effect should be considered for successive color evaluation tasks by a balanced experimental setup.
Experiment with regard to colors has to be aware of all the previous presented effects to receive reliable results.

2.3 Spotlight Design Basics

There are various possibilities to combine a light source and a secondary optics to create angularly defined far fields for spotlighting. LED light sources in combination with reflectors or TIR lenses are commonly used but often they project colors and patterns in the far field. Color mixing elements can be implemented in the optical systems to reduce color appearances. But this does not only lead to more uniformity in spotlights, it is usually associated with reduced efficiency or a weaker collimation of the light.

2.3.1 LED Light Source

A light emitting diodes (LED) is an electronic device of a semiconductor material allowing current only in one direction. LEDs emit discrete wavelength because of defined band gaps of the semiconductor material with doped impurities. The light emitted by the LED depends on the band gap. Thus, the emission spectrum of the LED is narrow depending on the material combination. Indium gallium nitride $InGaN$ is used for ultra-violet and blue LEDs, indium gallium aluminum phosphide $InGaAlP$ is used for green to red LEDs. The light is emitted in a solid angle of 180°, LEDs without primary optics are a Lambertian source.

LEDs provide many advantages. They are highly efficient, have a small size, and various chips can be combined to generate different levels of luminance, luminous flux, CCT, and tunable colors [Ohno, 2005]. LED chips can be combined in multi-chip and single-chip packages. Here, the focus is on multi-chip packages. In multi-chip packages, the single LED chips are directly mounted on a board closely together. The dimensions are smaller than typical surface mounted device (SMD) packages and offer cost down possibilities. They provide high luminance which is essential for narrow spotlight collimation. The smaller light emitting area is advantageous for light collimation and color mixing with regard to etendue, see page 28. [Uchida and Taguchi, 2005]
Three different types of LED light sources are presented in Figure 2.10. First, a multi-chip SMD package is shown. Each LED chip is housed and connected

separately to the board. Red and phosphor blended chips are combined to create white light. The second image b) shows a multi-chip package with blue LED chips and a complete phosphor cover as on board technology. The third image (Figure 2.10, c)) shows a multi-chip on board package with each LED covered separately by phosphor blend. Figure 2.10 d) shows a RGBW light source with four different single LED chips.

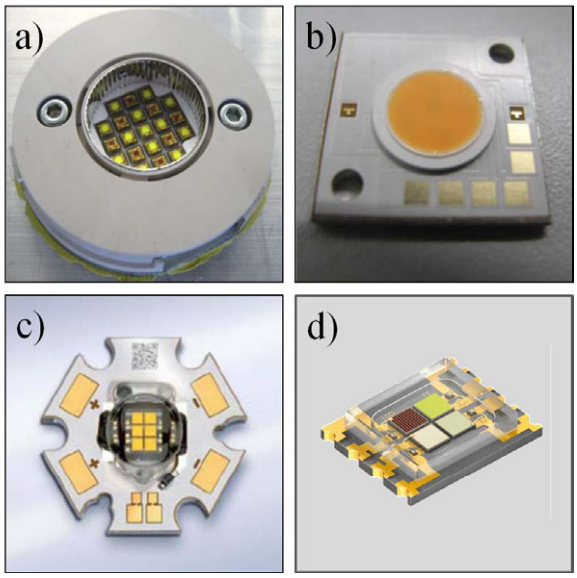

Figure 2.10: Three different LED light sources, a) single chip package, b) multi-chip package with complete phosphor blend, c) multi-chip package with single phosphor blended LEDs, d) RGBW LED [Osram GmbH, 2013]

The light engine is an LED module with a board, single LED chips and an electronic control gear which can be integrated in the module or can be placed in a separate housing. The light engine is usually put as a single light source or in combination with several sources in a housing as lamp or luminaire. This type of packaging achieves higher chip density and high luminance output. This advantage contributes to the design of narrow beams and spotlight solutions.
The LED module itself consists of a basic board. On top, the LED chips are mounted. The board links the chips with the package, and it serves as isolation between chip, package and heat sink. The chips are connected with wire bonds to the circuit path. They are available as surface emitters or volume emitters. Different LED chip types can be housed in the light engine as single chip package or multi-chip package. The final layer can have several shapes. It can be flat or round to change

the angular distribution of the light. For volume emitter and surface emitter with a flat or scattering layer, a reflective layer is put above the board for higher efficiencies. Depending on the application of the chip on board, the number of chips, their position, and the thickness of layers are variable. A light engine that will be used in following measurements and simulations is presented in Figure 2.11. It is assembled by several colored LEDs, covered by a silicone cast for light extraction. The scattering layer is optional and contains scattering particles. They are used to mix the light to create white light in the far field.

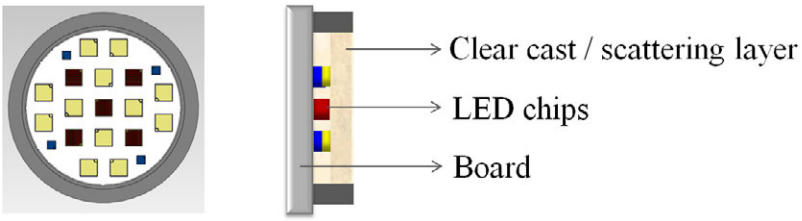

Figure 2.11: Top-view (left) and cross section (right) of a multi-colored light engine

The narrow spectrum of the single LED chips have to superposed for white light appearance in the far field. There are several possibilities to assembly a LED light engine to generate white light. The most frequently used method is phosphor conversion. Blue or rarely ultraviolet LEDs are covered by a phosphor layer. It can be done directly on the above the chip, called chip layer conversion; by a phosphor layer over all chips (volume conversion) or by remote phosphor more far away from the chip. The phosphor converts a part of the emitted light into light of longer wavelengths. Different phosphors can generate the desired CCT and chromaticity coordinates. The superposition of the blue and yellow light appears white in the human visual perception.
The second method is the combination of several LED chips with different emission wavelength (RGB or RGBW). Several LEDs chips with various emitting colors such as blue, green and red are placed next to each other. The separated light is mixed and appears white. The emitted light has narrow spectra but colors could appear more saturated, so bright colors are enlightened.
For professional lighting, a combination of both methods is applied to create white light. Red chips and converted blue chips are placed together, see Figure 2.11. The light spectrum is more balanced with this method. The spectral power distribution of all three methods is compared in Figure 2.12. The multi-colored method provides

less infrared radiation, less yellow but it enhances red and green. The combination of this spectrum reaches high CRI, high efficacy, complex color tuning is possible, and the colors appear bright and vivid. [Osram GmbH, 2013]

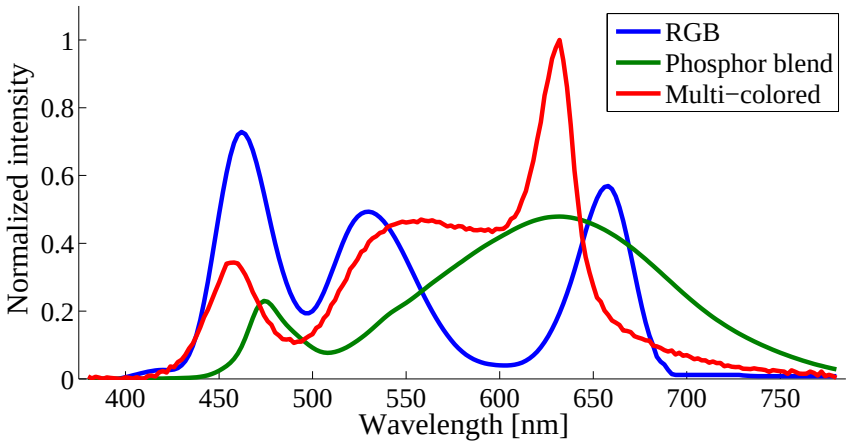

Figure 2.12: Spectral power distribution of several white light chip packages

The disadvantage of all methods is separated colors in the far field. Colors are spatially separated in multi-colored LED chips because the chips emit from slightly different positions. The phosphor conversion separates colors angularly. The emitted light passes different path lengths through the phosphor layer. At short path lengths, the light is converted less; it stays bluer and during longer transitions it becomes yellower. Due to spatial and angular separation of colors in the light source, the uniformity of spotlights is not always adequate.
Color mixing elements can be implemented to in the light engine to mix separated colors. To minimize color separation, scattering layers can be put on top of the chip level. The scattering layer can contain scattering particles. The color mixing level could be controlled by scattering particle concentration. The challenge is to determine the thickness, scattering particle density and chip position to reach a more uniform far field without to many efficiency losses. The color uniformity can be controlled by the amount of scattering particles in the layer.

Figure 2.13 compares the scattering process with different amounts of particles in the volume cast. Figure 2.13 a shows a ray bundle from a point source through a layer without scattering particles. The layer simulates the scattering layer of the volume cast. The light is directly emitted through the cast without further mixing.

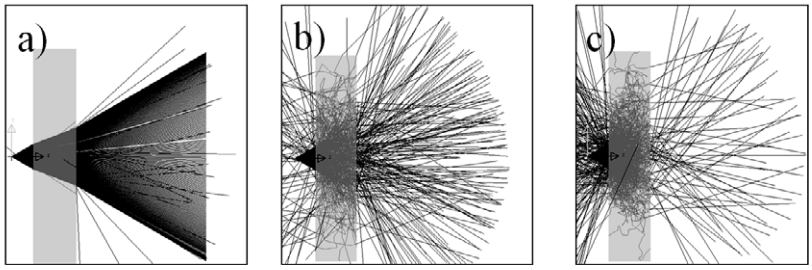

Figure 2.13: Comparison of scattering process at different scattering particle concentrations from a point source through a scattering layer, a) no scattering particles, b) few amount of scattering particles, c) large amount of scattering particles

The second image 2.13 b is related to light engine 2 and 3. The light is scattered partially dependent on the number of implemented scattering particles. Main part of light is emitted forward, small part is scattered backwards and to chip layer. Up to 70 % to 80 % of the light hitting the light engine is emitted again but the efficiency is decreased. The light which is emitted is mixed and improves color mixing but also enlarges FWHM angle. Figure 2.13 c presents a light engine with high concentration of scattering particles. Few light is emitted forward but most of the light is scattered around and backwards. The free mean path of the light is decreases dramatically and local scattering become important. Local scattering is to high too improve color uniformity further because only more direct rays are emitted forward. The efficiency drops clearly.
However, color mixing by scattering particles improves color uniformity up to a certain level but also decreases always the efficiency.

Although LEDs provide many advantages, the generation of white light by superposition of differently colored light is necessary. Either spatially separated (RGBW, multi-colored) or angularly separated (phosphor blending) colors from the light source are emitted. They have to be collected and collimated by the secondary optics to form the spotlight distribution.

2.3.2 Secondary optics

The secondary optics is essential for spotlights. It collects light of the light engine and collimates it into the defined angular distribution. Usually, reflectors or total

internal reflection lenses (TIR) are used for light collimation is spotlights. There are several additional types of optics for this propose: reflector with facets, TIR with micro lenses, RXI (reflection, refraction, total internal reflection), light pipe, and ripped light pipe.

In general, the rays going through the optical elements can be divided into two main groups. There are rays not interacting with the secondary optics, they go directly from the source into the target area. And there are rays redirected by the secondary optics, they change their direction during interaction. Furthermore, caution is needed for the threshold region. Figure 2.14 illustrate the different ray paths for a reflector (left) and ray paths in a TIR lens which are all redirected.

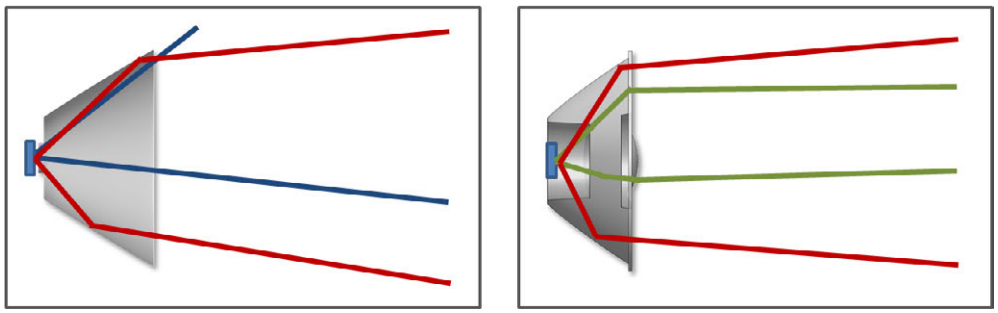

Figure 2.14: Different types of ray paths in secondary optics of reflectors (left) and TIR lenses (right): red are reflected rays, green are refracted rays, and blue are rays without interaction

The secondary optics have different possibilities to mix the light based on different physical processes. Light can be guided by the optical phenomenons of reflection (mirror), refraction (lens, prism) and diffraction (hologram, grating). Diffraction is not discussed further.

- Mixing via reflective randomized rays: reflectors, TIR lenses, mixing chambers or rods
- Mixing via refractive randomized rays: volume and surface diffusers
- Mixing via reflective and refractive randomized rays: TIR lens with collimation lens, micro lens arrays
- Mixing via color selective reflection and refraction: interference filter

There are various possibilities to combine the methods, the combination of reflection

and refraction is often favored [Dross, 2012]. It is common to all color mixing processes that the light is redirected to other directions so that the light interferes at different parts in the far field. This can be done continuously (Gauss scattering, mixing chamber, volume scattering) or sequential (facets, lens array).
The application of the presented methods ca be done by different types of additional elements or surfaces. They were added to the secondary optics to improve the color mixing level [Ding and Gu, 2007; Moreno and Contreras, 2007; Chaves et al., 2012]. Three common types o secondary optics and possible mixing elements are shown in Table 2.1

Table 2.1: Examples of secondary optical elements for illumination application

Optical element	Name	Variations
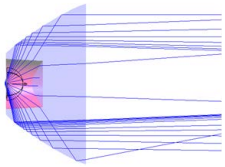	Total internal reflection lens (TIR)	even, faceted, Fresnel lens, micro lens array
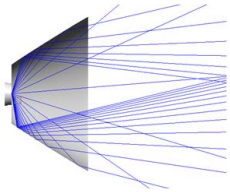	Reflector	even, faceted, rippled, micro lens array, shell mixer
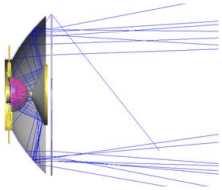	RXI	micro lens array, reflective

The additional implementation of those elements modifies system properties like full width half maximum (FWHM) angle, intensity distribution, and efficiency. Often such structures are accompanied by a wider far field and decreased efficiency. Lenses and reflectors have to be readjusted to the specifications especially FHWM angle. Often, the implementation of color mixing elements increases the angular distribution of the beam and thus the etendue. For etendue limited optics, it becomes more difficult to fulfill the requirements. Independent of the type of the optical elements presented in table 2.1, they have to be adjusted to the light engine. Only a complete defined system can be optimized to meet the requirements.

[Gorkom et al., 2007]

2.3.3 Spotlights Systems and Far Field Intensity Distribution

The spotlight system is a nonimaging system. In contrast to geometrical optics, the rays are free in their target position and are not forced to image an object. Nonimaging optics is a field of optics handling the transmission of light from a source to a defined target. The advantage of nonimaging optics is an additional degree of freedom for extended possibilities in design and system realization. [Chavez, 2008; Winston et al., 2005]

The etendue is an essential value in nonimaging optics. Every conceptual design has to consider the etendue for basic dimension and construction limits and efficiency. According to the optical system design, there is an explicit dependency of the construction of the optical system to the etendue. Design problems can be estimated. The etendue describes the extension of a ray bundle, while the ray bundle has a spatial and angular distribution. It is an integral property of the optical system. The calculation of the etendue E is based on the ray bundles of the system, the solid angle Ω, the area A and the refraction index n of the medium.

$$E = n^2 \int \int_{aperture} cos\Theta \; d\Omega \; dA \tag{2.12}$$

$$E = n^2 \cdot \pi \cdot sin^2(\Omega) \cdot dA \tag{2.13}$$

The application of the etendue results in some general design rules. For example an increased area results in a decreased angle and a defined area limit the degree of collimation as well as a specified angle needs an minimum area. The etendue is thus limiting the concentration of the light between the source and the target.

The relation of the coupling of a light bundle from the light source into the target is given by the etendue (see Figure 2.15). Ideally, an efficient optical system collects all light emitted by the source and collimates it into the defined target. This is only possible if the etendue of the target is similar or larger than the etendue of

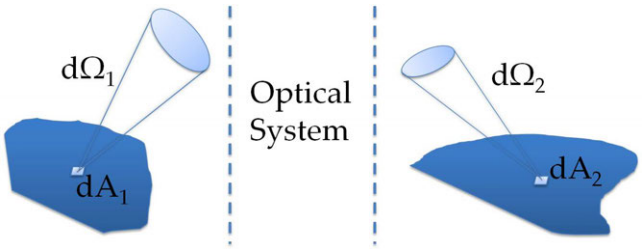

Figure 2.15: Etendue of the source and the target connected by the optical system

the source. It is a difficult task to design an optical system with high efficiency if the etendue of the source and the target are equally large. If the etendue of the source is larger, it is physically impossible to reach full efficiency. At the same time, the etendue of the target can be completely filled but only with efficiency losses. In other words, the size and the solid angle of the light source related to the illuminated target determine the minimum optical system size to reach full efficiency. The etendue is conserved in a perfect optical system.
One conclusion of the etendue calculations in spotlight systems is the demand for small emitting surface of the sources to keep the etendue low. The secondary optics collimates the large solid angle (Lambertian emitter) into a relative small spotlight area. Smaller light emitting surfaces enable better and compacter optical designs.

In a spotlight system, the etendue depends on the size, angle of radiation of the light source and size of the optics, FWHM of the spotlight. Two spotlight systems are illustrated in Figure 2.16. The upper system consists of a multi-colored light engine and a plain reflector. The second system consists of a phosphor converted light engine and a TIR lens as collimating secondary optics. The far fields of these systems appear very different with regard to colors and patterns. The reasons for non-uniform far fields are the combination of separated LED or phosphor conversion of LEDs and imaging properties or geometric boundaries of optics. [Steigerwald et al., 2002; Crawford, 2009]

The far field distribution appear very differently depending on the combination of light engine and secondary optics. The diversity results in very different spotlight solutions with varying level of collimation, luminance level and color distribution, some examples are presented in Table 2.2.

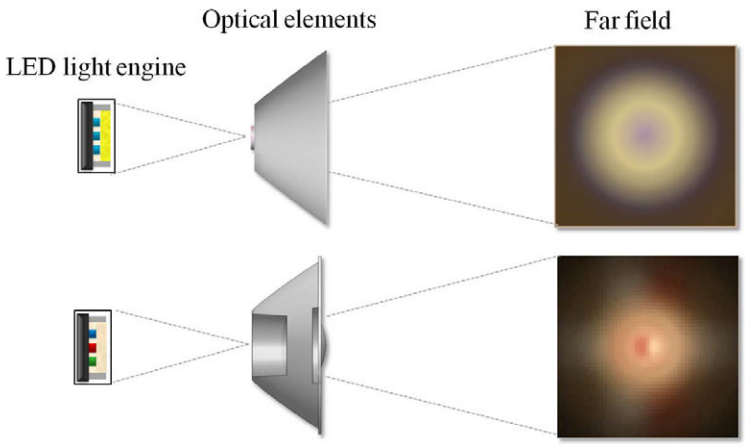

Figure 2.16: Two examples of spotlight designs consisting of light engine, secondary optics and illumination far fields

The first four examples were build up of the same reflector. Just the light source is different, especially the chip number and their position. Example 5 and 6 have the same light engine like example 2 and 3 but a TIR lens is implemented as secondary optics. The examples in Table 2.2 shows that the variation of one element can affect the color mixing in the spotlight clearly. The complete system is sensitive to small changes in one particular area.
Most far field artifacts consist of rings at the edge of the far field, segmented rings, shaped dots in variable amount and out of it several combinations. Most colors appearing in the far field are red and blue due to the wavelength of LED chips of the light engines.
A non-uniform far field can be avoided by an adjustment of light engine and secondary optics. The far field should be even and no colors or colored patterns should appear for excellent color uniformity. Both, the light engine and the secondary optics can contain additional color mixing elements. If the light engine provides color mixing elements, the optical design is less predetermined. If the light engine does not mix colors, the optics has to be adapted.
The light engine and related optic have to be calibrated together for adequate color uniformity in combination with high efficiency, high luminous intensity, and further properties in spotlights.

Table 2.2: Spotlights with different combinations of light engine (LE) and secondary optics

Nr.	Far field	Description	Nr.	Far field	Description
1		LE and reflector	2	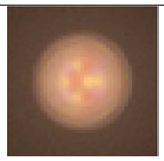	LE with many LED chips and reflector
3		LE with thin scattering layer and reflector	4	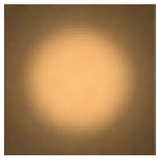	LE with enlarged scattering layer and reflector
5		LE and TIR lens	6		LE with scattering layer and TIR lens

2.4 State of the Art in Color Uniformity Quantification

The connection between objective mathematical description and the visual color perception is the main challenge in this topic.
The evaluation of color uniformity in available optical simulation programs is based on color differences calculations. In LightTools a weighted average of color differences ($du'v'_{wa}$) is calculated in the CIE 1976 (L*, u*, v*) color space. First, a reference color u'_{ref} and v'_{ref} is calculated from the data of a receiver. Each value is weighted with its illuminance Y_i. The counter i represents the number of test point of the receiver.

$$u'_{ref} = \frac{\sum_{i=1}^{n} u'_i \cdot Y_i}{\sum_{i=1}^{n} Y_i} \tag{2.14}$$

$$v'_{ref} = \frac{\sum_{i=1}^{n} v'_i \cdot Y_i}{\sum_{i=1}^{n} Y_i} \tag{2.15}$$

The reference chromaticity coordinates in u' and v' plane are used to calculate the color difference $du'v'_i$.

$$du'v'_i = \sqrt{\left(u'_i - u'_{ref}\right)^2 + \left(v'_i - v'_{ref}\right)^2} \tag{2.16}$$

The $du'v'$ value describes the color difference of each point to the reference color. The sum of the differences including luminance weighting results in $du'v'_{wa}$.

$$du'v'_{wa} = \frac{\sum_{i=1}^{n} du'v'_i \cdot Y_i}{\sum_{i=1}^{n} Y_i} \tag{2.17}$$

It describes the average color difference between the color value of each test point and the reference color. An illumination weighting is included to enhance the importance of color differences at high illuminance levels and decreased at lower illuminance levels. [LightTools, 2013]
The weighted average color difference is used in optical simulations and measurements for the evaluation of the color uniformity in spotlights. [Cvetkovic et al., 2012; Chen et al., 2014]

Another similar approach is described in Sun et al. [2012]. The color uniformity is calculated based on the standard deviation of color differences Δuv_{rms}.

$$\Delta uv_{rms} = \sqrt{\frac{1}{n}\sum_{i=1}^{n}\left[\left(u'_i - u'_{ref}\right)^2 + \left(v'_i - v'_{ref}\right)^2\right]} \tag{2.18}$$

The derivation for Δuv_{rms} is published in Moreno and Contreras [2007]. The color uniformity is defined as:

$$ColorUniformity = \frac{100}{1 + k \cdot \Delta uv_{rms}}[\%] \tag{2.19}$$

The fitting factor k is set to 138.9, that provided a color uniformity of 90 % for a very uniform far field measured in the laboratory and judged by the observers. The number of test points was limited to 37 and resulted from a spotlight divided into three circular zones that were divided into 12 sections and an additional center test point. Colored patterns which are smaller than the size of one test point would not be included in the $ColorUniformity$ calculation. However, depending on the distance between observer and spotlight and the size of the spotlight, the eye detects much smaller luminance and color patterns.
A fundamental approach is the implementation of visual sensitivity after the contrast sensitivity functions. The first implementation of achromatic contrast sensitivity that is applied to luminance distribution in spotlights were provieded by

Moreno [2010].
Apart from the mathematical descriptions calculating the color uniformity, a personal judgment of the color appearance in the far field by observers is still common. [Dross, 2012]

2.5 Summary

Spotlights are characterized by a light beam which illuminates a specific area in a defined angular distribution. The design of spotlights combines LED light source and secondary optics. Their combination often leads to color fragments and patterns in the far field because of spatially and angularly separated colors. The far fields of differently combined optical systems differ from each other. Various colors and patterns, basically rings and dots, occur. There are color mixing elements that can be implemented in the optical system but often these elements increase the angular distribution or decrease the efficiency.
A perfectly uniform far field is not absolutely necessary because of thresholds in color perception of the human eye. There are many visual influencing factors affecting the perception in spot lights. The luminance level, surrounding, contrast of the stimuli, and the personal constitution of the observer are essential factors. Thus, a subjective personal judgment of spotlight far fields is not practicable. An individual judgment would lead to very different estimations with regard to the color uniformity in spotlights.
Mathematical descriptions are available, most of them without an explained relationship to the perceived color uniformity. Thus, a mathematical description of color uniformities in spotlights with regard to visual color perception is necessary.

3 Mathematical Description of Spotlights

A mathematical description of the color distribution in the far field of the spotlights is required in order to receive objective function value. Until now, the personal subjective judgment is very important for color uniformity evaluations but should be avoided. Individual preferences are very divergent from person to person. It is necessary to reach an objective mathematical evaluation with regard to an average color perception. The mathematical evaluation should lead to a prediction of the perceived color uniformity in optical simulations and measurements of far fields as shown Figure 3.1. Therefore, the merit function for color uniformity has to implement many visual influencing factors of the previous section 2.2.

Figure 3.1: Three different far fields of spotlights

There are functions using direct measured or simulated data, called basic functions. There are functions which pre-process or post-process the data and apply the direct functions afterwards or before, called weighting functions.
All functions described in the CIELAB color space, see section 2.1.2 on page 9.

3.1 Basic Functions for Color Description

Each function describes different aspects of the color appearance in the far field of spotlights. They were selected with regard to the visual color perception (see

section 2.2.2 on page 14). Some functions were based on available functions from literature and simulation software. Additional functions were created to describe the aspects of visual perception more detailed. The correlation of the functions will be tested with the visual perception in the human factor experiments. The following functions to calculate a color uniformity value of a spotlight are explained in this section.

a) Maximum color difference
b) Color deviation
c) Gradient analysis
d) Symmetry analysis

a) Maximum color difference

The maximum color difference describes the color-color contrast in a spotlight. The function of the maximum color difference $\Delta E_{max\ Lab}$ refers to the color difference ΔE^*_{Lab} (equation 2.11 on page 10). ΔE^*_{max} is the Euclidean distance between the two test points $n_1(L^*_1, a^*_1, b^*_1)$ and $n_2(L^*_2, a^*_2, b^*_2)$ with the maximum difference in the CIELAB color space:

$$\Delta E^*_{max\ Lab} = \sqrt{(L^*_1 - L^*_1)^2 + (a^*_1 - a^*_2)^2 + (b^*_1 - b^*_2)^2} \tag{3.1}$$

Spotlights hold their own particular luminance distribution. ΔE^*_{max} depends on the luminance and is changed if luminance differs and hue and chroma stay constant. An adapted equation for spotlights without luminance impact is described as follows.

$$\Delta E^*_{max\ ab} = \sqrt{(a^*_1 - a^*_2)^2 + (b^*_1 - b^*_2)^2} \tag{3.2}$$

Now, the two test points n_1 and n_2 depend only on a^* and b^*. The maximum color difference $\Delta E^*_{max\ ab}$ in spotlights is independent of the spatial distribution of the color. The color distribution in between is irrelevant. Two points can be close to each other or far away and $\Delta E^*_{max\ ab}$ reaches the same value. However, the eye is not only sensitive to two extreme values in the far field distribution. The color characteristic between the two points is also crucial.

b) Color deviation

The color deviation *dab* is based on the average color difference function (Formula 2.17 on page 32) calculated by LightTool. The function is adapted to CIELAB color space. It describes the average of differences between a reference color and a test point n. The reference colors $a^*_{ref\ Lum}$ and $b^*_{ref\ Lum}$ are weighted with the luminance Y

$$a^*_{ref\ Lum} = \frac{\sum_{i=1}^{n} a^*_i \cdot Y_i}{\sum Y_i} \tag{3.3}$$

$$b^*_{ref\ Lum} = \frac{\sum_{i=1}^{n} b^*_i \cdot Y_i}{\sum Y_i} \tag{3.4}$$

The reference chromaticity coordinates are used to calculate the color difference to each test point $dab_{n\ wa}$.

$$dab_{i\ wa} = \sqrt{\left(a^*_i - a^*_{ref\ Lum}\right)^2 + \left(b^*_i - b^*_{ref\ Lum}\right)^2} \tag{3.5}$$

The luminance weighting results in the weighted average of color differences dab_{wa}.

$$dab_{wa} = \frac{\sum_{i=1}^{n} dab_i \cdot f(Y_i)}{\sum f(Y_i)} \tag{3.6}$$

Depending on the definition of the luminance weighting function $f(Y_i)$, the reference value a^*_{ref} and b^*_{ref} change as well as the final result dab_{wa}. The standard luminance weighting is linear as shown in Equations 3.3 and 3.4. Color differences at high luminance are enhanced in contrast to color differences at low luminance levels. Another weighting, e.g. with a logarithm function would emphasis the edges of the far field with lower luminance, edged colors and patterns become more important than centered colors. In contrast, an exponential weighting would suppress edge colors and clearly enhance colors and patterns in the center. The adequate functions without luminance weighting are the following.

$$a^*_{ref} = \frac{\sum_{i=1}^{n} a^*_i}{n} \tag{3.7}$$

$$b^*_{ref} = \frac{\sum_{i=1}^{n} b^*_i}{n} \tag{3.8}$$

The reference colors a^*_{ref} and b^*_{ref} are only the average color without luminance weighting. The color difference dab_i in a test point i compared to the reference color is then:

$$dab_i = \sqrt{\left(a^*_i - a^*_{ref}\right)^2 + \left(b^*_i - b^*_{ref}\right)^2} \tag{3.9}$$

And finally the color deviation dab results of the summation of dab_i.

$$dab = \frac{\sum_{i=1}^{n} dab_i}{n} \tag{3.10}$$

This equation does not only consider any maximum color difference but also the average of deviations between all test points.

c) Gradient analysis

The gradient is a mathematical expression considering the spatial color distribution in the spotlight and its local rate of change. An adaptation to spotlights considers only the CIELAB $a^* - b^*$ plane without luminance Y. The function $Grad_{ab}$ describes the variation of color over the spotlight in a^* and b^* direction and is the square of the modulus of the 4D vectors (∇a^*, ∇b^*).

$$Grad_{ab} = |\nabla a^*|^2 + |\nabla b^*|^2 \tag{3.11}$$

To create a function used for the prediction of color uniformity in spotlight, the difference in color between one test point and the immediate neighbor test point is added together for a^* and b^*. It results in the following equation.

$$\begin{aligned} Grad_{ab} =& \frac{1}{m \cdot n} \cdot \frac{1}{(\Delta\alpha)^2} \cdot \\ & \sum_{i=1}^{m \cdot n} \sum_{j=1}^{m \cdot n} \left[(a^*_{i,j} - a^*_{i,j+1})^2 + (a^*_{i,j} - a^*_{i+1,j})^2 + (b^*_{i,j} - b^*_{i,j+1})^2 + (b^*_{i,j} - b^*_{i+1,j})^2 \right] \end{aligned} \tag{3.12}$$

The parameters m and n are the number of test points in x and y direction, respectively. The $\Delta\alpha$ represents the visual angle for one test point pair. The function $Grad_{ab}$ is normalized to the number of pixels of the measuring zone and the distance between the screen and the observer to be independent of distance and size

of the measuring field. It allows the comparison of different measuring setups with each other.
The basic function $Grad_{ab}$ described the rate of change of color in the far field of the spotlight. It detects the slope of transition in the far field from one color to another color.

d) Symmetry analysis
The symmetry analysis is based on the assumption that visual perception is sensitive to symmetries in objects (see page 19). Symmetrical patterns are essential in human vision and have a high influence on the reception. [Corballis and Roldan, 1975; Carmody et al., 1977]
There are symmetry detection algorithms for imaging processing [Loy and Zelinsky, 2003; Chen et al., 2007]. In general, these algorithms try to detect several types of symmetries and number of symmetry axes in images. A basic function for color uniformity does not have to detect the presence of symmetry or symmetry axes but the level of symmetrical appearance. The symmetry calculation is divided into two aspects, the rotational symmetry and the linear symmetry. Thus, the smoothness of the radial and axial color distribution is analyzed.

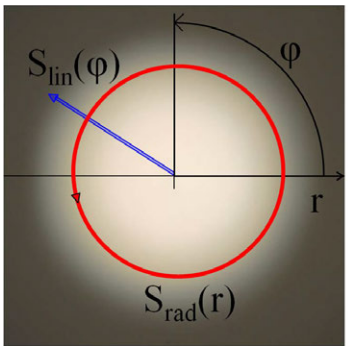

Figure 3.2: Algorithm of calculation of S_{rad} for defined r and S_{lin} for defined φ

For rotational symmetry the rotational smoothness of the far field is calculated. For each defined radius r the radial reference color $\bar{a}_r^*$ and $\bar{b}_r^*$ is calculated with n the

number of test points per radius.

$$\bar{a_r^*} = \frac{1}{n} \sum_{\varphi=0}^{2\pi} a_\varphi^* \tag{3.13}$$

$$\bar{b_r^*} = \frac{1}{n} \sum_{\varphi=0}^{2\pi} b_\varphi^* \tag{3.14}$$

In Figure 3.2 the red arrow illustrates the direction of the summation for $S_{rad\ r}$ that is calculated for each radius. The basic function S_{rad} results of the maximum value of all $S_{rad\ r}$ for each radius. S_{rad} is expressed as the maximum standard deviation of color at any radius.

$$S_{rad\ r} = \sqrt{\frac{1}{n} \sum_{\varphi=0}^{2\pi} \left(a_\varphi^* - \bar{a_r^*}\right)^2 + \left(b_\varphi^* - \bar{b_r^*}\right)^2} \tag{3.15}$$

$$S_{rad} = max\left[S_{rad\ r}\right] \tag{3.16}$$

The radial smoothness is considered because typical appearances in far fields are dots, rings and especially segmented rings. The S_{rad} function results in higher values for dots or segmented rings than for uniformly colored rings that do not affect the function.
In contrast to S_{rad}, the linear smoothness S_{lin} analyses the color differences in axial direction, it is illustrated in Figure 3.2 by blue arrow. Now, the reference colors $\bar{a_\varphi^*}$ and $\bar{b_\varphi^*}$ are calculated for each defined angle φ.

$$\bar{a_\varphi^*} = \frac{1}{n} \sum_{r=0}^{r_{max}} a_r^* \tag{3.17}$$

$$\bar{b_\varphi^*} = \frac{1}{n} \sum_{r=0}^{r_{max}} b_r^* \tag{3.18}$$

The standard deviation of color for each defined angle φ is calculated.

$$S_{lin\ \varphi} = \sqrt{\frac{1}{n} \sum_{r=0}^{r_{max}} \left(a_r^* - \bar{a_\varphi^*}\right)^2 + \left(b_r^* - \bar{b_\varphi^*}\right)^2} \tag{3.19}$$

$$S_{lin} = max\left[S_{lin\ \varphi}\right] \tag{3.20}$$

The basic function S_{lin} detects color differences on a specified angle. In contrast to S_{rad}, the function detects also multiple consistent rings. On the other hand, smoothed dot patterns do not influence the function so much.
For both function a minimum number of test points per radius or angle is necessary to be able to calculate the value. Therefore, the data are converted into polar coordinates and at least 10 test points are required to be included in the calculations of S_{rad} and S_{lin}. Thus, a small area in the center of the spotlight is not evaluated.

3.2 Preprocessing and post-processing of data

The previous presented basic functions calculate values direct form measured or simulated far field data. It could be necessary to preprocess the data or apply a further function afterwards. The following pre- and post-processing are tested.

a) Data preparation - noise reduction and luminance cutoff
b) Contrast sensitivity weighting
c) Luminance weighting
d) Cumulative distribution function

a) Data preparation - noise reduction and luminance cutoff
First, the measured or simulated data have to be prepared for the calculation of the basic function values. Therefore, the data are filtered for noise reduction, and a luminance cutoff is implemented to analyze circular data sets. These data modifications are done to all measured and simulated data independent of further processing.

The data are filtered to reduce the noise to be independent of measuring setup or number of simulated rays. In general, filtering is done by convolution of the function f and the filter h. Here, f are the data from measurements or simulations

of the far field in CIELAB. [Jähne, 2005; Annadurai and Shanmugalakshmi, 2007]

$$g = f * h \tag{3.21}$$

$$g_{i,j} = \sum_{\mu=-m}^{m} \sum_{\nu=-n}^{n} f(i-\nu, j-\mu) \cdot h(\nu, \mu) \tag{3.22}$$

Each test point $g_{i,j}$ of data is weighted by the filter with regard to control variables μ and ν where m and n are related to the size of the filter. To reach normalized values, the filtered value is divided by the sum of filter weights and normalized to the function values.

$$g_{i,j} = \frac{\sum_{\mu=-m}^{m} \sum_{\nu=-n}^{n} f_{i-\nu,j-\mu} \cdot h_{\nu,\mu}}{\sum_{\mu=-m}^{m} \sum_{\nu=-n}^{n} h_{\nu,\mu}} \tag{3.23}$$

The data of the far fields are given by f and are filtered with the lowpass filter h. As shape of the filter function h a boxcar function is selected. The size of the filter is variable and depends on the resolution of the data and the measuring noise. An example of a 3 filter is given by h.

$$h = \begin{bmatrix} 1 & 1 & 1 \\ 1 & 1 & 1 \\ 1 & 1 & 1 \end{bmatrix} \tag{3.24}$$

At the edges, the edge data are replicated to be able to apply the filter to the complete data set and to reach same size.

A luminance cutoff is necessary in combination with noise reduction . At very low luminance levels the noise increases clearly because of very low signal input or fewer simulated rays. The analyzed area of the far field is limited by the minimum luminance level L^*_{min}. All pixels with lower luminance values than L^*_{min} are skipped and not included in further calculation.

$$Data(L^*) = \prod (L^* / L^*_{min}) = \begin{cases} 1 & \text{if } |L^*| \leq L^*_{min} \\ 0 & \text{otherwise} \end{cases} \tag{3.25}$$

At the beginning, the luminance cutoff was set to 10 % of the maximum luminance for each spotlight. Thus, the spotlight area that had lower luminance levels did not belong the spotlight itself. Scattered light, background light or further light sources beside the spotlight was not considered.
The cutoff level has to be chosen carefully. Too high cutoff levels could exclude colors and patterns at the edge of spotlights, too low cutoff levels increase the spotlight and implement more noise and additional environmental light.

b) Contrast sensitivity function
The contrast sensitivity function (CSF) and its influence on vision is explained in section 2.2.2 on page 17. The CSFs express the relation between visual sensitivity and spatial frequencies of luminance and color patterns. The visual system has different sensitivities to detect achromatic and chromatic patterns, depending on spatial frequencies, The dependency was shown in Figure 2.9 on page 18.

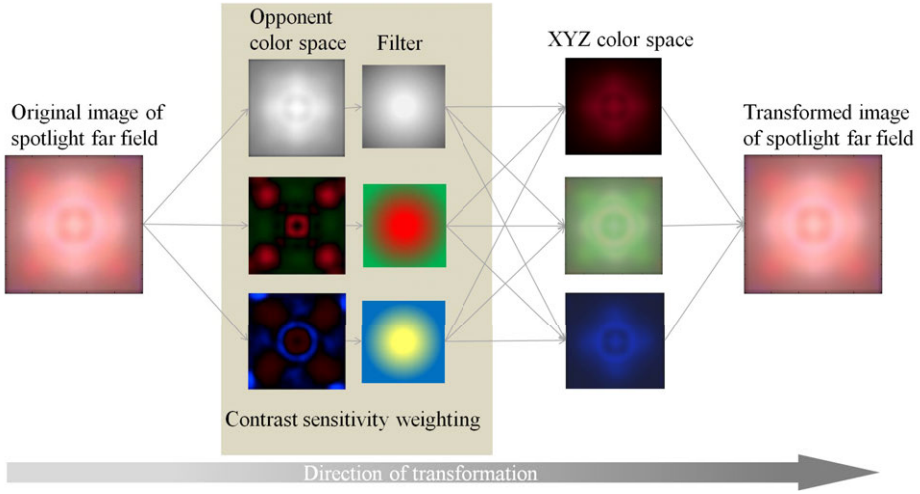

Figure 3.3: Steps of S-CIELAB transformation (after [Poirson and Wandell, 1993])

To implement the spatial sensitivity of the human eye, the S-CIELAB metric is used and schematically illustrated in Figure 3.3 [Poirson and Wandell, 1993; Zhang and Wandell, 1997]. The S-CIELAB metric performs a pre-processing analysis of the data. The spatial sensitivity of the human eye is used to filter the data. For the calculation of the corresponding S-CIELAB image, several assumptions and parameters are necessary. The main determined value is the viewing condition. It reports the number of test points per degree of visual angle in the image. A measurement of a spotlight with a resolution of 100x100 pixels projected at a screen of 1 m^2 and

viewed at a distance of 2 m results in 3.5 pixels per degree. Other specifications are the spectral power distribution of the light, the cone sensitivity function [Smith and Pokorny, 1975; Shevell, 2003], and the reference white point required by CIELAB. The parameters stay constant for same measurement or simulation setup.
The XYZ tristimulus data are transformed into the opponent color space for the processing and the SCIELAB calculations [Krauskopf, 2001; Fairchild, 2005]. It is a color space which represents the cardinal axis in vision based on the color opponent theory. It is similar to CIELAB color space but with differing axis. A conversion of CIEXYZ and reverse is defined by a transformation matrix. The decomposition of the image into opponent color space is necessary to achieve the separation of channels into green-red, blue-yellow, and luminance. In this color space the CSFs are applied to the three planes. Afterwards, the data are reassembled and transformed back into CIEXYZ. Now, further processing can be applied. The new data represents the visual perceived image under the defined viewing conditions. The SCIELAB conversion to implement the contrast sensitivity of the human eye was implemented as a pre-processing of data to all spotlights.

c) Luminance weighting
The importance of luminance level to visual color perception is explained in 2.2.2 on page 17. As explained by the Weber-Fechner law, a logarithmic increased luminance level is perceived linearly. Thus, a weighting of the color values a^* and b^* could adjust the basic functions and improve their correlation to the visual color perception of spotlights. Vision is sensitive to luminance and color, and color vision is not completely independent. It is expected that the correlation between the visual perception is improved by luminance weighting but not without restrictions. The luminance level in spotlights decreases clearly towards the edges. Two points with same a^* and b^* coordinates and only differing in luminance value L^* would result in a color difference although the luminance difference is not avoidable in spotlights and is not seen as color difference.
The implementation of a luminance weighing changes the impact of color differences in the center and the edge to the merit function. The impact of the luminance depends on the weighting function $f(Y)$. The luminance weighting of the color values $a^*_{i,j}$ and $b^*_{i,j}$ is obtained by multiplying the values with the corresponding luminance value $f(L^*_{i,j})$ or $f(Y_{i,j})$ of the test point i, j. This method was shown in the functions for $du'v'_{wa}$ 2.17 on page 32 and dab_{wa} 3.6 on page 37. The luminance

weighting implementation is possible for all basic functions. The luminance weighting is set to zero by $f(Y) = 1$ which results in the function without luminance impact, e.g. formula 3.10 on page 38.

d) Cumulative distribution function
Most of the basic functions results in a calculated average value of color difference or color change of the spatial distribution. The functions for color deviation *dab* (Formula 3.10), gradient $Grad_{ab}$ (Formula 3.12), radial smoothness S_{rad} (Formula 3.17), and axial smoothness S_{lin} (Formula 3.13) calculate averages of different spatial color formations. The processing of visual stimuli are spatially and frequency-depended averaged but the average has limitations. Thus, for spotlights with their spatial extension and long exposure durations, extreme values could be more convenient.
Not an average value but any other parameter used as function value can be described by the histogram to analyze the frequency distribution and its cumulative distribution function (CDF). The histogram described the distribution of function values and their frequency. The summation of the function values results in the CDF. Here, any percentaged number of test points can be defined as threshold for the function. It is not limited to the calculation of an average value. A threshold at 90 % of all test points could be defined. Then, the importance of more extreme values is increased. 3.4 shows an example of the distributions of the function values of dab_i for one spotlight. The histogram is on the left and the CDF in the middle. On the right side, the normalized cumulative distribution function is shown, the dab_i value at 0.9 could be used as threshold for the function value.

The variable definition of a threshold enables the testing of the correlation with the visual perception at different threshold levels. Depending on the basic function, there may be suitable results at different thresholds.

3.3 Conclusion

Various possibilities to analyze the spatial color distribution in the far field of spotlights are presented. But until now, there is a missing link between the visual

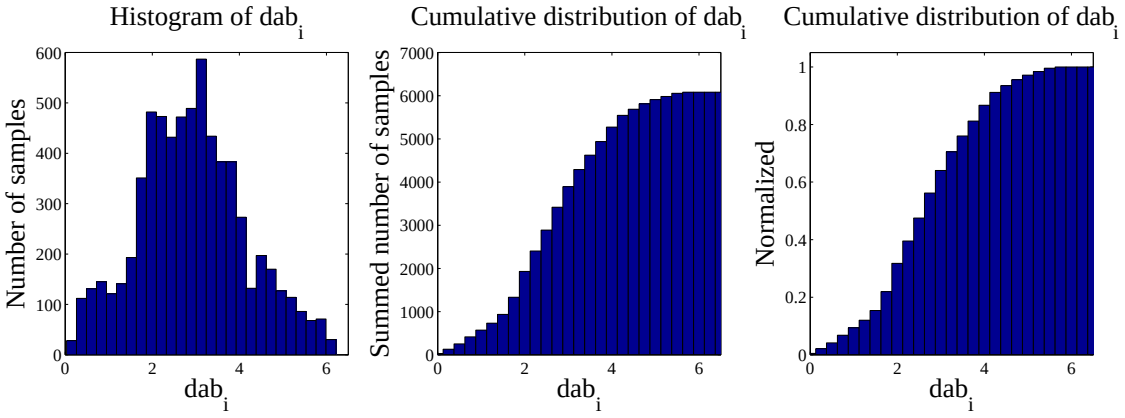

Figure 3.4: Histogram (left), cumulative distribution function (center), and normalized cumulative distribution function (right) of *dab* for one spotlight far field

perception and a consistent mathematical description. Several basic functions were proposed. They use the measured or simulated data of the far field to calculate a color uniformity value. These functions are the maximum color difference, the average color deviation, the gradient of spatial color distribution as well as the radial and axial smoothness. Each function refers to different visual influencing factors, and they have different handling of data. Thus, their effect to reproduce the visual perception of spot lights will differ. In addition, there are weighting functions which pre- and post-process the simulated or measured data. These functions are for noise reduction, luminance cutoff, the implementation of luminance weighting, contrast sensitivity function, and cumulative distribution function. They are either applied before or after the basic functions and thus, they can change the input data for the basic function or change their value afterwards, respectively. A combination of both, the basic functions and weighting functions, is possible.
All methods will be evaluated with regard to their accuracy to represent the visual perception of colors and patterns in spotlights. Therefore, two human factor studies were designed to test the correlation of the basic functions and weighting functions with the visual perception. A final merit function should lead to a mathematical description to estimate the perception.

4 Quantitative Merit Function of Color and Pattern Quality in Spotlights

A merit function describing the color uniformity in spotlights based on the human color perception is required. In the present chapter, the human factor experiments are described. The results provide the correlation between an average visual perception of color uniformity in spotlights and the required merit function. Therefore, two human factor studies were carried out to evaluate the visual perception of colored far fields. A perceived rank order was generated out of the results of the first experiment. The perceived rank order was used to verify the basic functions in various combinations with the pre- and post-processed data to define the merit function. The resulting merit function was analyzed in the second human factor experiment. Levels for excellent to insufficient color uniformity were defined.

4.1 Spotlight Appearance

Only few references can be found about the visual perception of colored spotlight far fields. Currently it is difficult to say, up to which level spotlights have to be uniform in color and luminance distribution to be accepted by customers. There are no standardized merit functions to quantify the level of color uniformity because many aspects influence the visual perception of light.

The visual perception of far fields was tested in two human factor experiments. In the two human factor experiments, subjects had to assess the evenness of colors and patterns in the far fields of spotlights. For the experiments, adequate spotlight far fields were required. The spotlight patterns were chosen systematically to cover a wide range of appearances of typical LED spotlights. The design of the far fields

was based on optical simulations with multi-colored light engines in combination with TIR lenses or reflectors as secondary optics.
All together 46 spotlights were created. The 15 spotlight far fields with highest chroma level are presented in Figure 4.1 and show all used combinations of the colors and patterns.

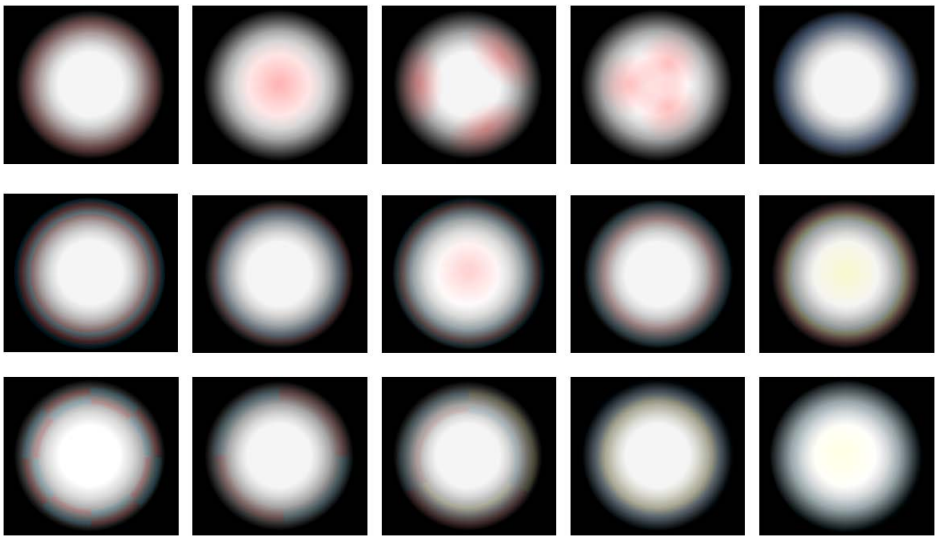

Figure 4.1: All 15 spotlights with highest chroma level used in the experiments

One reference was designed and it only had a luminance distribution. The luminance distribution was nearly the same for all spotlights (± 5 %). All spotlights had the nearly same peak luminous intensity of about 300 cd/m^2 and the same diameter of about 0.8 m.

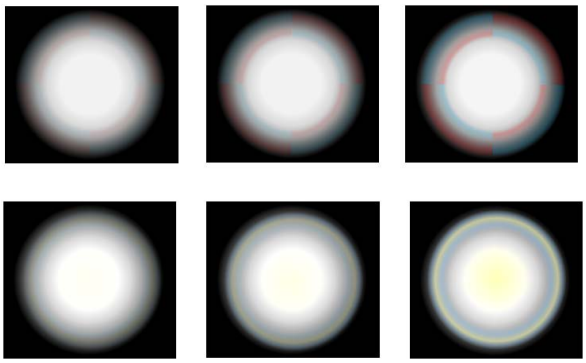

Figure 4.2: Two examples of a spotlight with the three different chroma levels of the colored pattern; left: lowest chroma level; center: medium chroma level; right: highest chroma level

To create several color uniformity levels, the 15 spotlights were replicated with two

lower chroma levels. Each spotlight pattern existed in three chroma levels. The color patterns of the spotlights with lowest chroma level were rarely discerned. The second chroma level showed colors and patterns more clearly, and the third level showed considerable colored patterns. Examples of two spotlights and their three chroma levels are shown in Figure 4.2. The pattern in each of the two spotlights was the same only the chroma level of the red-blue rings (first row) and yellow-blue rings (second row) differed. All other properties like luminance distribution and size were similar. The three levels were adjusted to optical simulations and tested in preliminary tests. All together, there were 46 different spotlights. The spotlights and their characteristic values are listed in Appendix A (see from page 141).

The spotlights were classified after four parameters to analyze preferences of subjects. The parameters were chroma (saturation), hue (number of colors), pattern, and existence of rotational symmetry. The different values for the four parameters are listed in Table 4.1.

Table 4.1: Four parameters of the far field description

Parameter	Scale	Values
Chroma level	ordinal	low, medium, high
Hue	ordinal/nominal	red, blue, red-blue, yellow-blue, rgb
Pattern	nominal	ring, dot, rings, dots, segmented rings, combination
Symmetry	nominal	rotational symmetry, non symmetrical

One value of each parameter was assigned to each spotlight. The analysis of these parameters provided information about the preferences of the subjects concerning preferred colors and patterns and their attention focus.

A slide projector and background light source were used for the projection of the far fields onto a screen. It offered a flexible and rapid changing of the slides and thus an experimental design with variable far fields. The illumination system used in the human factor experiments is shown in Figure 4.3.

The slide projector consisted of the light engine, followed by condenser lens of

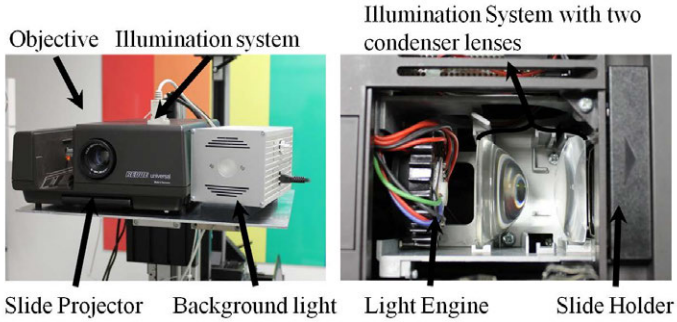

Figure 4.3: Slide projector with optical system (right) and background light

two plan-convex lenses. The lenses concentrated the light from the light engine to the sample plane to illuminate it uniformly. Afterwards, the sample holder was installed. It was the position of the slides containing the printed image of the far field. The slides were imaged by the projector objective onto the screen. The schematic optical systems is presented in Figure 4.4

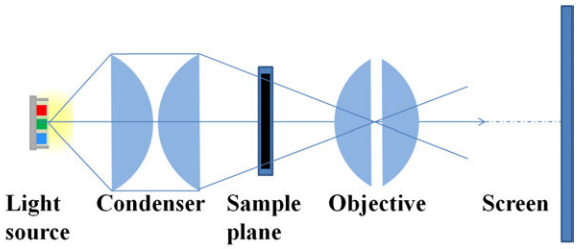

Figure 4.4: Optical system of the slide projector

The slide projector was equipped with a multi-colored LED light engine (see Figure 2.11 on page 23). The light engine replaced a traditional halogen lamp to obtain a more LED like light spectrum. The spectral power distribution (SPD) of the light engine in combination with the background light is shown in 4.5. The spectrum represented a typical multi-colored LED illumination. The light engine had a luminous flux of about 600 lm.

In addition to the slide projector, a background light was installed. The background light consisted of an identical light engine and provided the same spectral power distribution. The luminous flux was dimmed to 10 % of the maximum luminance in the reference spotlight. It was needed to provide a constant low luminance level during the whole procedure of the experiment, even when no slide was projected.

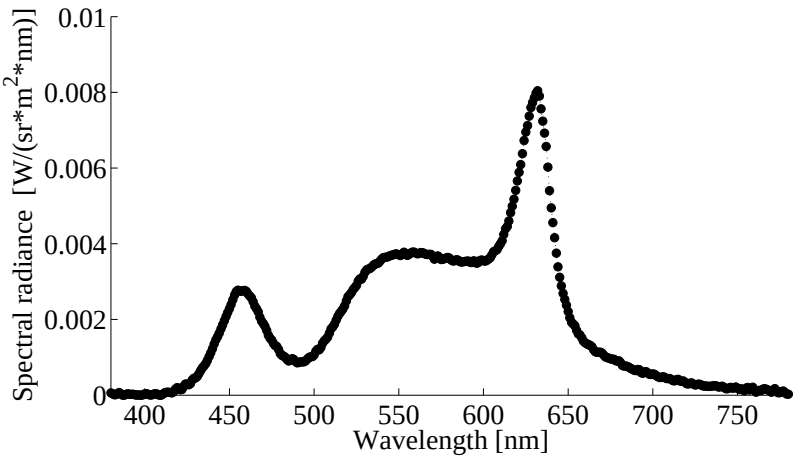

Figure 4.5: Spectral power distribution of the light source in combination with the background light

The subjects could keep adapted to photopic vision during the whole experiment. The projection of the different slides was accurate. The correlated color temperature (CCT) was 3200 K. All spot were within a 3 step MacAdam ellipse, the chromaticity coordinated of the mean value of the reference spotlights were $x = 0.426$ and $y = 0.408$. The illumination through the optical system and the slides reached a maximum luminance on the screen at 2 m distance of about 300 cd/m^2. The full width half maximum (FWHM) angle of all spotlights was about 18°.
All spotlights were measured by a luminance camera. It records the tristimulus values X, Y and Z (see page 6) by several filters with regard to the color matching functions of the human eye (see section 2.1.1 on page 5). The measurement setup was similar to the experimental setup of the human factor experiment. The illumination system was at 2 m in front of the projection screen. The measuring zone was 1 m^2 with the spotlights centered in the field. To reach statistical reliable measurements, each spotlight was measured five times.
The illumination system with slide projector and background light was able to project any far field of a spotlight by printed slide towards the screen.

4.2 Visual Perception of Far Field of Spotlights

there were several possibilities to analyze the light distribution in spotlights (see section 3 on page 35). The process of visual perception is complex and influenced by many parameters. Several studies tested perceived color difference thresholds and established values for perceivable color differences (see section 2.2.1 on page 11), but these results cannot completely be adapted to the spotlights of LED luminaires in any case.
A human factor experiment was designed to analyze the perception of colored patterns in spotlights of several observers. The main intention of the first human factor experiment was the creation of a perceived rank order of the spotlights. This order represented the visual perception of spotlights by subjects. It was correlated with the basic functions and weighting functions to find the best fitting mathematical description. Furthermore, preferences of color and pattern in spotlights were identified.

4.2.1 Setup of the 1st Human Factor Experiment

The setup of the first human factor experiment was aimed to the following four main aspects.

- Preference to spatial color distribution
- Correlation of spotlight parameters
- Definition of the perceived rank order
- Validation of mathematical descriptions

The first human factor experiment was performed as a successive two alternative forces choice test (2AFC), more precisely as a two interval forced choice test. The successive experiment represented more an everyday situation and typical applications for light spots e.g. series of spotlight luminaires illuminating several objects. Two randomly chosen spotlights in a successive order were presented to the subjects. After the presentation of the two stimuli the subject was forced to choose one spotlight. Thus, the answer of the subject was related to the subjective

experience about the two stimuli. There was no possibility to avoid an answer. Even if the subject did not assume a tendency for one stimulus, the subject had to make a choice, which was arbitrary. Over a larger number of subjects, a general tendency of subjective perception of the preferred stimuli was detectable. From all answers, the perceived rank order was calculated which is necessary for all further analyses. [McKee et al., 1985]
For the forced choice test, each observer used its own individual criteria. This criterion could differ between several observers and could also change for one observer over time as a result of training or previous experiences. There was no possibility to verify correctness of the answers due to personal criterion. There was no true or false in the answers of the subject. The answers were just evaluated in relation to all other answers of all subjects in the experimental group.

One disadvantage of a successive experimental setup is response bias. Often, successive presented stimuli lead to time order errors where subjects tend to select more often the first or second presented stimulus independent of the content of the stimuli. The observers tend to underestimate or overestimate systematically the magnitude of one stimulus proportional to the other. The reason for this effect is the sensitivity of the visual processing and its memory to time intervals and serial positioning of the stimuli [Schab and Crowder, 1988; Nachmias, 2006; Katkov et al., 2006]. Furthermore, they refer to the primacy-recency or serial position effect. The primacy effect indicates more importance on the first shown stimulus because the first stimulus is remembered better. In contrast, the recency effect states that later information have more importance to the subject. Depending on setup, task, and subject, one of the effects is predominant. [Schab and Crowder, 1988; Hellström, 2003; Patching et al., 2008]

The procedure of the first human factor experiment was divided into two parts.

a) Visual acuity tests and questionnaire
b) Spotlight evaluation

a) Visual acuity tests and questionnaire
The visual acuity, contrast vision, and color vision ability of the subjects were tested. The visual acuity and contrast vision were tested with the contrast sensitivity test of

the Freiburg Visual Acuity Test [Bach, 2006]. The color vision acuity was tested with the Fransworth-Munsell Dichotomous D-15 test [Farnsworth, 1943]. All participates had to pass all visual acuity tests to participate in the second part of the experiment, the evaluation of the spotlights.

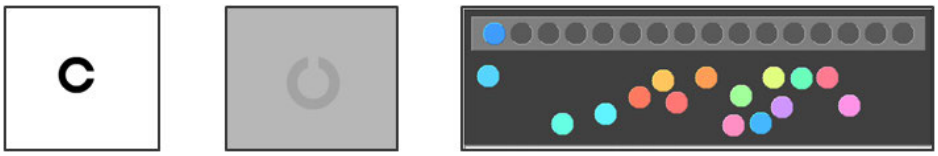

Figure 4.6: Vision acuity tests, left: visual acuity, center: contrast vision acuity, right: color vision acuity

In addition, the subjects had to answer several questions in a questionnaire. They should state general information about age, gender, and origin. They were asked about their experience in lighting engineering, illumination, and evaluation of light quality.

b) Spotlight evaluation

The second part of the human factor experiment was the evaluation of the far fields according to the 2AFC setup. Figure 4.7 shows the setup of the second part. The subject with unfixed head sat in front of the screen at a distance of about 2.2 m. The screen was a silver screen. The slide projector was positioned slightly behind the subject and projected the slides with the far fields onto the screen.

All sets of pairs were presented in the same way. The first spotlight was projected to the screen for four seconds, followed by a break of two seconds followed. During the break, only the background light was turned on to keep the subjects adapted to photopic vision. After the break, the second spotlight was shown at the same position and for the same duration of four seconds. Now, the subject had to make a choice with regard to the question: "Which spotlight looked more even regarding the color uniformity". The subject had to select spotlight one or spotlight two. They had to state the decision. Then, the next spotlight pair was shown successively.

Each subject had to evaluate 72 different spotlight pairs whereupon the procedure was divided into two parts. First, 36 spotlight pairs were shown, followed by a break of several minutes and then, the 36 spotlight pairs were shown again. The

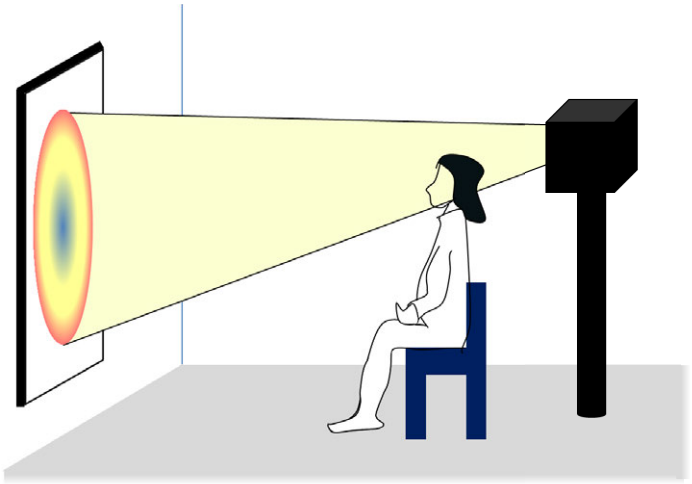

Figure 4.7: Experimental setup of the first human factor experiment, the observer sat in front of the screen where the spotlight appeared, behind the subject the slide projector and the background light was mounted

pairs in the first part were randomly chosen from all possible combinations of the 46 spotlights. One example of the first part could be the spotlight pair 1st: 1-2, 2nd: 30-46, 3rd: 9-4, ..., till 36th pair. In the second part, the same spotlight pair combinations were shown but the other way around: 2-1, 2nd: 46-30, 3rd: 4-9, ..., till 36th pair. This enabled the differentiation between real preference of the subjects and any arbitrary choice. The procedure was chosen to avoid systematic time order errors and bias in the selection of the spotlights.
Three observers had to evaluate the same spotlight pairs in the same order. The next three subjects saw another combination of pairs, e.g. 1st: 15-1, 2nd: 9-15, 3rd: 46-45, ..., till 36th pair and in the second part the other way around, 1st: 1-15, 2nd: 15-9, 3rd: 45-46, ..., till 36th pair. By a total number of 75 observers, there were 25 different groups formed each with different combinations. In total, 900 spotlight pairs were compared. Not all theoretically possible spotlights could be compared. The number of pairs was limited to stay at a manageable number of subjects. Therefore, the 46 spotlights were analyzed with the basic function $du'v'_{wa}$ (Formula 2.17 on page 32). The function $du'v'_{wa}$ was selected because it is used in optical simulation tools. The spotlights were sorted after $du'v'_{wa}$. Only spotlights which were next to each other in the range of ± 19 were combined as pairs.

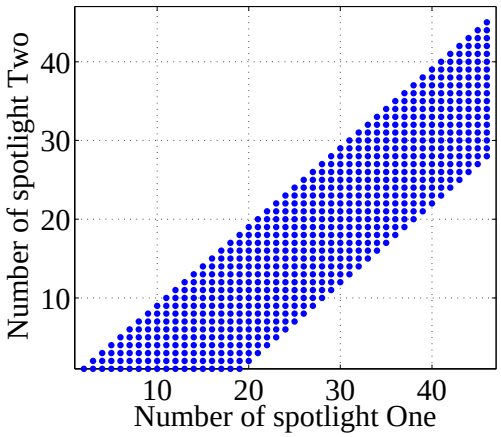

Figure 4.8: Combination of spotlight pairs for the first human factor experiment

All spotlight pairs evaluated in the experiment were marked in Figure 4.8. As an example, spotlight 23 was paired with spotlights from number 4 to 42. Spotlights further away according to this preliminary sorting were not compared. It was assumed, that these spotlights were clearly distinguishable form each other, proven by preliminary tests. However, with these diversified spotlight pairs, a wide range of color and patterns combinations could be evaluated against each other.

4.2.2 Results of the 1st Experiment

75 subjects took part in the first human factor experiment. They were aged between 23 and 60 years with a median of 35, there were 22 females and 58 males. One part of the experiment was executed in the Osram Corporated Technology department in Regensburg, Germany with 50subjects and the other 25 were from the Technical University Madrid (UPM), Spain.
Most of the subjects were experienced with lighting and had good knowledge in illumination technologies (50 subjects), the other had no or very little knowledge about lighting engineering. Many subjects (39) had experiences with the evaluation of light quality or spotlights.

The answers of the subjects were used to analyze the following two aspects of the human factor experiment before the main aspect, the calculaiton of the perceived

rank order and its correlation with mathematical descriptions, is presented.

a) Analysis of response behavior
b) Analysis of the four parameters: chroma level, hue, pattern and symmetry

a) Analysis of the response behavior
In general, the analysis of the response behavior showed a large number of spotlight pairs which were clear to the subjects. This means, the subjects selected the same spotlight as more even independent of its serial position. If five out of six subjects had selected the same spotlight, the pair was assumed to be clearly different. Otherwise, the preferences of the subjects were not unique. The response behavior of all subjects is presented in Figure 4.9.

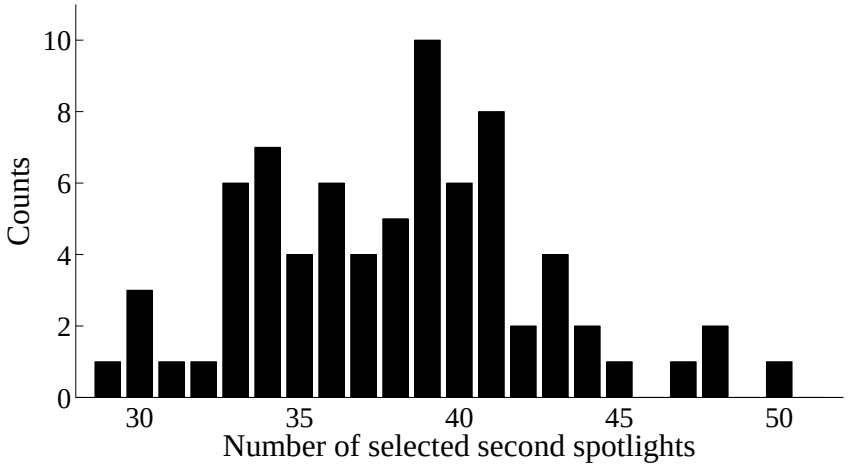

Figure 4.9: Response behavior of the subjects: number of selected second spotlights out of 72 pairs

The diagram shows the number of selected second spotlights.

If no response bias had occurred and all spot lights pairs had been clearly distinguishable, all subjects should have selected 36 times the second spotlight. In total, 72 spotlight pairs were shown, each spotlight once at the first position and once at the second position. The 48 subjects tended to select the second spotlight more often, only 21 subjects tended to select the first spotlight more often. The effect influenced the results just slightly, it increased the number of unclear pairs. However, most answers were consistent, subjects often selected the same spotlight

independent of its serial position. On average, 70 % of the answers of one subject were consistent and 64 % of the answers of one group ($\alpha = 0.05$). The accordance between consistent answers of subjects and consistent answers of a group indicated a good conformity in the perception of color uniformity in spotlights.

There were also several spotlight pairs which could not be distinguished clearly by the subjects. Either subjects selected both spotlight or the group was not consistent. On the one hand, two spotlights almost free of colors could often not be distinguished. Evidently the difference between the two spot was too small to be recognized and memorized. Hence, the subjects had to make an arbitrary choice. On the other hand, clearly colored spotlights could not be kept apart from each other. The subjects made again an arbitrary choice because both spotlights were unacceptable. However, the large number of discriminable spotlights made it possible to define the perceived rank order.

b) Analysis of the four parameters: chroma level, hue, pattern and symmetry
The four parameters described in Table 4.1 on page 49 were used to search for preferences of colors and patterns. The ordinal scaled parameters were tested with the Kruskal-Wallis test and the nominal scaled parameters were tested with the Wilcoxon signed rank test.

The Kruskal-Wallis test [Kruskal and Wallis, 1952] is a statistical non-parametric test to verify the variance of two independent samples by their rank positions. As a non parametric test, it does not assume normal distribution of the residuals. The Kruskal-Wallis test was performed with two parameter chroma level (1-3) and number of hues (1-3). The null hypothesis H_0 stated that there is no difference between the values of the parameters. If the null hypothesis had been rejected, there would be a significant difference between the values of the groups. At least one parameter would be dominating the other.
The results of the Kruskal-Wallis test are presented in Table 4.2 at a α level of 0.05. In a hypothesis test, the α level signified the maximum acceptable risk to reject a true null hypothesis. The results of the Kruskal-Wallis test were represented by several values. The median indicated the median value of the answer ratio for the pairs. The higher the median was the better the perception because more subjects selected spots with this value of the parameter. The rank was the average rank out

of 1800 ranks (2 times 900 showed pairs). High rank value indicates a preference of subjects, low rank values indicate rejected values. The z value described the relative position of the parameter value to the entire distribution normalized to the standard deviation. Negative z value signified that the value was below the average of all values of one parameter (regarding the ratio of preferences of this value, 0..6). Positive z value signaled that the value was higher than the mean value of all.

Table 4.2: Results of the Kruskal-Wallis test of chroma level 1-3, $\alpha = 0.05$

Value nr.	Value of parameter	Median	Rank	z value
1	Low chroma	4	985	8.08
2	Mid chroma	3	865	1.50
3	High chroma	2	665	-10.26

Table 4.2 presents the Kruskal-Wallis test results for chroma levels. The answers related to the chromaticity level showed significant difference in the evaluation. The subjects perceived the spotlights with lower chroma level more uniform than spotlights with higher chroma levels independent of all other parameters. The median of the different chroma levels were in accordance with the rank position and z value.

The parameter of number of hues inside the far field was analyzed with the Kruskal-Wallis test.

Table 4.3: Results of the Kruskal-Wallis test of number of hues 1 to 3, $\alpha = 0.05$

Value of parameter	Number	Median	Rank	z value
1 Red	1	1	643	-9.85
2 Blue	1	4	1038	4.49
3 Red-Blue	2	3	842	0.08
4 Blue-Yellow	2	4	1036	6.55
5 RGB	3	3	888	1.52

There was a difference between the values of the parameter hue but it was not correlated with the number of hues in the spotlight. Red and red-blue patterns were less preferred than blue or blue-yellow spotlight. It was not important for

the preference of the subjects if the spotlight contained one hue or several hues. The change of this parameter did not influence the preferences of the subjects much. Spotlights with only red color were clearly rejected. This was also caused by the pattern of three dots which was combined with the hue red. The direct comparison of the same pattern with red and another color did not show any significant rejection of red. The chroma in the distribution was more important for evenness perception than the total number of hues.

The parameters of pattern and symmetry were analyzed with the Wilcoxon signed-rank test [Wilcoxon, 1945]. It is a non-parametric test to verify a hypothesis by comparing two related samples with each other. H_0 stated the assumption that there was no difference between the two samples. The H_0 would be rejected if there was a difference between the two populations of the two samples after their ranking.
First, the difference in the preference for rotational symmetrical and non symmetrical color distributions was significant at $\alpha = 0.05$. Subjects clearly preferred patterns with rotational symmetry ($p = 8.3 \cdot 10^{-24}$, $p < \alpha$). The rotational symmetrical patterns were judged to be more even regarding the color uniformity.
The pattern analysis was not obvious. The patterns with three dots were perceived worst, followed by spotlight with one central dot. All patterns with rings (one or multiple) were preferred over dot patterns ($p = 0.0075$, $p < \alpha$). There was no significant difference between the various ring patterns ($p = 0.1725$, $p > \alpha$). Furthermore, the more the colors and patterns were concentrated in the center of the spotlight the more it was disturbing the perceived evenness.

In summary, spotlights with low chroma, rotational symmetry and rings were preferred by subjects, see Figure 4.10 a. Uneven perceived spotlights consisted mainly of high chroma, dots, or non rotational symmetries, see Figure 4.10 b.

4.2.3 Calculation of the Perceived Rank Order

The perceived rank order was needed to correlate the basic functions and weighted functions with the visual perception of color uniformity in the far fields. Based on

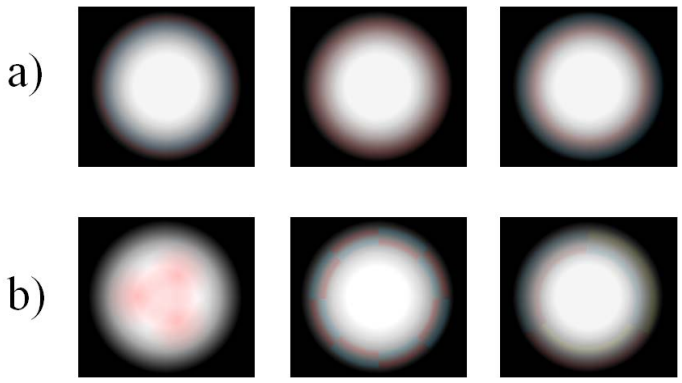

Figure 4.10: Comparison of preferred (a) and rejected (b) spotlights

the perceived rank order, the merit function was derived to objectively describe the color uniformity in spotlights. The order resulted from all answers of all subjects and reflected the order of spotlights after perceived evenness from even to uneven. The 2AFC setup enabled the calculation of the perceived rank order using the law of comparative judgment by Thurstone [Thurstone, 1927]. Other possibilities to estimate and calculate scale values for stimuli from a paired comparison experiment were the least square method by Bradley-Terry's logistic model [Bradley and Terry, 1952] or likelihood estimations.
The law of comparative judgment is defined as a method to determine a scale of stimuli which were not directly measurable. It describes the probability of how one stimulus is dominated at the ratio of another stimulus. One stimulus X is caused by an external object I, each stimulus with its own expected value μ_X and standard deviation σ_X. The expected values μ_i for each stimuli X_i are different but the standard deviations σ are assumed to be equal. The assumption of normal distribution enables the calculation of the perceived difference of two stimuli.

$$\Delta X = X_1 - X_2 \tag{4.1}$$

$$\Delta\mu = \mu_1 - \mu_2 \tag{4.2}$$

$$\sigma_\Delta^2 = 2\sigma^2 \tag{4.3}$$

The probability $P(X_2 > X_1)$ is reached by the distribution function of the normal distribution $F(z)$. The z score represents the differences of the value to the mean of

the population.

$$P(X_2 > X_1) = p_{12} = 1 - F(z_{12}) \tag{4.4}$$

$$= 1 - \frac{1}{\sqrt{2\pi}} \cdot \int_{-\infty}^{z_{12}} exp(-z^2/2)dz \tag{4.5}$$

The application of the inverse function F^{-1} results in the values z_{12}. The value z_{12} represents the difference between two objects I_1 and I_2.

$$z_{12} = F^{-1}(1 - p_{12}) \tag{4.6}$$

$$= (\sqrt{2}\sigma)^{-1} \cdot (\mu_1 - \mu_2) \tag{4.7}$$

To create the latent scale, several estimations for objects I_i are necessary. For the number of k objects (I_1, ..., I_k) with the comparison of each object with all other objects, a matrix $k \times k$ contain the dominated probability p_{ij} and the corresponding matrix with z_{ij}. The z-score $\overline{z_i}$ on the latent scale is calculated by summing up the row values in the z_{ij}-score matrix.

$$\overline{z_i} = \frac{1}{k} \sum_{j=1}^{k} z_j \tag{4.8}$$

$$= \frac{1}{k} \sum_{j=1}^{k} \alpha(\mu_i - \mu_j) \tag{4.9}$$

$$= \alpha \cdot \mu_i - \frac{\alpha}{k} \sum_{j=1}^{k} \mu_j \tag{4.10}$$

The α replaces $(\sqrt{2}\sigma)^{-1}$. The linear transformation of the subjective expected value μ_i is represented on an interval scale. As a result, not direct measurable stimuli X_i which are normal distributed with same variance and able to map onto a continuum, are represented by a interval scale only by an ordinal comparison. The important assumption of normal distribution of the answers of the subjects is needed for the scale but it is not possible to proof the assumption by observation. In general, it is assumed that each observer has a continuous preference for each of the two stimuli, both of these preferences are normally distributed over the entire population.

4.2.4 Correlation of Basic Functions

The sorting of the spotlights after their $\bar{z}$ values represented the perceived rank order. The $\bar{z}$ values were used to calculate the correlation between the basic functions (see section 3.1 on page 35) and weighting functions (see section 3.2 on page 41) and the perception of color uniformity in spotlights.
The correlations were expressed in terms of Pearson's and Spearman's correlation coefficients. Pearson's correlation coefficient r_p is used to express the linear correlation between two vectors. Spearman's rank correlation coefficient r_s describes a non linear monotonic correlation between the perceived order and the hypothetical order to be comparable, the data have to be pair wise ranked and based on ordinal or interval scale. The values of the correlation coefficients can be assigned to the following expressions of correlation levels. [Kvam and Vidakovic, 2007]

Table 4.4: Correlation levels

Correlation coefficient	Description
1 - 0.9	very strong
0.9 - 0.7	strong
0.7 - 0.4	moderate
0.4 - 0.2	weak
0.2 - 0	very weak

The correlation between the basic functions and the perceived rank order is presented in Table 4.5, it shows the correlation coefficients for Pearson's r_p and Spearman's r_s correlation coefficients.

Table 4.5: Correlation coefficients of the basic functions with $\bar{z}$ values

Correlation	E_{max}	dab	$Grad_{ab}$	S_{rad}	S_{lin}
r_p	0.64	0.72	0.71	0.63	0.64
r_s	0.64	0.75	0.82	0.60	0.60

The analysis of the correlation coefficients showed similar results for r_s and r_p, except for $Grad_{ab}$. All correlation coefficients were positive values, so low function values represented even far fields and high function values represented non-uniform far fields. For further analysis, Spearman's correlation coefficient r_s was

used because the correlation was not limited to a linear correlation. It was more important to generate a suitable rank correlation between the perceived order and the designated merit function.

Weakest correlations were reached by functions S_{rad} and S_{lin}. They represented smoothness of spatial color distribution in radial and axial direction. There was a correlation with the perceived rank order but several spotlights did not fit. The basic function E_{max} reached a slightly better correlation. But the value did not hold any information about the spatial color distribution in the spotlight. It was completely independent of the distance between the two pixels and the color distribution in between. Strong correlation was reached by function *dab* and best correlation was reached by $Grad_{ab}$. Both basic functions represented the visual perception of the tested spotlights in an adequate way. Figure 4.11 shows the progression of four basic functions dependent on the $\overline{z}$ values of the perceived rank order.

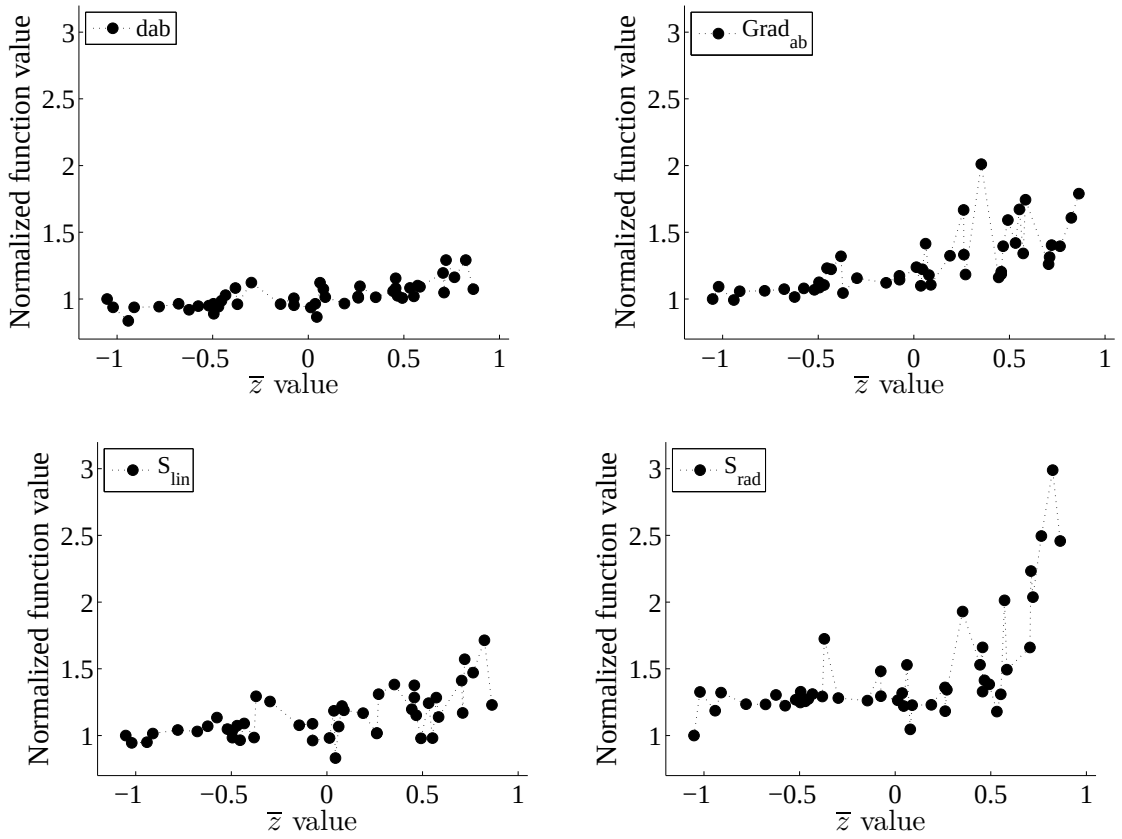

Figure 4.11: Comparison of the $\overline{z}$ values of four basic functions

It can be seen that the functions had a decent correlation with the perceived

color uniformity but there are systematical over- or underestimations of specific colors and patterns. Each basic function was created to represent different visual influencing factors and clearly one function alone cannot correctly rank the spots according to the perceived rank order. Table 4.6 shows the relationship between several visual influencing factors and the basic functions.

Table 4.6: Link between basic functions and visual influencing factors

	Basic function				
	E_{max}	dab	$Grad_{ab}$	S_{rad}	S_{lin}
Hue	X	X			
Contrast	X	X			
Chroma			X		
Shape			X		
Axial symmetry					X
Radial symmetry				X	

None of the functions combined all visual influencing factors. The visual influencing factors which were not included in the basic function could lead to systematical aberration with regard to colors and patterns.
The basic function *dab* evaluated single colored ring and dot patterns in spotlights differently from the visual judgment by subjects. Single ring patterns (Figure 4.12, 1), which were on position 1 and 16 at the perceived rank order, were places at position 21 and 36 according to *dab*. The spotlights were underestimated regarding the perceived color uniformity. Although the colored rings at the edge of these spotlights could be relatively colorful and saturated, the subjects did not perceive them as uneven as predicted by *dab*.

The functions for symmetry detections S_{rad} and S_{lin} had also systematical errors. S_{rad} overestimates the color uniformity of unique colored ring patterns since it was only sensitive to radial changes of colors. The function value was low for spotlights with unique colored rings, which had no color change on radial directions. Therefore, the estimation errors occurred, and the positions of those spotlights in the perceived rank order was worse than the estimation of the function S_{rad} (Figure 4.12 1, 2). Actually tested spotlights were on the perceived rank order on position

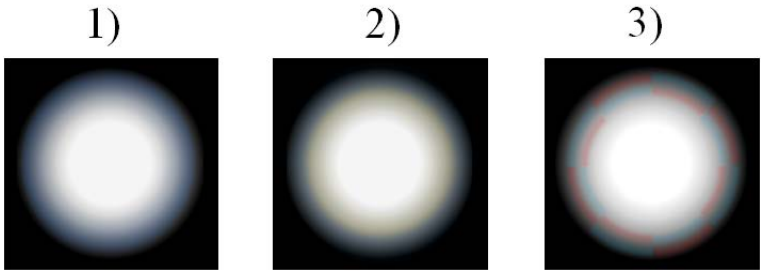

Figure 4.12: Typical patterns for over- and underestimation of the basic functions

28 and 38, whereas the calculated function values of S_{rad} would be at position 4 and 23.
The behavior of the function S_{lin} was opposite to S_{rad}. It was not sensitive to radial color changes, it reacted only on axial color changes. Thus, spotlights with multi-colored rings (Figure 4.12, 3) were overestimated. The calculated function value of color uniformity would be too low because the color changes in radial direction were not detected.

Especially these parameters which were not included in the function but described an important visual impact in the spotlight occurred as outliers of the basic functions. There were no basic functions which handled all visual influencing factors. Therefore, one basic single function was not recommended to be used as a merit function for a wide range of different spatial color distributions in spotlights.
However, there were further possibilities to improve the correlation of basic functions with the visual perception. The pre- and post-processing functions (see on page 41) were applied to the basic functions.

Table 4.7: Possibilities to weight the basic functions and change their thresholds

Weighting	E_{max}	dab	$Grad_{ab}$	S_{rad}	S_{lin}
Luminance		X	X		
Cumulative distribution function (CDF)		X	X	X	X

Table 4.7 lists several possible combinations of basic functions and weighting functions. It was possible to apply the weighting functions to all basic functions except E_{max}. The luminance weighing would be implemented during calculation by

scaling the chromaticity coordinates of the test point with their luminance value. The cumulative distribution function (CDF) would be applied as post-process to change the threshold of the function value. The correlation of *dab* and $Grad_{ab}$ were highest with the perceived rank order, thus these functions were tested with the weighting functions. Some correlation coefficients of the basic functions *dab* and $Grad_{ab}$ are shown in Table 4.8

Table 4.8: Spearman's correlation coefficients r_s for selected weighted basic functions

	dab	$Grad_{ab}$
Basic function	0.75	0.82
Luminance weighting	0.72	0.77
CDF 0.3 %	0.67	0.45
CDF 0.6 %	0.71	0.82
CDF 0.9 %	0.67	0.60

As seen in Table 4.8, the correlation could not be improved by weighting the basic functions. The weighted functions do at their best reach the same correlation coefficient as the basic functions but without further improvements. In conclusion, there is no evidence that the luminance influences the way these spotlights are perceived.

Figure 4.13 shows the progression of four weighted basic functions. In most cases the behavior at the beginning for even perceived spotlights was sufficient. The accordance to higher $\bar{z}$ values degraded. There are large deviations from the trendline of the function and there was no clear trend identifiable. Especially for the weighted gradient function the performance decreased. Except E_{max}, the basic functions calculated an average value according to their definition, this seemed to match the visual perception most.

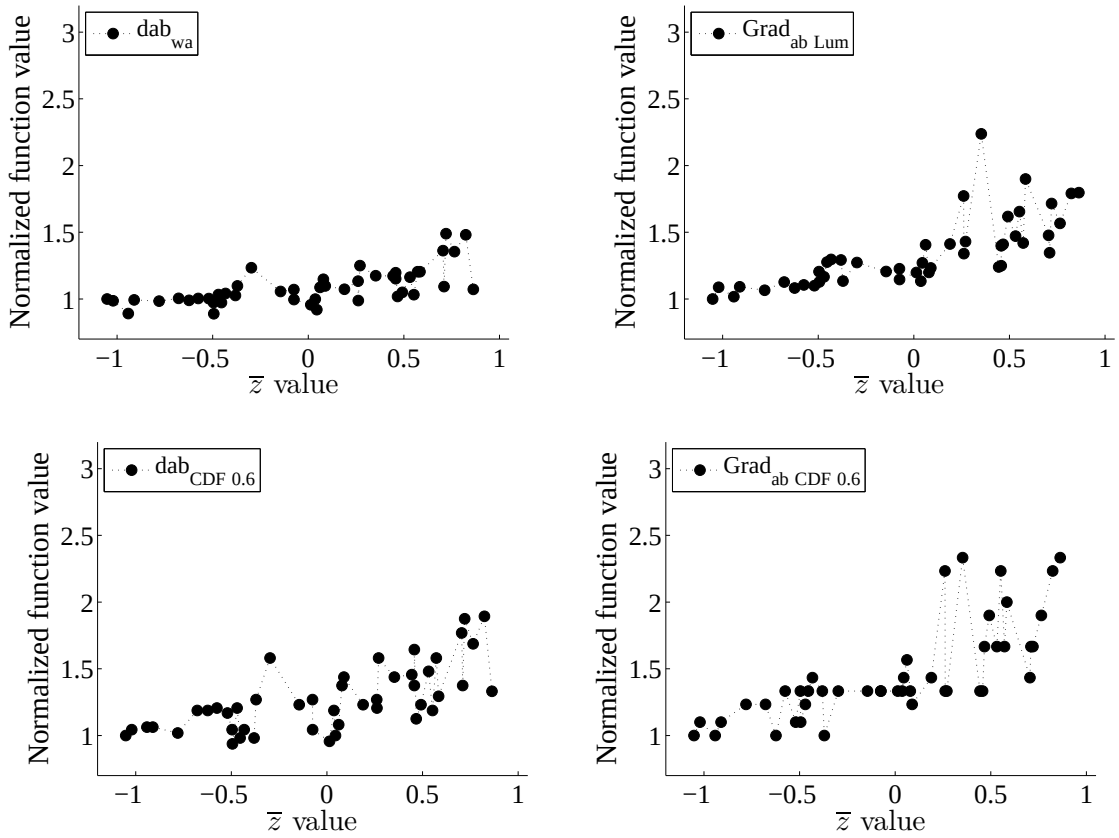

Figure 4.13: Comparison of four weighted basic function

4.2.5 Merit Function for Color Uniformity

As seen in the previous analysis, an implementation of many visual influencing factors becomes necessary to fit the visual perceived rank order. Many visual influencing factors were combined to derive a merit function with a more reliable prediction of the perceived color uniformity. A linear regression based on the presented basic functions was proceeded.

The regression analysis provides a connection between several independent variables. It can be used to describe relations in a quantitative way. The regression analysis is applied to predict values out of x without knowing the y by the regression model received relation. The received function allows the calculation of the y value only from the x value. In general, the regression model is described as

follows.

$$F = f(x_1, x_2, ..., x_n) + \epsilon \tag{4.11}$$

With F as the regression model, f the function and ϵ is the residuum of the model. One specific application of the regression analysis is the linear regression. The linear regression assumes that the data have a linear relation between the dependent and independent variable. Hence, homogeneity of variance is required to combine several functions. The linear regression considers only a linear function F and results from a linear system of equations, called multiple linear regression.

$$F = \beta_1 x_1 + \beta_2 x_2 + ... + \beta_n x_n + \epsilon \tag{4.12}$$

The β_n coefficients are determined by minimization of the residuum ϵ. The method to minimize ϵ depends on the model, e.g. least squares or other robust methods. After the derivation of the linear regression model, a validation of the model is required. This proves, if the linear regression model is an adequate description of the relation.
The merit function for the color uniformity was called U_{sl} (Color Uniformity of Spotlights). The multiple linear regression for the color uniformity in spotlights is expressed as follows.

$$U_{sl} = \beta_1 \cdot f_1(a^*, b^*) + \beta_2 \cdot f_2(a^*, b^*) + ... + \beta_n \cdot f_n(a^*, b^*) \tag{4.13}$$

It should describ the perceived color uniformity level in spotlights. Table 4.6 on page 65 showed that at least the four functions dab, $Grad_{ab}$, S_{rad} and S_{lin} were necessary to consider all main visual influencing factors in the merit function.

$$U_{sl} = \beta_1 \cdot dab + \beta_2 \cdot Grad_{ab} + \beta_3 \cdot S_{rad} + \beta_4 \cdot S_{lin} \tag{4.14}$$

The coefficients β_1 to β_4 were optimized by least squared method to reach the best possible correlation with the perceived rank order. In addition, the basic functions were adapted to the same slope in a linear regression of type $y = m \cdot x + n$ to estimate the influence of each single basic function. Table 4.9 lists the four basic functions with the linear regression. The function $Grad_{ab}$ had the largest increase, indicated by m. The other basic functions were adapted to the increase of $Grad_{ab}$.

Table 4.9: Linear functions of basic functions

	$y = m \cdot x + n$
dab	$y = 0.011 \cdot x + 1.365$
$Grad_{ab}$	$y = 0.027 \cdot x + 2.474$
S_{rad}	$y = 0.019 \cdot x + 0.574$
S_{rad}	$y = 0.017 \cdot x + 1.214$

Table 4.10 shows the normalized basic functions y_{normed} to the same slope and with $n = 0$.

Table 4.10: Linear regression of basic functions and adaptation to the same slope of $Grad_{ab}$

	$y_{normed} =$	$(x_i - n(x)) \cdot (m(grad_{ab})/m(x))$ $+n(x) \cdot m(grad_{ab})/m(x)$
dab	$y =$	$dab_i \cdot 1.36 \cdot (0.027/0.11) + 3.41$
$Grad_{ab}$	$y =$	$Grad_{ab\ i} \cdot 2.47 \cdot (0.027/0.27) + 2.47$
S_{rad}	$y =$	$S_{rad\ i} \cdot 0.57 \cdot (0.027/0.19) + 0.84$
S_{rad}	$y =$	$S_{rad\ i} \cdot 1.21 \cdot (0.027/0.17) + 1.91$

Figure 4.14 shows the four normalized basic functions. In comparison to Figure 4.11 on page 64, the functions were more congruent to each other, and they did not show different slopes.

The normalized basic functions were used for the linear regression. Figure 4.15 presents the results of the linear regression (Formula 4.14) with the coefficients $\beta_1 = 2.5$, $\beta_2 = 8.0$, $\beta_3 = 3.0$, and $\beta_4 = 1.0$.

$$U_{sl} = 2.5 \cdot dab + 8.0 \cdot Grad_{ab} + 3.0 \cdot S_{rad} + 1.0 \cdot S_{lin} \tag{4.15}$$

The *dab* function described the average of the differences from each pixel to reference color. The reference color was the average color of all pixels included in the calculation. It referred to general visual perception of the complete spotlights. Function $Grad_{ab}$ was the summation of the difference between neighboring pixels. It was a criterion for the contrast in the spotlight in color plane. The functions S_{rad}

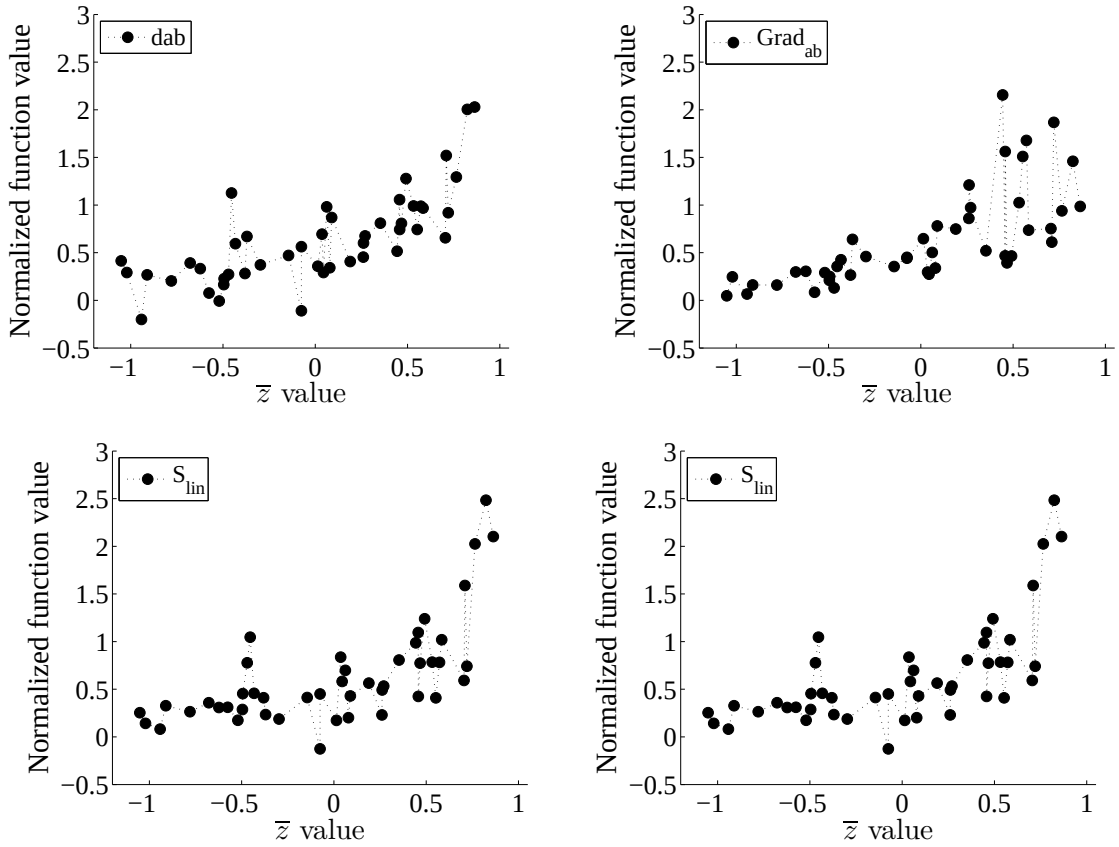

Figure 4.14: Basic functions with same slope used for liner regression

and S_{lin} described the smoothness of the spots in radial and axial direction. S_{rad} was related to rotational symmetry which is important for object detection in vision. A very strong correlation of $r_s = 0.934$ was reached.
The data for calculation include the luminance cutoff, noise reduction, contrast sensitivity function filtering, and same slope of the basic functions. In comparison to the basic functions, the correlation was clearly improved and reached a very strong correlation with the visual perception. The linear regression resulted in an adequate description of the visually perceived color evenness of the far field of spotlights. The function trend was more precise with less outliers of systematical aberrations. Low merit function values indicated better color uniformity and higher merit function values represented poorer color uniformities.

Further validations and statistical discussions with regard to the merit function U_{sl} is presented in section 5 on page 87 in combination with the absolute scale of U_{sl} resulting from the second human factor experiment.

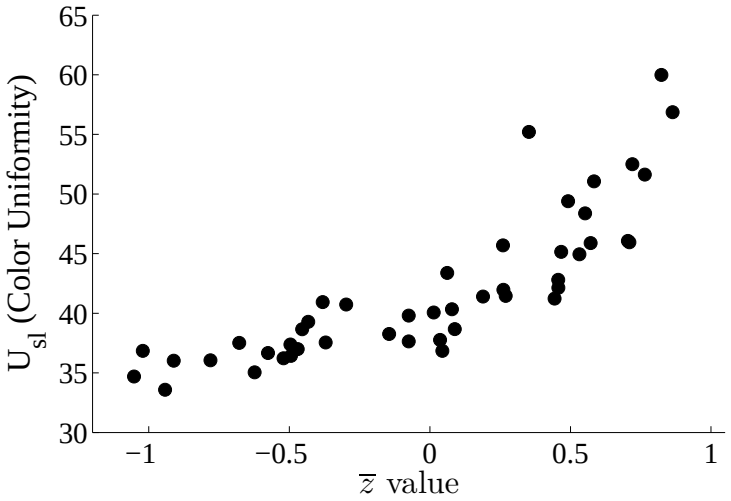

Figure 4.15: Color uniformity of spotlights $\overline{z}$ values of the perceived rank order

4.3 Grading the Impression of Spotlights

The first human factor experiment was proceeded to define the perceived rank order of the presented spotlights and to derive the merit function. The same spotlights were used to investigate the visual perception of spotlights further in a modified experimental setup and procedure
The $\overline{z}$ values of the first experiment enabled a prediction of the color uniformity level but it were not related to the visual impression of excellent or insufficient color uniformity in the far field of spotlights. A definition of thresholds for excellent to insufficient color uniformity level was required to apply the merit function U_{sl} to measurements and optical simulations and to make a prediction about the visual impression of the spotlight. Furthermore, the second human factor experiment investigates the perception during changed environmental conditions.

4.3.1 Setup of the 2nd Human Factor Experiment

The setup of the second human factor experiment was similar to the setup of the first human factor experiment (see Figure 4.7 on page 55). In this experiment, the question was about the entire impression of the spotlight appearance. The subjects

had to grade their impression on a rating scale.
In the second human factor experiment 48 subjects form the first human factor experiment took part. Thus, no visual acuity tests were required. The experiment started with an introduction about the procedure. A test procedure followed. The subject saw several spotlights with various color uniformity levels. The subject could evaluate the spotlights with the software and had time to clarify concerns. Afterwards, the experiment started. The subjects sat in front of the screen at a distance of 2.2 m, the slide projector imaged the spotlight towards the screen. Each spotlight was shown for four seconds. Then, the subject had time to evaluate this spotlight. The question was concerning the overall impression of the spotlight. To evaluate the spotlight, the subjects used a tablet computer. The user interface is shown in Figure 4.16. The subject had to decide between very good impression and very bad impression on a 7-point scale.

Figure 4.16: Evaluation software for the second human factor experiment (language: German)

After the subject graded the spotlights, the next spotlight was shown. Again, subjects were forced to give an answer for each spotlight. Altogether each subject had to evaluate 84 spotlights divided into two parts. The first part included the evaluation of all 42 spotlights on a white wall and the standard background light like in the first human factor experiment. In the second part the same spotlights were shown but under a different environmental setup and in a different order. Either the luminance level of the background light (Setup 2, Figure 4.17) or the white wall (Setup 3, Figure 4.17) was exchanged.

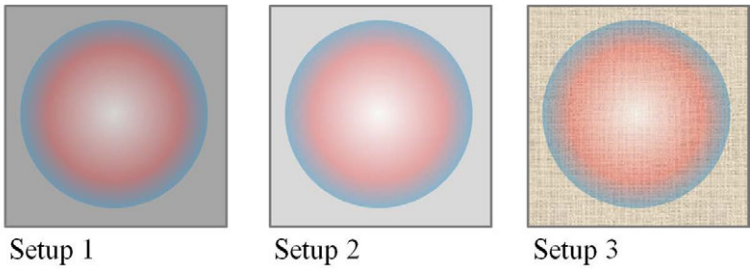

Figure 4.17: The difference between the three experimental setups, setu 1: standard environmental, setup 2: higher luminance level, setup 3: colored projection background

The first half of the subjects (1 to 24) evaluated the same spotlights but with a higher luminance level of the background light in the second part of the experiment (Setup 2). An additional LED lamp was turned on and the luminance level was increased by 30 % to the maximum luminance of 400 cd/m^2 of the reference spotlight. The other subjects (25 to 48) evaluated the spotlights on a colored wall in the second part of the experiment. Therefore, a panel of cotton fabric in beige color was hung down directly in front of the wall. The spotlights were projected onto this panel. Each subject saw another random order of spotlights to avoid systematical errors due to order and adaptation of the subjects. The presented spotlights were selected from the first human factor experiment and 26 of the 46 spotlights were used again. In addition, 16 new spotlight distributions were designed. The additional spotlights contained same patterns but in different color combinations, each combination again in three chroma levels.

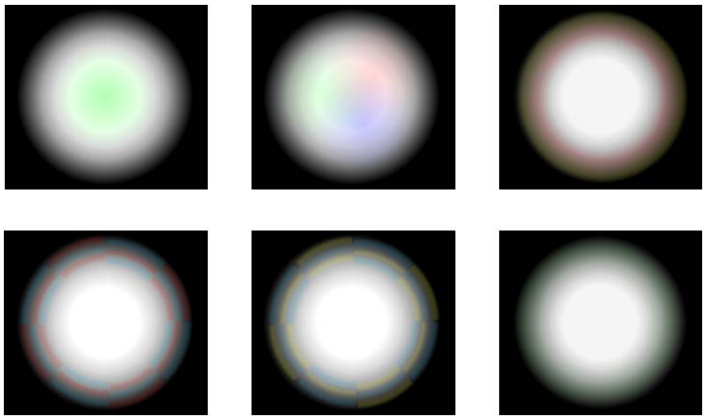

Figure 4.18: Additional presented spotlights with highest chroma level in the second human factor experiment

The new spotlight designs should enable further analysis of the preferences of subjects regarding defined colors and patterns. They made it possible to compare the perception between colors and patterns separately.
The additional experimental setups 1 and 2 were designed to change the appearance of the spotlights in a defined way. The aim was to analyze the visual perception of the same spotlights under slightly different conditions. Through the additional light source, the contrast of colors and patterns in the spotlights was reduced and better gradings were expected. The panel of cotton fabric changed only the appearance of the spot lights slightly and put a light structure inside the spotlights without contrast changing. The second human factor experiment showed the influence of modified spotlight appearances on the visual perception.
However, the main aspect of the setup was to determine a classification of the U_{sl} function. Form excellent to insufficient color uniformity a scale should enable a fast assignment of optical systems to color uniformity levels. A relation to the perceived impression of excellent or poor color uniformity in spotlights was applied to the U_{sl} values from the first human factor experiment.

4.3.2 Results of the 2nd Experiment

The evaluation of the response behavior of the subjects is

a) General evaluation of the response behavior
b) Evaluation of the three experimental setups
c) Comparison to the first human factor experiment

a) General evaluation of the response behavior
Starting with all answers during the human factor experiment, the analysis of all answers showed a large diversity. Overall, 69 % (33 out of 48) of the subjects used the entire grading scale from 1 to 7. But there were a notable number of subjects which avoided to grade spotlights with the best rating 1 or the worst rating 7 (15 %, 7 out of 48). Some subjects used 5 6% or 4 10 % rating values. Figure 4.19 shows the histogram of median grade (left) and the grade range (right) for all subjects. The left diagram indicates that most subjects had an average grading of 3 or 4.

Therefore the subjects used mainly the entire rating scale (right diagram)

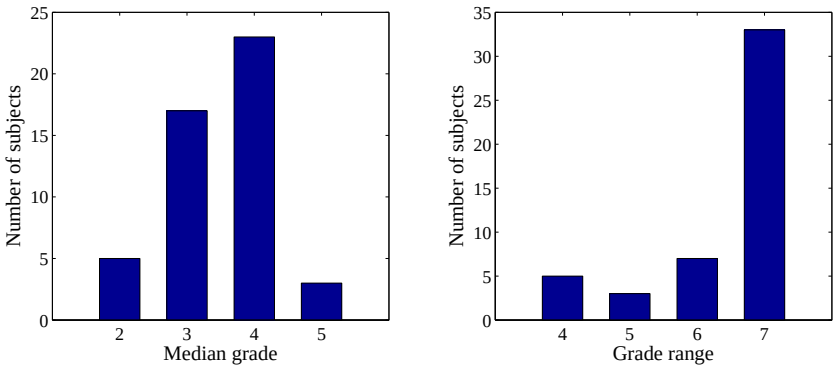

Figure 4.19: Median grade and grade range for all subjects

The median of the answers were mainly at 3 (36 %) and 4 (48 %), some tend to better ratings (10 %) or worse ratings (6 %). The mean of the rating scale was 4 and half of the subjects reached this rating value as their median value. But most of the subjects tended to give better grades to the spotlights.

The responsiveness of the subjects varied. They had different impressions of the spotlights on their own inherent scale. At the beginning of each session a sequence of spotlights was shown to the subjects that included excellent and insufficient examples of color uniformity. It should accustom the subjects to the light of spotlights and to the extent of the appearance of colors and patterns. Nevertheless, sensitivity and inherent scale differed from subject to subject.

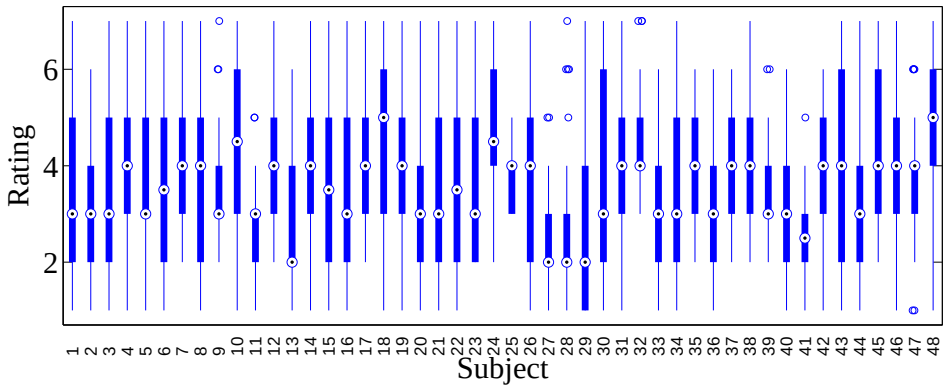

Figure 4.20: Distribution of given grades (1 to 7) to all spotlights from each subject (1 to 48)

Figure 4.20 shows the distribution of answers for each of the 48 subjects separately. The centered circle of each bar represents the median of grading. The bar indicates

the range from 25 % to 75 % of the answers, the 25th and 75th percentile. The thin line limits the answers within $\pm 2.7\ \sigma$, the outer unfilled circles are outliers, which do not fit within $\pm 2.7\ \sigma$ standard deviation (99.3 %) of the answers.
Subjects were able to distinguish between several spotlight appearances. Most of the spotlights reached a mean grade of 3 (38.1 %) or 4 (21.4 %). From the other spotlights 16.6 % reaches a grad 2, 14.3 % reaches a grad 5 and 9.5 % of the spotlights were assigned to grade 6. There was the tendency of the subjects to assign better ratings 1 to 3 (50.6 %) more frequently than worse ratings 5 to 7 (30.6 %), all other spotlights were assigned to 4 (18.8 %). Although most of the subjects used most gradings, the answers for one defined spotlight were rather different, see Figure 4.21. There were spotlights which got all grades from 1 to 7. It implied, that some of them thought this was an excellent spotlight and yet other thought it was a spotlight with poor color uniformity.

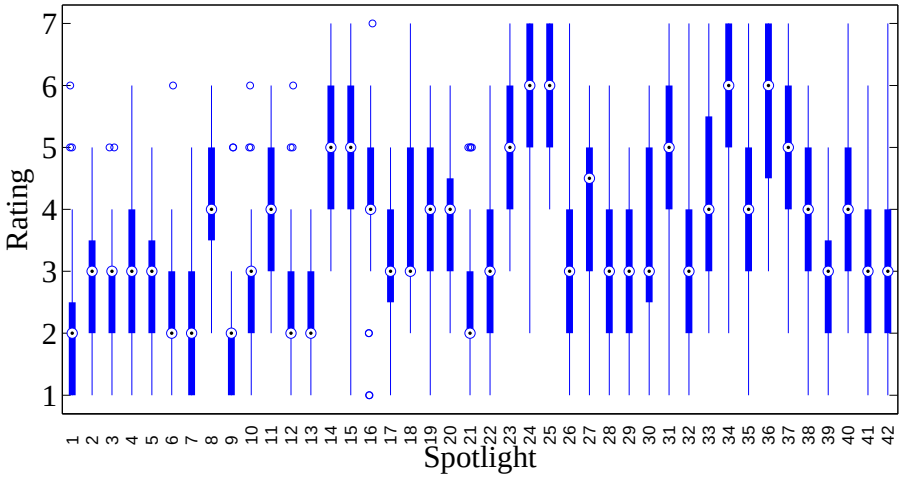

Figure 4.21: Grades for each spotlight in the standard environment

Although many subjects used a wide range of the scale, there were many spotlight with a large divergence in grading. There was only one spotlight (2.4 %) within $2.7\ \sigma$ which held only 3 grades. Most of the spotlights had a much wider range, 4 grades were valid for 24 % of the spotlights, a range of 5 grades for 26.2 % spotlights, a range of 6 grades for 33 % spotlights, and 14 % of the spotlight were evaluated with all grades from 1 to 7. The grading range could be limited to the evaluation of the $25th$ to $75th$ percentile. Now, there were 8 (19 %), 7 (16.7 %) and 24 (57.1 %) spotlights with a range of 1, 1.5, and 2, respectively. Only 3 spotlights (7.2 %) had a range of 3. There were no spotlights with larger grading range. This

showed that a least the half of the subjects allocated very similar or same grades to most of the spotlights in the standard environment. The difference between the gradings analyzed for $25th$ to $75th$ and 2.7σ is illustrated in Figure 4.22.

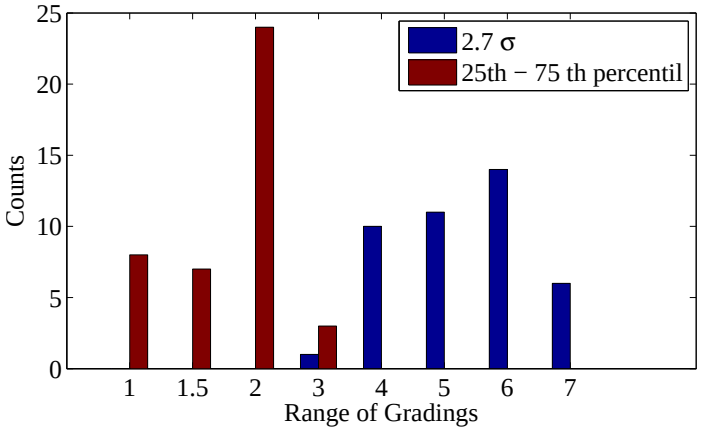

Figure 4.22: Comparison of grade range for 2.7 σ (blue) and 20th-75th percentiles (red) for all spotlights and all subjects

The red bars represent 50 % of the answers around the median, the blue bars represent the range of answers for spotlights within 99.3 %. The accordance of many subjects enabled the derivation of a scale for color uniformity levels.

b) Evaluation of the three experimental setups

In addition to the standards environment (setup 1) in the first half of the experiment, a modified setup was tested. Either the luminance level (setup 2) or the consistence of the projection wall (setup 3) was changed. Through the changed setups, the sensitivity of the subjects to different environments could be tested. The comparison of each grading of the subjects in the three different setups is shown in Figure 4.23.

The statistical analysis of the grading between setup 1 and setup 2 showed a significant difference. For the comparison of setup 1 and setup 3, no difference in grading was received.

Comparison of setup 1 and setup 2

The standard setup 1 was compared with second setup having an increased luminance level. An additional LED lamp increased the entire luminance level by 30 % of the maximum luminance in the reference spotlight. Thus, the contrast was

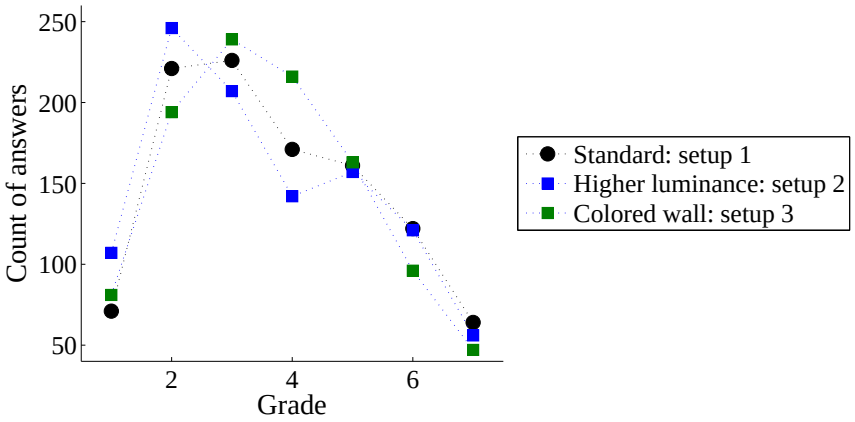

Figure 4.23: Comparison of answers for the different setups

reduced. The analysis of the answers showed a significant difference between the grading of the subjects.

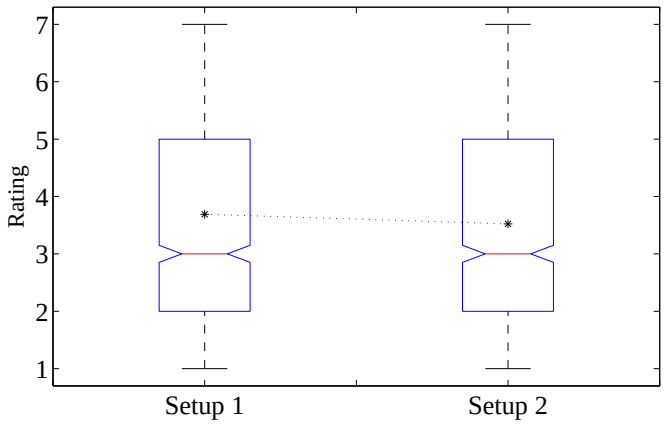

Figure 4.24: Comparison of median, average and standard deviation for setup 1 and 2

The boxplot (explained on page 77) represents the statistical analysis. The median of 3 for all gradings was the same for both setups, the mean changed from 3.69 for setup 1 to 3.52 for setup 2.

A t-test was used to judge the null hypothesis H_0 of no difference between the setups. It is a method to test statistical hypothesis of similarity of two samples and determines if means are significantly different. It assumes normal distribution of the data and follows the application of Student's t distribution for a small sample size and unknown standard deviation.

The t-test was significant at $p = 0.012$ at $\alpha = 0.05$, $p < \alpha$. There was a difference in gradings of the subjects for setup 1 and setup 2. The nonparametric Mann-Whitney

U test resulted as well in significant difference between the two setups at $p = 0.018$, $p < \alpha$. In contrast to the t-test it did not assume normal distribution. Therefore the Mann-Whitney U test was preferred. The improved evaluation of the spotlights was also represented by U_{sl} values of the spotlights of setup 2.

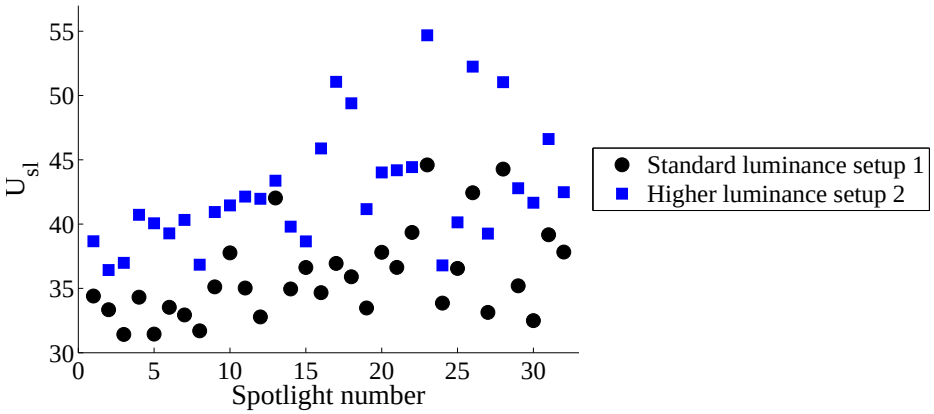

Figure 4.25: Comparison of U_{sl} values of spotlights for setup 1 and setup 2

Figure 4.25 presents U_{sl} values of spotlights for the standard setup 1 (black circles) and the second setup 2 (blue squares). Most U_{sl} function values for setup 1 were higher than in setup 2. The merit function evaluated spotlights in setup 2 at higher luminance more uniform than in setup 1. Through the additional lamp, the contrast between the background and the foreground was reduced. Subjects graded the spotlights in setup 2 also better. The calculation of the U_{sl} function values were in accordance with the visual impression of subjects.

Comparison of setup 1 and setup 3

The second half of the subjects had to evaluate the spotlight on a panel of cotton fabric. It had a slightly beige color with waving pattern. There was no significant difference in rating of the subjects between setup 1 and setup 3. The subjects evaluated the spotlights in the same way, they did not see any differences between the standard setup 1 and setup 2 with structured background.

Figure 4.26 presents the statistical analysis between answers of setup 1 and setup 3. Although the median changed from 4 to 3, there was no significant difference in the gradings of the subjects. The mean of setup 1 (3.66) was very similar to

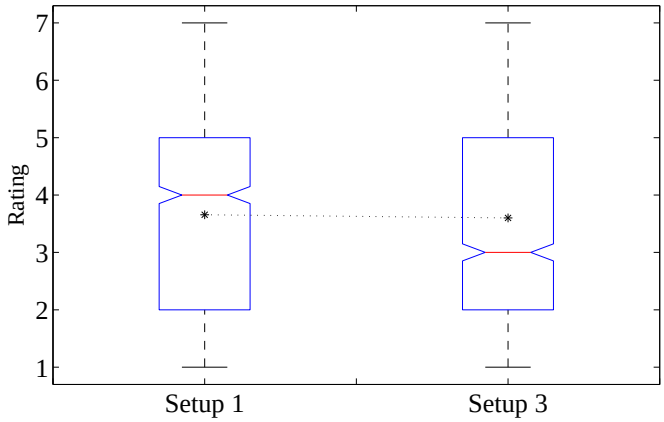

Figure 4.26: Comparison of median, average and standard deviation for setup 1 and setup 3

setup 2 (3.60). The two sampled t-test reached $p = 0.775$. The null hypothesis that there was no significant difference between the two samples could not be rejected at $\alpha = 0.05$ ($p > \alpha$). The Mann-Whitney U test resulted in $p = 0.584$ ($p > \alpha$) and H_0 could not be rejected.
There were some imperfections in the wall and slightly changed color but it did not influence the perception of the spotlights much. However, the contrast between background and foreground as well as the color and pattern contrast in the spotlight remained the same. Thus, the rating of the subjects for both setups was similar. The perception of colors was independent of slightly structured background.

c) Comparison to the first human factor experiment
The responds of the standard environment in setup 1 were compared with the function values of U_{sl} to define levels for perceived excellent to insufficient color uniformity. Figure 4.27 presents the comparison between the results of the first experiment and the setup 1 of the second experiment. The merit function values U_{sl} of the first human factor experiment were compared with the median of the evaluation for spotlights in the second human factor experiment.

The accordance between the first and the second human factor experiment was principally consistent. The merit function was optimized to fit the data from the first human factor experiment and was then applied to the median values of the grading of the subjects.

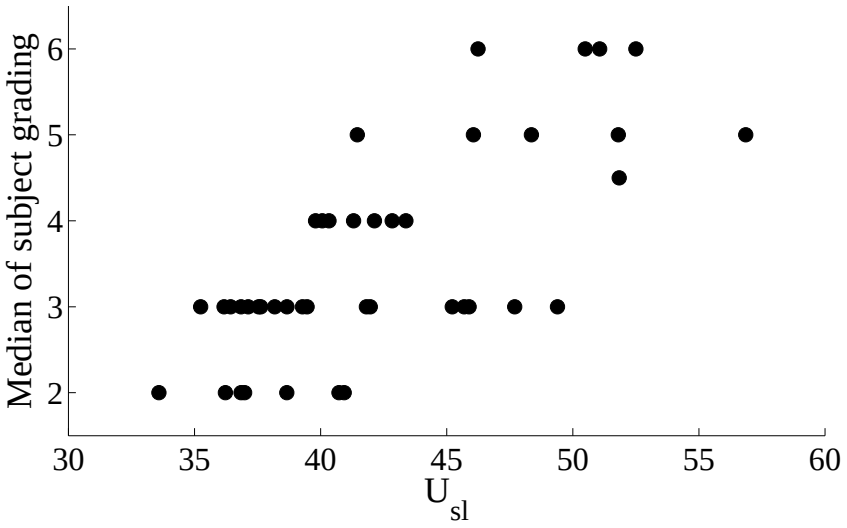

Figure 4.27: Comparison of color uniformity U_{sl} and subject grading

The first human factor experiment explicitly asked about the color uniformity of successive shown spotlights, the second human factor experiment asked about the impression of one spotlight. The question was aimed to the complete spotlight and not only on the color uniformity. The complete spot caused the impression, so the task was more widely arranged. The different questions could lead to different individual evaluation criteria and scales. It was assumed that the question about the impression of the spotlights was mainly influenced by the differences in the perception of color and patterns because luminance distribution and further experimental properties stayed constant. The second human factor experiment showed that U_{sl} was able to estimate the color uniformity at different luminance levels similar to the observers. The evaluation of spotlights under different contrast levels by subjects was confirmed by U_{sl} values of measurements of these spotlights. Just variation of background did not influence the perception necessarily. The subjects grading remained the same due to similar contrast appearance of the spotlights.

4.3.3 Semantic interpretation of U_{sl}

The merit function U_{sl} needed to be classified into several color uniformity levels. The response from the standard setup was used to classify U_{sl} into several levels from excellent to insufficient color uniformity. The assignment of spotlights to a color uniformity level enabled a simplified comparison of different spotlight systems at the same visual perception.

The levels were derived from the distribution of spotlights regarding median and merit function in Figure 4.27. The color uniformity scale was expanded over the U_{sl} function values to be prepared for excellent and insufficient spotlights because these spotlights were not included in the experiments. The U_{sl} range of the spotlights used in the human factor experiments was about 30 to 60. Lower levels were defined as excellent color uniformity for $U_{sl} \leq 30$. Higher levels were defined as inadequate color uniformity for $U_{sl} \geq 60$. For spotlight which did not even reach this level, a level for insufficient color uniformity $U_{sl} \geq 100$ was defined. The range between 30 and 60 was divided into good and acceptable color uniformity. The threshold value was set to 40. This was the critical value for grade 4. All spotlights which were graded with 4 or worse had U_{sl} value larger than 40. Therefore, the threshold was fixed here. More uniform spotlights with grade 2 were better than 40, except two spotlights which were really near by at about 41. Spotlights with grade 3 were widely distributed, there was no clear range to allocate the grade 3 to any level. Figure 4.28 presents the levels of U_{sl} for the visual perception of color uniformity in the far field of spotlights and the classification from excellent to insufficient color uniformity.

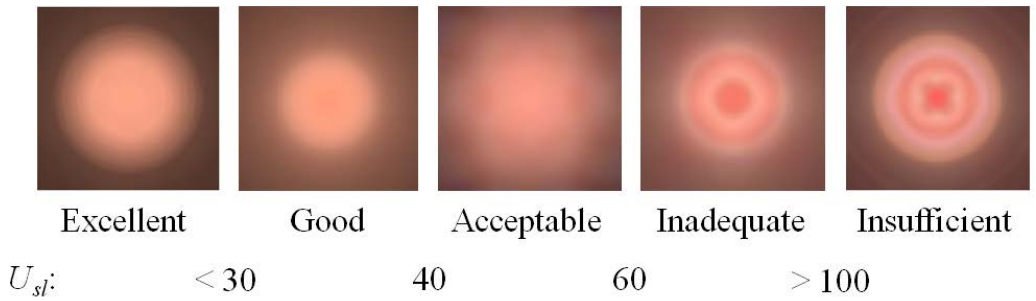

Figure 4.28: Levels of color uniformity U_{sl}

Spotlights assigned to excellent color uniformity showed no perceivable colors and patterns in the far field. Acceptable spot lights contained visible but not disturbing colors and patterns. Colors and patterns were highly disturbing and clearly visible at insufficient color uniformity level. Table 4.11 explains the difference between the color uniformity levels.

Table 4.11: Description of color uniformity levels of U_{sl}

Level	U_{sl} range	Description
Excellent	$U_{sl} \leq 30$	No colors or patterns visible in the spotlight
Good	$30 \leq U_{sl} \leq 40$	Slightly visible colors and patterns
Acceptable	$40 \leq U_{sl} \leq 60$	Visible, but may not disturbing (depending on application and requirements)
Inadequate	$60 \leq U_{sl} \leq 100$	Immediately visible and disturbing colors and patterns
Insufficient	$U_{sl} \geq 100$	Clear colors or patterns with assured disturbing impression

The classification enabled a relation between U_{sl} and the perceived uniformity in spotlights. Different spotlight systems could be compared at same color uniformity level under similarly perceived spotlights.

4.4 Conclusion

Two human factor experiments were performed to evaluate the visual perception of typical spotlight patterns. The results of the human factor experiments were used to derive the merit function U_{sl} for the estimation of the perceived color uniformity in spotlights.
Many spotlights with different color and pattern combinations were created based on optical simulations with multi-colored light engines and reflector or TIR lens as secondary optics and tested in human factor experiments. The first human factor experiment resulted in the perceived rank order of the spotlights. The perceived

rank order was used to correlate the basic functions and weighted function concerning the spatial color distribution. Finally, a linear regression of four basic functions reached a very strong correlation with the perceived rank order. This merit function U_{sl} was able to estimate the visually perceived color uniformity in spotlights. The second human factor experiment tested the perception of spotlights under different environmental conditions. The impression of subjects of spotlights could be rather reproduced by U_{sl} . Furthermore, a classification of U_{sl} into several levels form excellent to insufficient color uniformity was reached.
The semantic interpretation of U_{sl} enables the analysis of different spotlight systems and their comparison of perceived color uniformity. An objective evaluation method could be derived from the visual perception of many subjects under various conditions. The subjective personal opinion of individuals could be replaced by a standardized merit function.

5 Validation of the Color Uniformity Function U_{sl}

The results of both human factor experiments lead to the merit function U_{sl} for the color uniformity in the far field of spotlights. A classification of U_{sl} into several color uniformity levels enabled a comparison of similar perceived spotlights.
In the present chapter, the validation of the function is presented concerning the application range and conditions as well as limitations and restrictions. Measured and simulated data of various optical several systems were compared to adjust U_{sl} as a reliable method.

5.1 Adjustment of Measurement and Simulations

The merit function U_{sl} (see Formula 4.15 on page 70) was derived using experimental measured data collected with a luminance meter. The luminance meter measured the tristimulus values X, Y, and Z which were converted into CIELAB coordinates. Simulated results have to be adjusted to measured results to validate the function. Then, the application will be the estimation of the color uniformity in simulations of optical systems. The adjustment of simulation parameters was required to be able to use U_{sl} to simulations. Afterward, it would not be necessary anymore to build prototypes to generate spotlights. The estimation of the color uniformity level will be possible already during optical simulation and optimization.
Figure 5.1 shows the different appearance of a measured (left) and simulated (right) spotlights after data processing for visualization. The color pattern with four red dots in the center of the spotlight and the outer red ring are visible in both data. The luminance appearance and hue of red/ yellow vary from each other. The differences between the two pictures in Figure 5.1 may occur due to differences in data collections and the conversion into RGB color space for computer screen

visualization. A comparison of U_{sl} of measured and simulated would show realistic deviations independent of visualization processing.

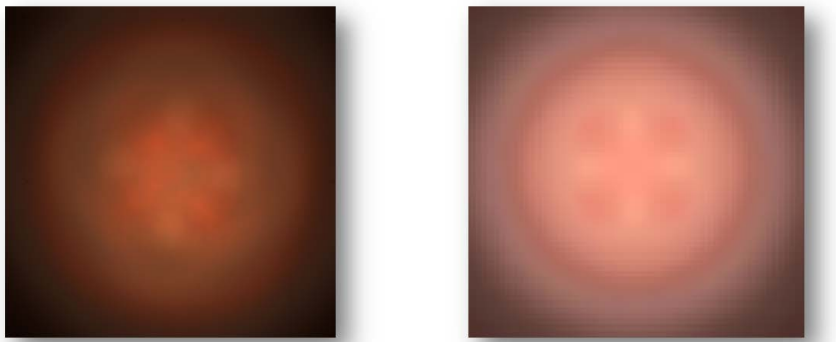

Figure 5.1: Comparison of measured (left) and simulated (right) far field of the same optical system

The measurements and simulations of four different systems were used. For the comparison, spotlights which were available from manufactures or as prototypes were selected. They are shown in Figure 5.2. A large reflector with specular reflection (Figure 5.2, 1), a small reflector with Gaussian reflection (Figure 5.2, 2), a very flat Fresnel lens with facets especially designed for color mixing in a narrow spotlight (Figure 5.2, 3), and a TIR Fresnel lens (Figure 5.2, 4) were used for comparison. All four secondary optics were measured and simulated with the same light source, the multi-colored light engine presented in Figure 2.11 on page 23. The light engine provided no scattering particles or color mixing structures.

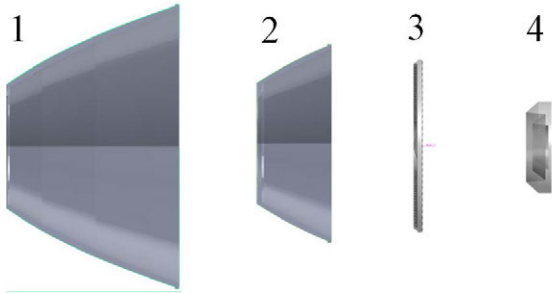

Figure 5.2: Optical elements for adjustment of measurement and simulation, 1) specular reflector, 2) Gaussian reflector, 3) thin Fresnel lens, 4) TIR Fresnel lens

Due to very different sizes of the elements, the angular distribution of the spotlights and the FWHM angle differed. Consequently, U_{sl} was tested with regard to various optical properties. Table 5.1 lists the different optical properties of the four elements.

The measured data were received by a luminance meter with the same setup as for the measurements of the far fields of the human factor experiment.

Table 5.1: Comparison of size and FWHM angle of optical elements

	1	2	3	4
	reflector 1	reflector 2	thin Fresnel lens	TIR Fresnel lens
Size [$mm \times mm$]	120×70	80×30	60×3	30×8
FWHM angle	$10°$	$15°$	$17°$	$24°$

For simulation data, the systems were built in a standard ray-tracing program (LightTools). The prototype and simulation model of the multi-colored light engine matched in the spectral distribution, luminous output, spatial and angular light distribution. The optical elements were built as accurate as possible after properties of the prototypes.
During simulation, the number of rays was set to 2500000000 (2.5 bn). The large amount was necessary to reach a comparable noise ratio to measured data. The calculation of chromaticity coordinates always needed a large amount because each ray held only the color information of one wavelength. A receiver was set 2 m in front of the system to record the rays. It imitated the projection screen of measurements. The resolution was set to 100×100 which was the same resolution as for measurements.

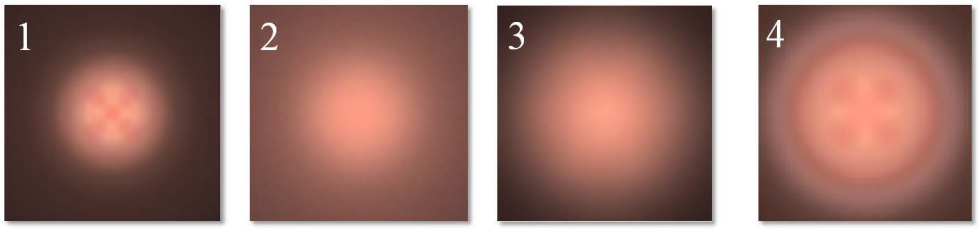

Figure 5.3: Results of the simulated far fields of the four optical elements with multi-colored light engine

Figure 5.3 shows the far field at 2 m distance. Reflector 1 imaged clear colors and patterns due to its specular reflection but it had a quite narrow beam. In contrast, reflector 2 did not show colors or patterns but it had a larger FWHM angle. The thin Fresnel lens performed well concerning the color uniformity whereas the TIR

Fresnel lens projected clear colors and patterns onto the screen. There were two systems with good color uniformity and two systems with clearly visible colors in the far field and poor color mixing ability.

Table 5.2: Comparison of measured and simulated U_{sl}

	1	2	3	4
	reflector 1	reflector 2	thin Fresnel lens	TIR Fresnel lens
U_{sl} measured	59	28	32	122
U_{sl} simulated	61	31	35	115
Deviation	3%	10%	9%	6%

Table 5.2 presents an overview of the results of U_{sl} calculations for the measurements and simulations. Although all four systems were very different, the deviation between measured and simulated U_{sl} values was smaller than 10 %.
The deviations had several reasons. On the one hand, the measurement noise and systematical errors of the luminance meter were existent. Especially, in measured areas with low luminance level, noise was present. The measurement method with colored filters caused color shifts at color gradients and results in discrepancies and limited color resolution. On the other hand, the simulation model had limitations in its replication of the real system. The light engine was adjusted to experimental data. Due to complex physical processes like phosphor conversion and advanced scattering, it was an approximation. For simulation, only a limited number of rays could be calculated. In addition, the resolution of the receiver was limited because a minimum number of rays per receiver bin were needed for accurate color calculations. The optical elements and surfaces had ideal properties, no tolerances or production effects like rounded edges were implemented. As a result, the simulation could only be an approximation of the prototype.
The calculated differences of Table 5.2 were within inaccuracies between the model of measurement and simulation as well as different way of data generation. Comparable U_{sl} values were obtained in simulations and experiments under defined conditions. It could be used for the analysis in measured optical systems as well as for simulation data. The U_{sl} merit function is applicable as reliable standardized value to estimation the color uniformity level with regard to the visual perception in various systems.

5.2 Validation and Restrictions

The validation of U_{sl} is discussed with regard to the following three aspects.

a) Covariance of the function U_{sl}
b) Sensitivity of correlation coefficients β_n
c) Visual perceptual application range

a) Covariance of the function
In general, the merit function U_{sl} was derived for circular illuminated areas and especially spotlights. A circular luminance distribution or evaluation area is absolutely necessary. The function S_{rad} and S_{lin} were designed to find color differences on radial and axial directions. The luminance distribution itself is not determined because luminance is not implemented in the merit function.

Performing a linear regression, it was necessary to test the sensitivity and stability of fitting. There were several methods to avoid an over prediction to particular data sets and to define the best fitting for a linear regression. First, the covariance of the basic functions was calculated. In statistics, covariance represents the measure of monotonic relation between two random variables. The covariance of each basic function is shown in Table 5.3 in relation to the other functions in matrix form.

Table 5.3: Covariance of the four basic functions

	$Grad_{ab}$	dab	S_{rad}	S_{lin}
$Grad_{ab}$	0.082	-	-	-
dab	0.046	0.085	-	-
S_{rad}	0.042	0.044	0.196	-
S_{lin}	0.004	0.037	-0.001	0.054

At the main diagonal, the matrix contains the variances of each basic function. The variance of two variables is symmetrical, therefore only once the value between two functions is mentioned. All covariances except S_{rad} - S_{lin} were positive. All coefficients had a positive sign and greater function values indicate larger non-

uniformities in color. The variance of $Grad_{ab}$ was larger than the covariances of $Grad_{ab}$ together with the three other functions ($Grad_{ab}$ column). It was the case for all functions, the covariance of the function to itself was larger than covariance to the other functions. The clearly lower covariance values to other functions implied that the functions did not analyze the same properties of the far field. The linear behavior differed for all functions. All four functions described different influencing factors which were reflected in the covariance. A combination of these four basic functions was reliable and applicable for a fitting of the visual perception.

b) Sensitivity of correlation coefficients

The coefficients of each basic function in U_{sl} were analyzed regarding their sensitivity to changes and their impact on the overall correlation. Figure 5.4 presents the trend of Spearman's correlation coefficient r_s. The coefficients β_n of each basic function were shifted in the range of $\pm$ 20 %, separately from each other. During the change of one coefficient the other coefficiencts were unchanged.

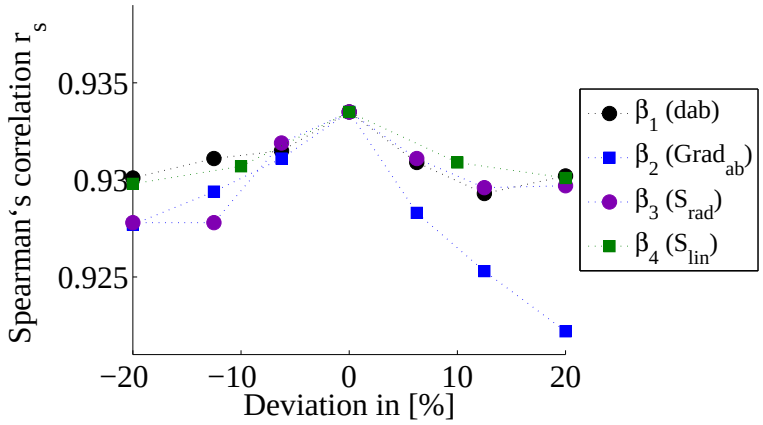

Figure 5.4: Sensitivity of correlation coefficient r_s by changing coefficient β_n of each basic function

The shift of one coefficient always lead to a reduced correlation. The strongest effect can be seen for the basic function $Grad_{ab}$. It had already as basic function the highest correlation with the perceived rank order. Here, the sensitivity to overall correlation was largest. The correlation decrease by shift of the other functions was similar. The correlation coefficient did not drop below the correlation value of any of the single each functions. Then, the three other coefficients would be 0.
Of course the same correlation of 0.934 is reached by a multiple of the coefficients 2.5,

8, 3 and 1, e.g. 1.25, 4, 1.5, 0.5 or 5, 16, 6, 2. The presented coefficients were selected to let U_{sl} be within a range of 0 to 100 for excellent to insufficient perceived color uniformity. The function range of U_{sl} is set to $0 \leq U_{sl} < \infty$. The function value 0 indicates perfect color uniform surface and increased values indicate decreased color uniformity in the spotlight.

c) Application range

The experiments were proceeded under defined conditions and therefore the function U_{sl} implied some restrictions for its application. The luminance level in the first human factor experiment was one fixed condition. The second human factor experiment tested also another luminance level.

Previous studies about color discrimination and visual search at different illumination conditions provide detailed information (see page 17). Color vision is constant over a wide luminance range and various environmental conditions in the range between 50 cd/m^2 and 1000 cd/m^2. Lower luminance levels result in scotopic vision with active rods, and color vision ability clearly degrades and should be avoided. Thus, the function U_{sl} could be applied in the above mentioned range for various spotlights.

The implemented luminance cutoff defined a threshold to the outer edge of the spotlight. The threshold had to be selected differently for different systems to either get the same spotlight size or the same luminance cutoff level. To get comparable function values, the spotlight size should be similar for absolutely compared spotlights.

In addition, the luminance distribution is excluded of U_{sl} calculations. Although the luminance distribution was nearly the same in all spotlights during the human factor experiments, it could not be avoided that the luminance distribution had an effect on the evaluation of the subjects. It was difficult to distinguish between color and luminance distribution in reality. Due to very low differences in luminance levels in the spotlights, the effect was minimized. However, the implementation of luminance weighting to *dab* (see Table 4.8 on page 67) did not improve the correlation with the visual perception. Thus, the merit function was derived without luminance weighting and calculated values were independent of luminance distribution in the spotlight.

One important factor for the perception of uniformity was colored patterns. Therefore, the contrast sensitivity function (CSF) was implemented in the U_{sl} calculation. Based on the perception of the spatial frequencies of luminance and colored patterns, the eye has different sensitivities. The frequencies of color patterns in the tested spotlights were larger than 1 $cycle/^{\circ}$. Higher frequencies were not tested during human factor experiments. The color CSFs are constant for frequencies lower than 1 $cycle/^{\circ}$. For frequencies higher than 10 $cycle/^{\circ}$ the visibility decreases rapidly till colored patterns are invisible. Although higher frequencies were not tested in the experiments, the implementation of the CSF enables an estimation of the perceived color uniformity in spotlights with smaller patterns which contain higher spatial frequencies. The implementation of CSFs into data sets was done before calculating U_{sl} for each spotlight. Thus, it is an inherent part of the U_{sl} calculation.
As seen especially in the second human factor experiment, hue had lower influence on the perception than chroma level. The sensitivity was higher at different color categories like red, green yellow and not for colors of one color category (several red hues). The usage of other light sources e.g. differently colored LED chips or other phosphor types would cause changes in hue. The tested hues red, green, yellow and blue were mostly existent in the spotlights in several variations. The perception of spotlights with same pattern but slightly different color combination of e.g. blue-yellow would not change the perception of uniformity.

5.3 Conclusion

The merit function U_{sl} based on for basic function combined by liner regression is an appropriate function to estimate the perceived color uniformity at the far field of spotlights. The function U_{sl} is not limited to the experimental conditions of the human factor experiment but it can be applied to spotlights with various spatial and angular color distributions. Very different spotlight systems with varied luminance levels, spotlight size and patterns can be evaluated and the perceived color uniformity can be estimated.
The adjustment of U_{sl} from measured to simulated optical systems resulted in related values. Now, the function can be applied to simulations of optical systems.

An estimation of the color uniformity is received already from the simulation results and no prototypes for real illuminations are necessary. The color uniformity is applicable as a optimization constraint in simulations. Systems can be compared objectively regarding their perceived color uniformity of the far field among other properties like efficiency, peak luminous intensity and system size.
For an absolute comparison of U_{sl} values, the data basis should be similar with regard to the resolution and the measurement noise. The viewing distance, the luminance level, the luminance distribution, and FWHM angle of the compared systems can differ and have no predefined values. These variations of parameter influences also the U_{sl} values but in similar way as the visual perception in influenced.

6 Spotlight Optimization

The visual perception of spotlights lead to the merit function U_{sl} by linear regression including many visual influencing factors. U_{sl} is valid in a wide range of environmental conditions including luminance levels, size, viewing distance and spatial color distributions. The adjustment of measurements and simulations enables an accurate estimation of color uniformity already from simulated illumination systems.
The merit function U_{sl} is now used to evaluate different spotlight systems regarding several properties. Different optical systems consisting of multi-colored light engine and secondary optics, mainly reflectors and TIR lenses were optimized and compared with each other. The focus was on color uniformity of the far field and further properties efficiency, peak luminous intensity, and sensitivity to colored shadows. The spotlights often have restrictions to size, collimation angle, luminance distributions and other depending on the focused properties. Furthermore, the influence of light mixing by additional structures or elements in the secondary optics as well as different amounts of scattering particle concentration in the light engine were analyzed.
Defined constrains for all spotlights enable a direct comparison of the systems. The performance of the spotlights was evaluated to be able so select suitable spotlights for defined applications.

6.1 Optimization Constrains

Several optics were selected for further optimization and comparison between each other. The optimization of the systems was done to adjust them to the same FWHM angle and to find best performing systems as a combination of light engine and

secondary optics for defined color uniformity levels.

Several specification were assumed to get comparable results from the optimization of different optical systems. The main specification was the definition of the FWHM angle, it was set to 20°. The restriction was limited to a medium spotlight beam. For more collimated spotlights 12° are available and for broader distributions 24° and 36° spotlights are used. Formula (2.13) was used to calculate etendue of source E_{source} and target E_{target} and to define the minimum size of the secondary optics. The etendue E_{source} of the light engine is defined by its radius r_{source} of 4.5 mm and the half angle of radiation $\alpha_{source} = 85°$. The flat cover layer makes that the effective n to be considert in the etendue calculation is $n = 1$.

$$E = n^2 \cdot \pi \cdot sin^2\Omega \cdot A \tag{6.1}$$

$$E_{source} = n^2 \cdot \pi \cdot sin^2\alpha_{source} \cdot \pi \cdot r_{source}^2 \tag{6.2}$$

$$E_{source} = 1 \cdot \pi \cdot sin^2(85°) \cdot \pi \cdot (4.5mm)^2 \tag{6.3}$$

$$E_{source} \approx 180\ sr \cdot mm \tag{6.4}$$

The etendue of the light source was fixed. To be able to reach full efficiency, the etendue of the target E_{target} should be at least as large as the etendue of the source E_{source}. It was set to be equal to the etendue of the target.

$$E_{source} = E_{target} \tag{6.5}$$

The half angle of the target luminous distribution α_{target} was set to 10° to calculate r_{optic}.

$$E_{target} = n^2 \cdot \pi \cdot sin^2\alpha_{target} \cdot \pi \cdot r^2 \tag{6.6}$$

$$E_{target} = 1 \cdot \pi \cdot sin^2(10°) \cdot \pi \cdot r^2 \tag{6.7}$$

$$r_{optic} = \sqrt{180/\ (\pi^2 \cdot sin^2(10°))} \tag{6.8}$$

$$r_{optic} \approx 25\ mm \tag{6.9}$$

At least the radius r_{optic} would be necessary to collimate all light from the source into the spot field with a FHWM angle of 20° if the luminous distribution had an abrupt slope. The final radius could be slightly smaller because the luminous

distribution does not end at 10°. Depending on the luminous distribution, most of the light would remain in about 30° FWHM angle (sums up to a radius of 16.5 mm). The initial value of the diameter was set to 16.5 mm.

The optimization was started with light engine 2 as initial light source. During optimization, the light engine was unchanged, only parameters of the secondary optics were set as variables. The main optimization parameter was the FWHM angle of 20°, followed by the efficiency and peak luminous intensity as lower weighted optimization targets.
After optimization of secondary optics, the resulted optics were combined with the other two light engines 1 and 3. By the combination of all three light engines with all secondary optics, various spotlights systems resulted. Either the light engine provided color mixing or the secondary optics or both elements which depended on the combination.

After optimization and simulation of each combination, the data of the optical systems were analyzed by three different receivers. The first receiver was a spherical far field receiver around the encased optical system. It was used to measure the optical system efficiency. Two further receivers were positioned in 2 m distance of the light emitting surface of the light engine. The distance was selected to be the same as the setup of the human factor experiments. One receiver recorded the 1 m^2 measuring area of luminance meter. The second receiver with a size of 2.5 $m \times 2.5$ m recorded a larger area to detect the complete spatial color and luminance distribution. The resolution of both receivers was set to 100×100 because for calculating chromaticity coordinates many simulation rays per receiver bin were necessary to reach robust color values (tristimulus values X, Y, and Z). Thus, the simulations were done with 250000000 rays. In the region of interest at least 20000 rays per receiver bin should be available for reliable chromaticity coordinates.

6.2 Optical Systems Used for Optimization

The assembly of light engine and optical elements resulted in various systems and far fields. The wide range of LED light sources and secondary optics offered a very flexible design of spotlights with regard to FWHM angle, luminance distribution, luminous flux and CCT. The multi-colored light engine and basic TIR lenses and reflectors were used to assembly the spotlight systems which were used for further optimizations.

6.2.1 Multi-colored LED Light Engine

A multi-colored LED light engine was selected with fixed size and chip positions for the optical simulations and their optimizations. The prototype of the light engine consisted of 12 green converted chips, 5 red and 4 blue chips, the light emitting area had a diameter of 9 *mm*, the CCT was 3000 *K*.
For the optical simulations, three light engines with above described assembly were used. The three light engines differed only in the volume cast which covered the chips. They are presented in Figure 6.1. They were chosen out of 16 light engines with gradually increased scattering particles concentration which result in a gradually increased color mixing.

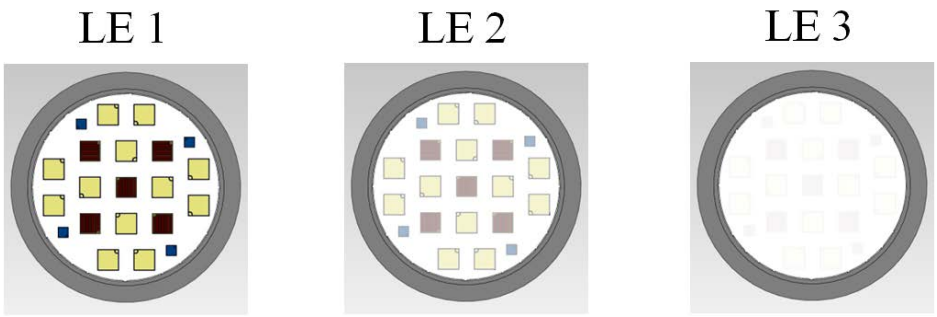

Figure 6.1: Top-view of the three different light engines (LE) setups with different color mixing ability, left: without scattering particles, center: few scattering particles, right: most scattering particles, included in the cover layer

The light emitting area was filled with a silicone cast for better light extraction from the LED chips. The volume cast of each light engine contained different

concentrations of scattering particles. The scattering particles were incorporated in the volume cast layer to provide mixing of the spatial separated colored LED chips. Increased scattering particle concentration lead to improved color uniformity but also decreased extraction efficiencies. The reasons were losses in scattering processes and the absorption of backscattered light. The properties of each light engine are listed in Table 6.1. Light engine 1 had a nominal luminance output of 1900 lm, it was set to 100 %.

Table 6.1: Setup parameters of the three light engines (LE)

Parameter	LE 1	LE 2	LE 3
Type of cast	clear cast	few scattering particles	many scattering particles
Weight percentage [%] of scattering particle	0	0.1	0.4
Efficiency [%]	100	99.5	94.5

The far field of the optical systems behaved similar. Figure 6.2 presents the far fields of simulated light engine 1 to 3 in combination with a specular reflector without facets.

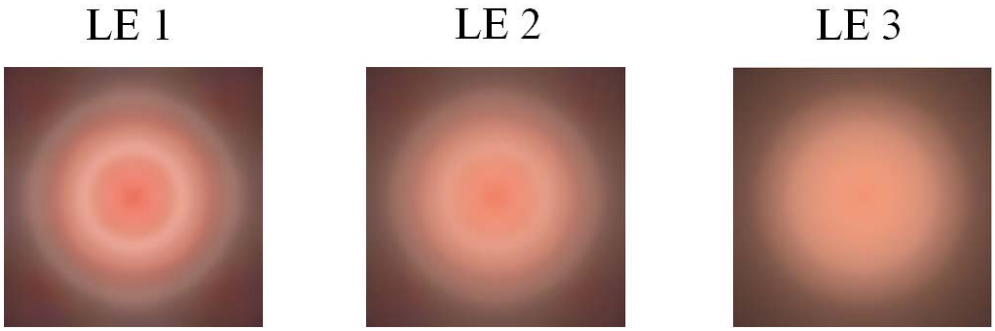

Figure 6.2: Far field of light engines 1 to 3, light collimated by specular reflector

The different levels of color uniformity in the far field of the spotlight were clearly visible. In combination with light engine 1 colored rings were visible in the center and at the edge of the spotlight. Light engine 2 decrease the colored rings but they were still visible and light engine 3 avoided nearly all colors in the spotlight.
The scattering process was explained in Figure 2.13 on page 25. It was necessary to balance the color mixing ability of the light source by scattering particles with its

efficiency. Color mixing in the light engine was possible up to a certain level. The absence of colored sections at the light emitting surface of the light engine allowed the use of nearly every secondary optics without colored far fields. By this method, colored far fields can be avoided but there is a large efficiency decrease. Another possibility to control the color uniformity level was the secondary optics which could also provide color mixing properties.

6.2.2 Secondary Spotlight Optics

To form a spotlight, the light engine have to be connected to the secondary optics which collimated the light into a narrow beam. There are different types of optics used for collimation. The following list contains possible secondary optics spotlights with defined angular distributions. [Dross, 2012]

- Total internal reflection (TIR) lens
- Faceted TIR lens
- Reflector
- Faceted reflector
- Rippled light pipe and lens system
- RXI
- UFO
- Additional elements: Köhler array

For product design of spotlights mainly TIR lenses and reflectors are used. These optical elements are widely distributed and can be fast optimized to requirements. Reflectors and TIR lenses are investigated in several designs and with additional light mixing structures or elements.
Based on an initial optical design of a TIR lens and reflector, the system optimization was started. Elements and structures for color mixing in the secondary optics were implemented in the initial design gradually. Scattering surfaces, facets, Fresnel modifications or micro lens arrays were used to test the color mixing performance of the optical system.

The TIR lenses were first designed as plain lens with and without focusing center (Figure 6.3 TIR2). To the plain lens, modifications of several surfaces were done. A TIR lens without focusing center was designed (Figure 6.3 TIR1). Another TIR lens was provided with a rough outer surface to reach not a specular reflection but a diffuse reflection. Different reflection modes were tested. A lens array was implemented at the front surface of the TIR lens (Figure 6.3 4, TIR5). Further possibility to generate color mixing were tailored TIR lenses, Fresnel TIR lenses and combinations of these methods.

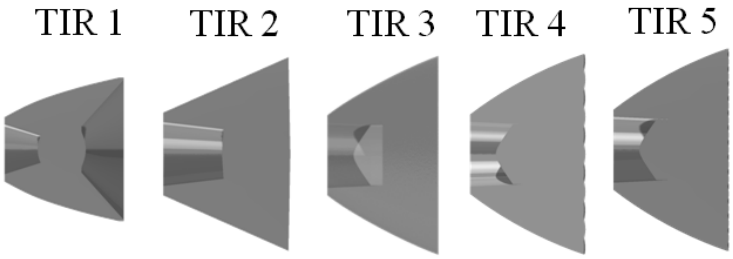

Figure 6.3: TIR lens designs: 1) plain TIR lens, 2) plain TIR lens, 3: rough outer surface, 4) large lens array at front surface, 5) small lens array at front surface

All TIR lenses consisted of PMMA with a refractive index of 1.494. Fresnel losses and reflection were implemented in the simulation models. Furthermore, all TIR lenses were designed with a rotational symmetric shape.

The iterations for the reflector design stared with a plain standard reflector (Figure 6.4 REF1 and REF2). It was a plain parabolic reflector with specular reflections and without any other mixing elements. The initial form of the reflectors was parabolic. During optimization, the form changed to a more elliptical shape to reach the defined FWHM angle of 20°. Then, rough surfaces with several reflections properties were added (Figure 6.4 REF3). Another possibility to influence color mixing were facets. Finally, to the first plain reflector an optical element called shell mixer was added [Chaves et al., 2012]. It was a dome element and contained a double sided Köhler lens array. It was designed to provide color mixing in already existing illumination systems (Figure 6.4 REF5).
All reflectors were simulated with a reflectivity of 90 % and had a rotational symmetry. In further work a standard reflector refers to RREF1 and REF2, the rough reflector refers to REF3 and a faceted reflector refers to REF4 and REF5.

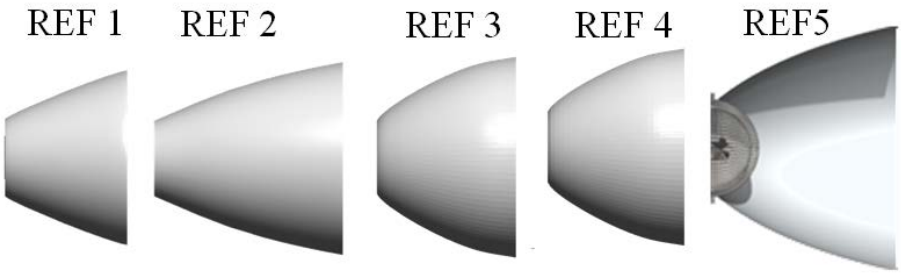

Figure 6.4: Reflector designs: 1) standard specular reflector, 2) standard specular reflector, 3) reflector with diffuse reflection, 4) faceted reflector, 5) reflector and shell mixer in combination

The size of TIR lenses and reflectors are presented in Table 6.2.

Table 6.2: Comparison of TIR lenses and reflectors, the elements are specified as the product of the size of each elements length and its diameter [mm]

TIR lenses	TIR1	TIR2	TIR3	TIR4	TIR5
	23×32	22×47	23×58	23×48	23×47
Reflectors	REF1	REF2	REF3	REF4	REF5
	30×47	41×49	29×51	32×51	45×68

The TIR lens TIR1 was the smallest optical element of all. Modifications of surfaces and additional facets did not change the size of the lenses significantly, only the shape of the outer shell was changed to reach the defined FWHM angle. The reflectors were a bit larger than the TIR lenses. The standard reflector REF1 was set to its profile to fit FWHM angle. The adding of facets or rough surfaces changed the size only marginally. Similar to TIR lenses, mainly the shape of the reflector was modified. The combination of reflector and the shell mixer REF5 resulted in the largest optical system due to additional optical element which had to fit into the reflector.

The optimization lead to systems with the same FWHM angle in a range of $20° \pm 1°$. The optics were analyzed with regard to their color mixing ability, occurrence of color shadows, efficiency and peak luminous intensity.

6.3 Comparisons of Optimized Systems

First, the systems were compared with regard to the color uniformity. Afterwards, the effects to color shadows, efficiency, and peak luminous intensity were analyzed. In general, the results of the optimizations and simulations were presented in tabular form for each property. The resulted values are highlighted with either red, yellow or green color. There are three levels of performance. The classification of red, yellow and green highlighting was related to the visual perceived color uniformity after U_{sl}. Green indicates excellent color uniformity $U_{sl} < 30$, yellow indicates good and acceptable color uniformity $30 \leq U_{sl} \leq 60$ and red indicates inadequate and poorer color uniformity $U_{sl} > 60$.

6.3.1 Color uniformity

The color uniformity was compared based on U_{sl} merit function. The optimization to the same FWHM angle for all systems allowed an exact comparison of the systems. Out of many simulated optimized systems, five systems TIR lenses and five reflectors were selected and discussed.

First, TIR lenses were compared (see Figure 6.3). Each TIR lens was simulated with the three light engines 1 to 3 separately. Light engine 1had a clear cast and did not provide any color mixing. Light engine 2 included some scattering particles and light engine 3 the highest number of scattering particles. Thus, light engine 3 had best color uniformity but lowest efficiency. Table 6.3 lists the U_{sl} values of each combination of light engine and TIR lens.

The color uniformity U_{sl} reached by TIR lenses covered a wide range. Excellent to insufficient color uniformity was created by the lenses. On the one hand, the color uniformity was influenced by the mixing level of the light source. On the other hand, it could be controlled by the optics itself with additional mixing elements.
The light engine with clear cast showed the poorest color uniformity for all secondary optics. With increased scattering particle number in the volume cast the color uniformity was increased. The better the light mixing in the light source

Table 6.3: Comparison of color uniformity U_{sl} of far fields from TIR lenses; table entries with the green background donate excellent color uniformity levels while yellow and red background entries denote acceptable and insufficient color uniformities, respectively

		TIR1	TIR2	TIR3	TIR4	TIR5
LE1	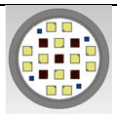	199	118	114	77	29
LE2		109	76	76	52	26
LE3		40	36	31	25	20

was the better the color uniformity in the far field of the spotlight appeared. In combination with light engine 1, U_{sl} depended clearly on the design of the optics. A well mixed light engine in combination with a specular reflector as secondary optics reached an acceptable color uniformity. But the higher the uniformity in the light engine the lower the efficiency. Furthermore, the color uniformity could not always be improved to excellent color uniformity level for all optics. Therefore, the number of scattering particles had to be increased further (e.g. to reach excellent color uniformity for TIR1 and TIR2). Then local scattering effects would be predominant, the mean free path reduced and again only more direct scattered light was emitted by the light source. The more direct light was less colored mixed because of the separated single LED chips. The systems did not reach better color uniformities. Especially, TIR1 could not reach excellent color uniformity only by increased scattering particle concentration, it should be chosen another light source.

Table 6.4 showes the far fields of the six TIR spotlight systems in real color rendering images. The TIR lenses themselves show clearly different far fields with the same light engine. The plain variants had low color mixing abilities, their U_{sl} values were high. There was a difference between the two standard lenses. The TIR lens with collimating centered lens TIR1 had worst color uniformity. It clearly imaged the LED chips into the far field. The second standard lens TIR2 performed better but still mostly with insufficient color uniformity. Dependent on additional elements,

Table 6.4: Comparison of far fields with different color uniformity levels of some TIR spotlight systems

LE1 TIR1 $U_{sl} = 199$	LE2 TIR3 $U_{sl} = 76$	LE3 TIR3 $U_{sl} = 31$
	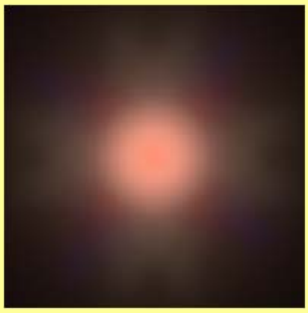	
LE1 TIR2 $U_{sl} = 118$	LE2 TIR4 $U_{sl} = 52$	LE3 TIR5 $U_{sl} = 20$
		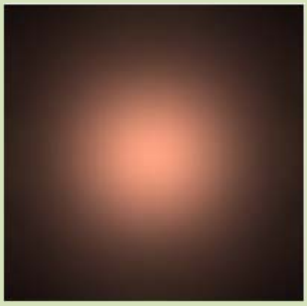

the improvements were distinct. A rough outer surface (TIR3) did not concede advantage over standard TIR lenses as well as the TIR4 with a large lens array. An adapted lens array could provide excellent color uniformity already with unmixed light sources (LE1 TIR5). A better mixed light engine increases the color uniformity further at an excellent level.

The second comparison dealt with the reflector spotlight systems (see Figure 6.4). Each reflector was simulated with the three light engines. The results of the simulations for each combination are listed in Table 6.5

The reflectors showed similar trends like the TIR lenses in color uniformity. The better the color mixing in the light engine was the better was the far field of the spotlights. The standard reflectors REF1 and REF2 had clearly poorest color

Table 6.5: Comparison of color uniformity U_{sl} of far fields from reflectors; table entries with the green background donate excellent color uniformity levels while yellow and red background entries denote acceptable and insufficient color uniformities, respectively

		REF1	REF2	REF3	REF4	REF5
LE1	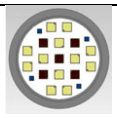	121	145	61	87	21
LE2		60	65	46	48	22
LE3		30	34	29	29	13

uniformity. Additional elements like rough surfaces or facets were able to improve the value. The effect was highest with unmixed light engine 1, and was lower with mixed light engines. In combination with light engine 3 most reflectors reached excellent color uniformity. The shell mixer in combination with plain standard reflector resulted in best color uniformity of all optical systems. The shell mixer was especially designed for color mixing. The double sided lens dome fulfill the procedure of color mixing perfect. It gave an enormous advantage to unmixed light engines. Already with light engine 1, the color uniformity was excellent. It was further improved with better mixed light engines.

In general, the color uniformity of the reflector systems was slightly better than the color uniformity of TIR lens systems. The color mixing process could be done in the light engine or in the secondary optics. The results of the evaluation of U_{sl} values for several TIR lenses and reflectors indicated a large influence of the light engine on the far field uniformity. The better the emitted light was mixed the better the color uniformity level of the spotlight. Implementation of scattering particles in the volume cast improved the color uniformity of the spotlights clearly but only up to a certain level.
Another important fact was additional elements in the secondary optics. They improved the color uniformity of both optics, TIR lenses and reflectors. For reflectors they were mainly useful with unmixed light sources, for TIR lenses it depended on

Table 6.6: Comparison of far fields with different color uniformity levels of some reflector spotlight systems

LE1 REF1 $U_{sl} = 121$	LE2 REF2 $U_{sl} = 65$	LE1 REF5 $U_{sl} = 21$
		
LE1 REF4 $U_{sl} = 87$	LE2 REF4 $U_{sl} = 48$	LE3 REF3 $U_{sl} = 29$
		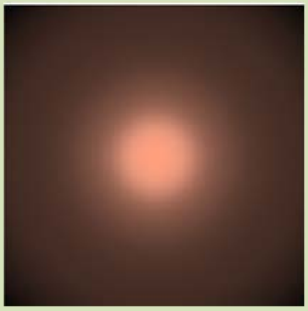

type of elements.
The overall excellent performance in color uniformity provided the standard reflector in combination with shell mixer REF5. The best TIR lens system was the TIR lens with small lens array at the front surface TIR5.

6.3.2 Color Shadows

Multi-colored LEDs with different colors and spatially separated arranged chips are sensitive not only to colored patterns and fringes but also to colored shadows. An object between the spotlight system and the target plain could cause multiple and colored shadows. The sensitivity to color shadows may be important in spotlights

for shop lighting where people stay inside the light beam. Another common application for spotlights is wallwashing where objects are near the optics. Then colored shadows should not appear.

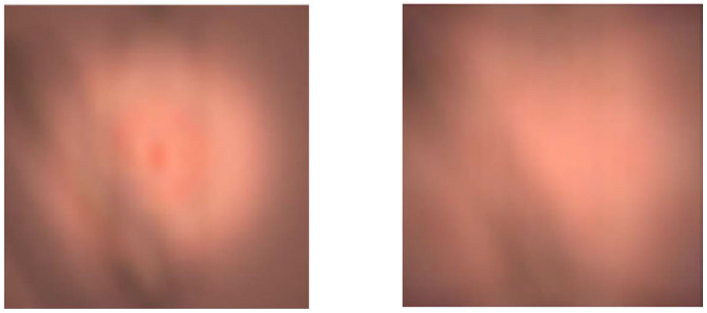

Figure 6.5: Two examples of spotlights with an object in the ray path and resulted far fields; left: reflector REF4, right: TIR lens TIR4, both secondary optics in combination with light engine 2

Figure 6.5 shows two different optical systems with differing colored shadows. All TIR lenses and reflectors in combination with each of the three light engines were simulated with objects in the ray path and again analyzed with U_{sl}.

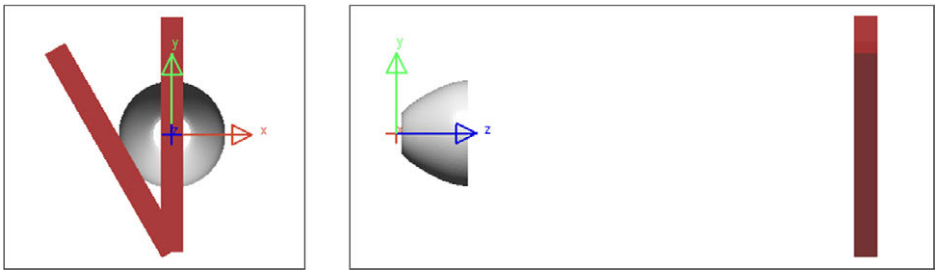

Figure 6.6: Colored shadows simulation setup, shown with reflector REF1 and absorbing objects in front of the reflector

The function U_{sl} could be used for evaluation because it is independent of the luminance distribution. If the colored shadows were only luminance variations, the color uniformity value would not have been influenced. Thus, there were no restrictions to apply the function U_{sl} to non-uniform spotlights. Figure 6.6 shows the simulation setup for far fields with colored shadows. An absorbing object was inserted in front of the optical element. The two elements had dimensions of $100\ mm \times 10\ mm \times 10\ mm$. Table 6.7 presents the U_{sl} values for the simulations with the absorbing object of all optical systems.

Table 6.7: Comparison of color uniformity U_{sl} of far fields from TIR lenses (first part) and reflectors (second part) and their colored shadows; table entries with the green background donate excellent color uniformity levels while yellow and red background entries denote acceptable and insufficient color uniformities, respectively, in relation to standard systems

		TIR1	TIR2	TIR3	TIR4	TIR5
LE1	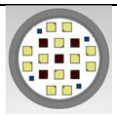	231	138	137	89	39
LE2		128	89	89	60	32
LE3		47	43	38	30	23

		REF1	REF2	REF3	REF4	REF5
LE1	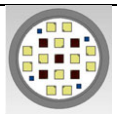	169	157	82	128	29
LE2		60	69	59	76	26
LE3		30	39	32	38	14

All U_{sl} values were increased with absorbing objects in the ray path. The color uniformity of all far fields was poorer and more colors and patterns were visible. The absolute differences between the U_{sl} values of the standard systems and the U_{sl} values of implemented absorbing objects (colored shadows) is shown in Figure 6.7.

Although all far field had poorer color uniformity, there were differences in the characteristics. The assembly of the light engine had a strong influence on the effects of objects in the ray path. The difference between the standard system and the systems with colored shadows optical system were largest for light engine 1.

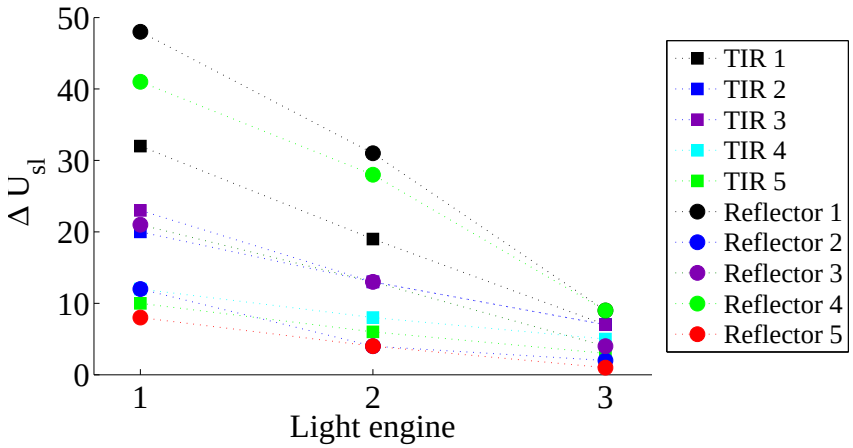

Figure 6.7: Comparison of ΔU_{sl} ($U_{sl\ ColoredShadows} - U_{sl\ Standard}$) from standard far field simulations to simulations with absorbing objects in the ray path

Most systems had not well mixed far fields. The color uniformity was still reduced by implemented objects in the ray path. It was similar for systems with acceptable or excellent color uniformity level. For light engine 1, the separated colors were only mixed by the secondary optics in the far field of the spotlight. Thus, an object in the ray path could absorb defined ray bundles form single LED chips and at the imaged edges of the object colored shadows occurred. The better the light was premixed in the light engine the lower was the influence of those objects to the color uniformity. Largest differences occurred with light engine one, up to $\Delta U_{sl} = 50$. Whereas, color uniformity for optics with light engine 3 decreased only up to $\Delta U_{sl} = 10$.
The absolute color difference between standard simulation and simulation with objects in the ray path depends on the specific form and profile of the secondary optics. The better the colors were mixed inside the optical system and secondary optics the fewer colored shadows occurred.

6.3.3 Optical System Efficiency

The optical system efficiency Φ_v is an important characteristic of optical systems. It represents how much of the light emitted by the light source is collimated into the target. The optical system efficiency was measured with a spherical far field

receiver. The receiver was installed around the optical systems. The optical system was surrounded by a housing and no light was emitted marginally. Only light emitted forwards through the output area of the secondary optics was recorded.

In the comparison, all efficiencies of the optical systems were set in relation to the most efficient system LE1 REF1 which was set to 100 at a real efficiency of 88.5 %. The other systems were specified as percentage of the system LE1 REf1. Table 6.8 present the optical system efficiency.

Table 6.8: Comparison of optical system efficiency of TIR lenses (first part) and reflectors (second part); table entries with the green background donate excellent color uniformity levels while yellow and red background entries denote acceptable and insufficient color uniformities, respectively, in relation to the standard system

		TIR1	TIR2	TIR3	TIR4	TIR5
LE1	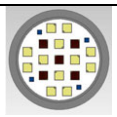	99.4	96.7	97.3	97.6	97.6
LE2		99.2	96.3	97.1	97.1	97.1
LE3		94.2	91.5	92.6	92.6	92.6

		REF1	REF2	REF3	REF4	REF5
LE1	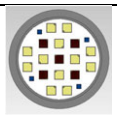	100	99.3	96.5	98.5	91.9
LE2		99.7	98.9	96.1	98.2	91.7
LE3		94.8	94.3	91.4	94.8	85.6

In general, the efficiency was reduced by about 5 % for all optical systems from LE1 to LE3. TIR lenses had Fresnel reflections and only part of the back reflected light

was emitted again by the light engine. The efficiencies of most TIR lenses (expect TIR1) were very similar because of ideal properties of surfaces and materials. They had nearly the same shape and size, thus their efficiencies were comparable. TIR lens TIR1 had highest optical system efficiency due to its geometrical shape. Less light under extreme large angles was lost. In production it would be more realistic that tolerances in gaps and edges leaded to lower efficiencies.
The efficiency of the reflectors depends on different aspects. On the one hand, the efficiency of the reflector system depend on the performance of the light engine as it was for TIR lenses. On the other hand, the efficiency depend on the reflectivity of the reflector material. A reflectivity of 90 % was assumed which was an ambitious value for standard available reflectors. In addition, the length and size of the reflector, its aspect ratio (length $\times$ diameter) had an influence. The smaller the aspect ratio was, the more rays hit the reflector surface and so the efficiency was reduced but the spotlight was better collimated. Furthermore, additional elements like the shell mixer had a clear effect. All light went through the shell mixer, most was transmitted and some light was reflected backwards by Fresnel reflection of 8 %. Only part of the reflected light by Fresnel reflection was emitted again. Clearly, the application of two elements as secondary optics was clearly reducing the efficiency. There was no distinct difference between the efficiency of TIR lenses and reflectors. However, the efficiency of the reflector was highly variable due to their reflectivity index. Increasing or decreasing of the reflectivity index affected the efficiency value immediately.

6.3.4 Peak Luminous Intensity

The peak luminous intensity is a further critical property for spotlighting. The peak luminous intensities were measured in the center of the receiver which corresponded to the center of the spotlight. The optimization was concentrated on the FWHM angle and the efficiency, the peak luminous intensity was not considered as main factor. Only from the results of the optimization to FWHM and efficiency, the peak luminous intensity values were compared. Table 6.9 presents the peak luminous intensities of the optical systems. All table entries were given as a percentage of the system LE2 TIR1 which reached highest peak luminous intensity

of all systems.

Table 6.9: Comparison of peak luminous intensity of far fields from TIR lenses (first part) and reflectors (second part); table entries with the green background donate excellent color uniformity levels while yellow and red background entries denote acceptable and insufficient color uniformities, respectively, in relation to standard system

		TIR1	TIR2	TIR3	TIR4	TIR5
LE1	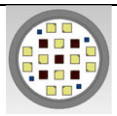	99.6	89.5	85.3	85.1	80.5
LE2		100	89.4	86.9	85.2	80.5
LE3		96.6	87.1	83.9	83.5	77.0

		REF1	REF2	REF3	REF4	REF5
LE1	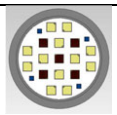	69.2	74.7	64.9	59.8	58.2
LE2	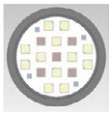	70.9	75.2	66.1	60.2	58.5
LE3		66.3	72.4	60.6	57.4	56.6

The differences in luminous intensity were larger than the differences in efficiency between the optical systems. Due to the optimization on FWHM and efficiency, the intensity distributions were very unequal.

The peak luminous intensity was highest for TIR lens TIR1 in combination with light engine 2. Both parts of the TIR lens were collimating the light, the outer shell as well as the centered lens part and light engine 2 was the initial light source for optimization. Additional color mixing elements like rougher surface or micro lens array at the front surface enlarged the luminous distribution and resulted in lower peak luminous intensities. The peak luminous intensities of TIR lenses TIR2 to TIR4

were similar because of similar shape and additional structures of the lenses. TIR lens TIR5 had lowest luminous peak intensity of all TIR lenses because the small lenslets of the micro lens array enlarged and smoothed the luminous distribution most.
The peak luminous intensities of the reflectors were lower than the intensities of the TIR lenses. The size of the reflectors were adapted to the size of the lenses. An increased size of the reflector would provide higher number of collimated rays and an increased peak luminous intensity. Part of the differences between the peak luminous intensity could be explained by different intensity distributions.

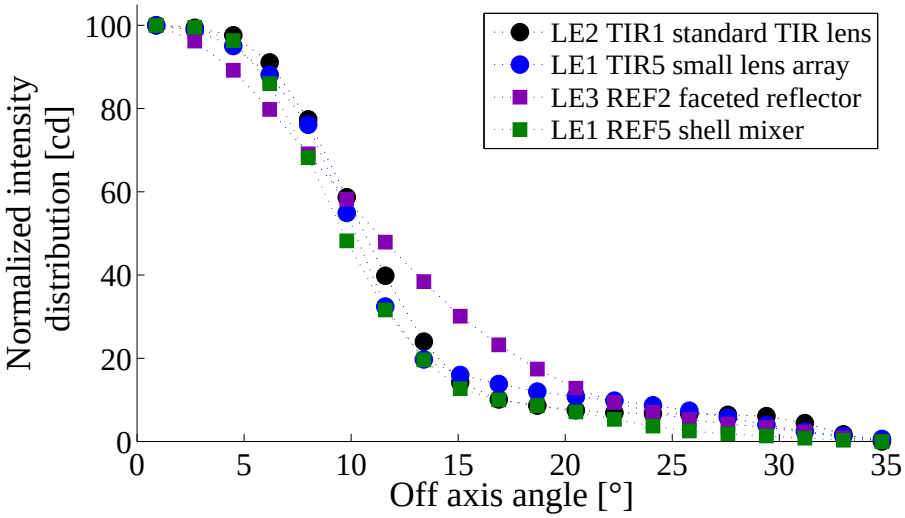

Figure 6.8: comparison of luminous intensity distribution of four optical systems, all systems normalized to 100

Although the FWHM angle was similar at $20° \pm 1°$ for all systems, the slope of the intensity distribution differed clearly. The luminous distribution of selected optical systems is presented in Figure 6.8.
The TIR lens with small lens array TIR5 had a wider distribution in comparison to the standard TIR lens TIR1. Larger amount amount of light outside the FHWM angle lead to lower peak luminous intensity. More light was guided towards the edge of the spotlight. This effect was enhanced by the reflector with facets. The slope of the luminous distribution was very flat in comparison to the other distributions. Large amount of light was not collected within the FWHM angle. The optical system of reflector and shell mixer showed a quite narrow distribution

but because the efficiency of the system was lowest, the peak luminous intensity did not reach high values.
An optimization of the optical systems with regard to the peak luminous intensity could lead to improved values and the large difference between TIR lenses and reflectors could change.

6.4 Evaluation of Spotlights

Spotlights are compared with each other to identify best fitting systems for spotlight application with defined boundary conditions. The compared values are the previous analyzed properties of the optical systems: color uniformity U_{sl}, sensitivity to colored shadows, efficiency, and peak luminous intensity.
In additions, a comparison of existing systems of traditional and professional spotlights with the simulated optical systems in relation to the color uniformity U_{sl} is performed.

6.4.1 Best Solutions for Color Mixing Systems

After the comparison of TIR lens systems and reflector systems separately in each category, the systems were compared with regard to all properties together. To find best solutions for color mixing systems, the four properties of color uniformity, sensitivity to colored shadows, efficiency, and peak luminous intensity were analyzed together.
The systems were classified according to their color uniformity U_{sl} of the far field. The three best levels of color uniformity were distinguished. First, systems with excellent color uniformity $U_{sl} \leq 30$ were compared. Then, systems with good color uniformity $U_{sl} \leq 40$ and finally, spotlight with acceptable color uniformity $U_{sl} \leq 60$ were compared.

Spotlights with excellent color uniformity did not show colors or patterns in the far field. The TIR lens systems are shown in Figure 6.9. There were four TIR lens

systems which reached excellent color uniformity.

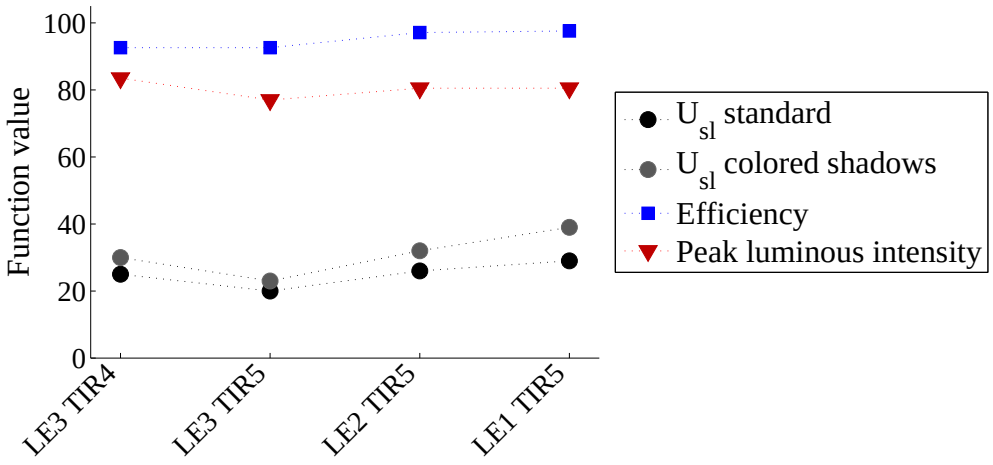

Figure 6.9: Comparison of TIR lens systems with excellent color uniformity

The TIR lens systems reached excellent color uniformity either by well mixed light engine 3 or with an adjusted lenslet array at the front surface of the TIR lens. Best color uniformity was reached by the combination of both, well mixed light engine LE3 and lenslet array TIR5. But this system had also lower efficiency and lowest peak luminous intensity of all systems with excellent color uniformity.
Figure 6.10 shows the comparison of six reflector systems which reached excellent color uniformity.

The reflector systems reached excellent color uniformity with well mixed light engine LE3 or with additional mixing elements like the shell mixer. Best color uniformity of all system was reached by light engine 3 and the shell mixer but at the same time with lower efficiency and lower peak luminous intensity. High efficiency and peak luminous intensity together with excellent color uniformity was reached with light engine 3 and standard specular reflector.
Light mixing either in the light engine or secondary optics lead to best results of the entire system for excellent color uniformity. Only if perfect color uniformity would be required, a combination of both, mixing in the light engine and the secondary optics, would be required. Here, the shell mixer was essential.

Excellent color uniformity would not be needed for all applications. Optical systems

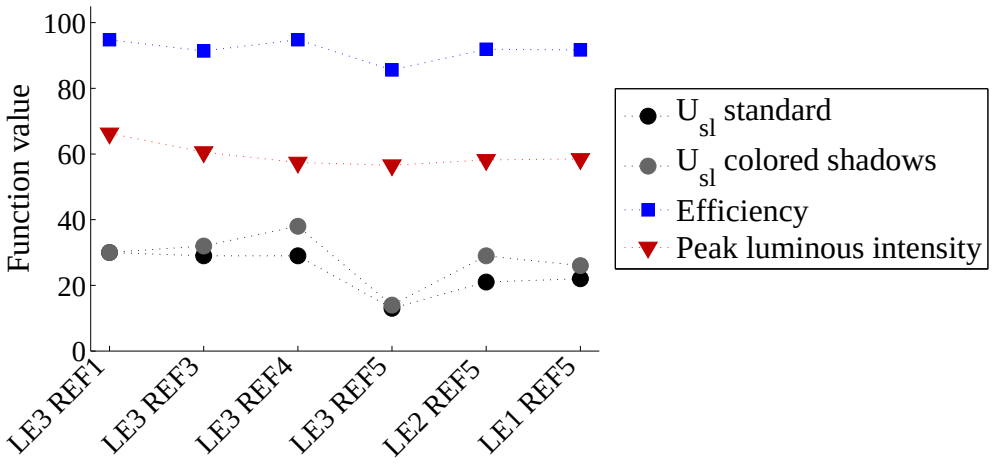

Figure 6.10: Comparison of reflector systems with excellent color uniformity

with good color uniformity could be sufficient in some cases. Spotlights with good color uniformity showed colors and patterns in the far field. These colored patterns were visible and not disturbing. There were three TIR lens systems which reached good color uniformity and one reflector system in this category. The systems are compared in Figure 6.11.

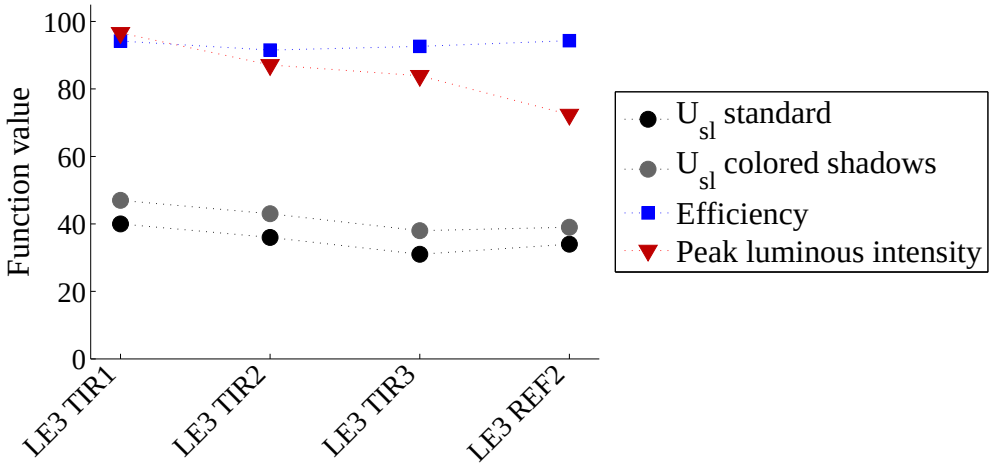

Figure 6.11: Comparison of TIR lens systems and reflector system with good color uniformity

Several combinations were possible for good color uniformity. The TIR lens systems with well mixed light engine and the standard TIR lens reached good color uniformity and high peak luminous intensities. The reflector system with well mixed light

engine and a standard reflector also reached good color uniformity. But the peak luminous intensity was lower at slightly higher efficiency. The efficiency of systems with only good far fields was not higher than the efficiency of most systems with excellent color uniformity. For good color uniformity a well mixed light engine was necessary. Higher peak luminous intensity values could be reached for by the standard TIR lenses.

If even less color uniformity would be required, spotlights with acceptable color uniformity in the far field could be used. These spotlights show visible color and patterns but may not disturb the visual perception. There were three reflector systems and one TIR lens system which reached acceptable color uniformity. The comparison is shown in Figure 6.12

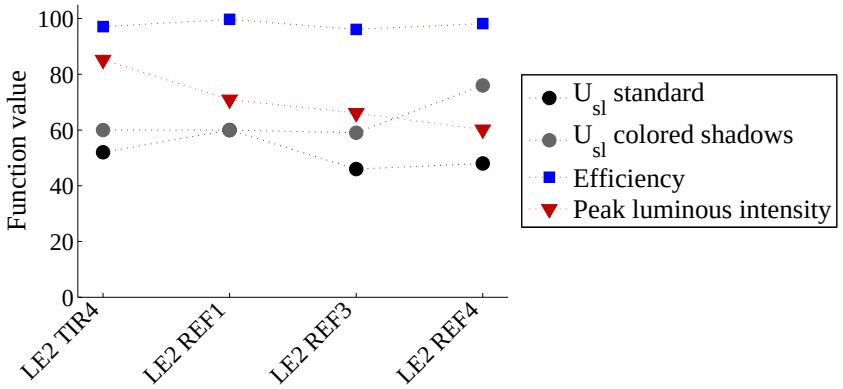

Figure 6.12: Comparison of optical systems with acceptable color uniformity

The acceptable spotlights reached U_{sl} values lower than 60. For acceptable color uniformity, color mixing of light engine 2 was sufficient. It was not necessary to use a well mixed light source to reach this level. Thus, the efficiency of these systems was high than the efficiencies of good or excellent color uniformity systems. The peak luminous intensity depended on the secondary optics.
A slightly mixed light engine in combination with standard reflector (or rough surface or facets) reached acceptable color uniformity. For TIR lens systems also a slightly mixed light source and TIR lens with facets were sufficient. Furthermore, highest peak luminous intensity and efficiency were reached with this system combination.

Table 6.10: Comparison of spotlight systems by their color uniformity level of the far fields, the combination of light engine (LE) and secondary optics as well as efficiency Φ_v and peak luminous intensity $I_{v\ max}$ were listed

U_{sl} level	LE	Optics	U_{sl}	Phi_v	$I_{v\ max}$
Best U_{sl}	LE3	REF5 shell mixer	13	85.6	56.6
Excellent U_{sl}	LE3	TIR4 faceted	25	92.6	83.5
Excellent U_{sl}	LE1	TIR5 faceted	29	97.6	80.5
Excellent U_{sl}	LE3	REF1 standard	30	94.8	66.3
Good U_{sl}	LE3	TIR1 standard	40	94.2	96.6
Acceptable U_{sl}	LE2	TIR4 faceted	52	97.1	85.2
Acceptable U_{sl}	LE2	REF1 faceted	60	99.7	70.9

The results showed that there was no system which had an outstanding performance in all categories. It was necessary to define the required color uniformity level of the spotlight. Then, best performing system for each color uniformity level could be chosen. It would be advantageous to define the main focus either on efficiency or peak luminous intensity. The best performing systems for each color uniformity level for TIR lens systems and reflector systems are listed in Table 6.10

There were different combinations of light engine and secondary optics to reach a specific color uniformity level. The single properties depend on this combination and the direct comparison showed that not all properties could be perfect at the same time.
There were excellent systems with high efficiencies or high peak luminous intensity values. For lower color uniformity qualities higher values for efficiency and peak luminous intensity could be reached at the same time.

6.4.2 Comparison to Traditional and Professional Spotlights

There are still traditional lamps like incandescent, halogen or high-intensity discharge (HID) lamps in usage for spotlights applications for consumer and professional lighting. Furthermore, LED spotlights for high-end illumination where absolutely highest light quality is required are available.

Five different spotlight lamps and luminaires were selected for the comparison with the previous presented spotlight systems (section 6.3 form page 105 ff). There were a traditional halogen spotlight lamp with a FWHM of 36° (Figure 6.13, left), and two consumer LED spotlight retrofits available at market (LED retrofit 1 is shown in Figure 6.13, right). These lamps were typical consumer products.

Figure 6.13: Halogen lamp (left) and consumer LED retrofit 1 (right), [Osram GmbH, 2013]

The two professional luminaires were a HID spotlight with high luminance output and a professional LED spotlight for high-end applications in museums. Both luminaires have a FWHM of 12°. The luminaires are shown in Figure 6.14.

Figure 6.14: HID luminaire (left) and professional spotlight luminaire (right), [Osram GmbH, 2013]

The color distribution of the far fields was measured with the luminance meter, then the U_{sl} values were calculated with the presented function (see Chapter 5, on page 87). The far fields of the spotlights, their FWHM angle and the U_{sl} values are listed in Table 6.11.

The visualization of the spotlights looked very similar. Slightly different CCT val-

Table 6.11: Comparison of traditional and professional spotlight luminaires

Spotlight	Type	FWHM	U_{sl}	
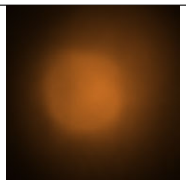	Halogen lamp	36°	18	excellent
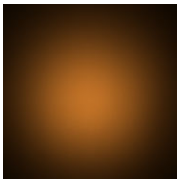	Consumer LED retrofit 1	36°	33	good
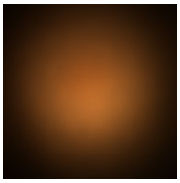	Consumer LED retrofit 2	36°	54	acceptable
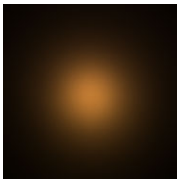	HID luminaire	12°	33	good
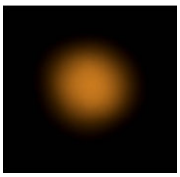	Professional LED spotlight	12°	16	excellent

ues could be recognized. In none of the spotlights were colors or colored patterns visible, the spatial color distribution seemed very uniform in the images of the far field. But the U_{sl} values indicated differences in the color uniformity of the spotlights.

The traditional halogen lamps were widely used by costumers and the performance of color uniformity was excellent. The coiled filament emitted a continuous spectrum without peaks. Thus, there were no colored patterns in the far field visible. However, the U_{sl} function did not include luminance distributions. The luminance distribution of the halogen lamp was very non-uniform. It did not look like a round spotlights but showed edges and fragments of luminance, the luminance decreases not constantly from the center towards the edge.

The two LED spotlight retrofits were designed to replace traditional lamps. The performance of the two lamps was rather different. LED retrofit 1 reached a good color uniformity which was nearly excellent. The second retrofit reached only acceptable color uniformity. In this spotlight colors and patterns were visible. It illuminated a yellowish center with bluish rings at the edge of the far field. The luminance distribution of both retrofits was very uniform.
The HID luminaire reached a good color uniformity of the far field. The luminance distribution was also quite uniform. The best performance with regard to color uniformity was reached by the professional LED spotlight. The spot was designed for museum lighting and a very high light quality was required. Especially the color and luminance distribution needed to be very uniform. The professional spotlight showed no color inhomogeneities or colored patterns. A clear difference between the color uniformity of the two consumer LED lamps was detected. Depending on the combination of LEDs and secondary optics, the color uniformity was different. The presented luminaire systems reached good and excellent color uniformity. These was comparable to many spotlights optimized in the simulations.

6.5 Conclusion

The simulated optical systems were compared in relation to all analyzed properties. The color uniformity U_{sl}, sensitivity to colored shadows, efficiency, and peak luminous intensity were compared together. There was no single system which performed best in all categories. There were recommended optical systems which performed best at the specific color uniformity level. It was necessary to define the most important property and afterwards optical systems with focused optimization on this property could be identified by compromising other properties.

"Excellent" color uniformity could be reached by two different system assemblies. One system was a TIR lens with small lens array at the front surface in combination with unmixed light engine, the other system was a standard reflector with a well mixed light engine. If perfect color uniformity would be required, a reflector in combination with the shell mixer could be used but with slightly decreased efficiency, luminous intensity and increased system size.

For spotlights systems with "good" color uniformity, a standard TIR lens with a well mixed light source performed sufficient. And for acceptable color uniformity light engines with only slight color mixing could be used and thus these systems reached higher efficiencies.
With the presented multi-colored light engine, it was necessary to pay attention for the color uniformity in the far field of spotlights. At least acceptable color uniformity was not reached by each system combination.

The comparison of traditional lamps and luminaires with professional products and the simulated spotlights systems demonstrated that color uniformity varied clearly over different technologies. Although many advantages of LED technology, color uniformity in the far field of spotlights was a new challenge but the color uniformity was not automatically excellent. But as showed with a professional luminaire color uniformity can be perfect with multi-colored LED light sources.
Nevertheless, excellent color uniformity could be reached with multi-colored light engines by an adjusted combination of light engine and secondary optics. It was necessary to pay attention not only to efficiency or peak luminous intensity but also to color distribution in the far field. The separated colors of the light source had to be mixed in an adequate way to reach good or excellent color uniformity.

7 Conclusion and Futrther Line of Reaseaarch

7.1 Conclusion

Spotlights are one application field for LED lighting for highlighting outstanding objects or illuminate areas. The use of LEDs as light source has advantages in terms of efficiency, size, light quality, and design opportunities but also involves a disadvantage. A combination of multi-colored LEDs or phosphor blended light source and a secondary collimating optics of the light into a narrow spotlight beam were necessary for spotlights. It could causes chromatic effects and color non-uniformities in the far field of the spotlight due to spatially and angularly separated colored light.
There are several possibilities to reach a uniform far field by mixing the colors in the light engine or in the secondary optics. Scattering layer in the light enging, rough surfaces, micro lens arrays, or additional optical elements in the optics could be used. However, color mixing typically reduces the efficiency and enlarge the luminance distribution of the spotlight.
A mathematical description of this spatial color distribution in spotlights was required. It should enable an optimum relation of the color uniformity in the spotlight concerning the visual perception and further optical properties like system efficiency and peak luminous intensity.

The visual perception of spotlights was tested by two human factor experiments with various colored and patterned far fields. The first human factor experiment resulted in the perceived rank order of 46 different projected spotlights by a two alternative forced choice test. The perceived rank order was used to correlate various mathematical descriptions of the light distribution in the spotlight with the visual perception of subjects. A multiple linear regression of four basic func-

tions led to a very strong correlation with the perceived rank order number. The implementation of many visual influencing factors resulted in the merit function U_{sl}, which represents the perceived color uniformity in the far field of spotlight.
A classification of U_{sl} from excellent to insufficient color uniformity enabled a systematical analysis of various spotlight systems with each other. The comparison of measured and simulated optical systems proved the validation of U_{sl} for simulations. Therefore, it is not necessary to build prototypes of the system and to evaluate the far field subjectively. It could be done already objectively during simulation of the optical systems.

The merit function U_{sl} was used to optimize spotlight system of a multi-colored light engine in combination with TIR lenses and reflectors. The color mixing ability of various scattering layers, rough surfaces, facets, and additional elements in the optical system were tested. At a FWHM angle of 20° the systems were compared with regard to color uniformity U_{sl}, sensitivity to colored shadows, system efficiency, and peak luminous intensity.
Color uniformity was not automatically excellent by using scattering layers in the light engine or mixing structures in the secondary optics. There was no simulated optical system performing best for each property. An adjusted system of light source and optics can provide excellent color uniformity but by compromising with the other properties. Thus, it is essential to define the required color uniformity level to optimize teh other properties.
For perfect color uniformity a combination of mixed light source, reflector and shell mixer should be applied. The best systems for excellent color uniformity were a combination of TIR lens with facets and unmixed light engine or a standard reflector with a well mixed light engine. For lower color uniformity quality, a slightly mixed light engine together with a faceted TIR lens or reflector performed suitably. They reached clearly higher efficiencies due to lower losses in the light engine.

A standardized evaluation method for the estimation of the perceived color uniformity in the far field of spotlights is presented. It is possible to implement the estimation of the color uniformity already in optical system simulations. The function U_{sl} provides an objective calculation method for the visual perception of color uniformity.

7.2 Further Line of Research

Nevertheless, further investigations could be necessary. One the one hand, the merit function for evaluation could be further reflected. On the other hand, further optical system optimizations are of interest.
Further, detailed analysis of the merit function U_{sl} should include other human factor experiments with varied luminance level and varied spot size. Thus the application range of U_{sl} would be further confirmed and extended.
A filtering of initial data of measurement and simulation of the noisy data could better approximate the human vision system and singal filtering of the brain. All frequencies with an amplitude below $\Delta E = 1$ would be equivalent to a constant and could not be distinguished by vision [Kelly, 1979], and [Burr et al., 1986]. Then, further mathematical descriptions of the merit function will be possible. Currently, the merit function is based on a linear regression of four basic function merging important visual influencing factors. Another method could be the fitting by orthogonal polynomial. Representing a wavefront, polynomial coefficients could correlate with the visual perception of spotlights (Polynomials of Zernike or Forbes).
The merit function U_{sl} and optical system optimization should be applied to other constrains of spotlights. Spotlights systems with FWHM angle of 12° and 36° are also widely. These spotlights sizes were typically used in professional and consumer lighting. The optimization could result in different preferable combinations of light source and secondary optics for different color uniformity levels. Therefore, the direct implementation into optical simulations as optimization parameter will lead to optical systems which reach the defined color uniformity level, efficiency and further properties together.
And finally, the function could be validated with the presented spotlight systems. Prototypes of the simulated systems could be visually evaluated. The comparison of visual judgment and calculated U_{sl} function value would be given and lead to matching merit function for various spotlight appearances. This new adjustment cycle would be necessary to prove the accuracy of the merit function U_{sl} for various kinds of spotlights.

Bibliography

Abramov, I., Gordon, J., and Chan, H. (1991). Color appearance in the peripheral retina: effects of stimulus size. *Journal of the Optical Society of America A*, 8(2):404–414.

Abrams, A. B., Hillis, J. M., and Brainard, D. H. (2007). The relation between color discrimination and color constancy: When is optimal adaptation task dependent? *Neural Computation*, 19:2610–2637.

Amano, K., Uchikawa, K., and Kuriki, I. (2002). Characteristics of color memory for natural scenes. *Journal of the Optical Society of America A*, 19(8):1501–1514.

Annadurai, S. and Shanmugalakshmi, R. (2007). *Fundamentals of digital image processing*. Dorling Kindersley (India) Pvt. Ltd.

Bach, M. (2006). The freiburg visual acuity test - variability unchanged by post-hoc reanalysis. *Graefe's Archive for Clinical and Experimental Ophthalmology*, 245(7):965–971.

Barlett, N. R., Brown, J. L., Hisa, Y., Mueller, C. G., and Riggs, L. A. (1965). *Vison and Visual Perception*. John Wiley & Sons, Inc.

Bloj, M. G., Kersten, D., and Hurlbert, A. C. (1999). Perception of three-dimensional shape influences colour perception through mutual illumination. *Nature*, 402:877–879.

Bollmann, M. and Mertsching, B. (1996). Opponent color processing based on neural models. In *Advances in Structural and Syntactical Pattern Recognition. Lecture Notes in Computer Science*, pages 198–207. Springer Verlag.

Bouma, P. J. (1971). *Physical Aspects of Colour: an introduction to the scientific study of colour stimuli*. MacMillan and Coltd, London, Basingstoke.

Bouman, C. A. (2013). Digital image processing. Internet.

Boynton, R. M. and Kambe, N. (1980). Chromatic difference steps of moderate size measured along theoretically critical axes. *COLOR Research and Application*, 5(1):13–23.

Bradley, R. A. and Terry, M. E. (1952). Rank analysis of incomplete block designs. i. the method of paired comparison. *Biometrika*, 39(3/4):324–345.

Brainard, D. H. and Wandell, B. A. (1992). Asymmetric color matching: how color appearance depends on the illuminant. *Journal of the Optical Society of America A, Optics and image science*, 9(9):1433–1448.

Brown, R. O. and MacLeod, D. I. A. (1997). Color apperance depends on the variance of surrounding colors. *Current Biology*, 7:844 – 849.

Brown, W. R. J. (1951). The influence of luminance level on visual sensitivity to color differences. *Journal of the Optical Society of America*, 41(10):684–688.

Brown, W. R. J. (1952). The effect of field size and chromatic surroundings on color discrimination. *Journal of the Optical Society of America*, 42(11):837–844.

Brown, W. R. J. and MacAdam, D. L. (1949). Visual senitivites to combined chromaticity and luminance differences. *Journal of the Optical Society of America*, 39(10):808–834.

Burr, D. C., Ross, J., and Morrone, M. (1986). Smooth and sampled motion. *Vision Research*, 26(4):643–652.

Carmody, D. P., Nodine, C. F., and Locher, P. J. (1977). Global detection of symmetry. *Perceptual and motor skills*, 45:1267–1273.

Chaves, J., Cvetkovic, A., Mohedano, R., Dross, O., Hernandez, M., Benítez, P., Miñano, J. C., and Vilaplana, J. (2012). Inhomogeneous source uniformization using a shell mixer köhler integrator. In *Optical System Design, Proc. of SPIE Vol. 85502X*.

Chavez, J. (2008). *Introduction to Nonimaging Optics*. Taylor & Francis Group, LLC, Boca Raton, London, New York.

Chen, E., Wu, R., and Guo, T. (2014). Design a freeform microlens array module for any arbitrary-shape collimated beam shaping and color mixing. *Optics Communications*, 321:78–85.

Chen, P.-C., Hays, J., Lee, S., Park, M., and Liu, Y. (2007). A quantitative evaluation of symmetry detection algorithms. Technical Report CMU-RI-TR-07-36, Ronotics Institute, Carnergie Mellon University.

CIE (1976). Cie colorimetry - part 4: 1976 l*a*b* colour space. ISO 11664-4:2008(E)/CIE S 014-4/E:2007.

CIE (2004). Guideline for the evaluation of gamut mapping algorithms. ISBN 978 3 901906 26 8.

Clery, S., Bloj, M., and Harris, J. M. (2013). Interactions between luminance and color signals: Effects on shape. *Journal of Vision*, 13(5):1–23.

Corballis, M. C. and Roldan, C. E. (1975). Detection of symmetry as a function of angular orientation. *Journal of Experimental Psychology: Human Perception and Performance*, 1:221–230.

Crawford, H. M. (2009). Leds for solid-state lighting: Performance challenges and recent advances. *IEEE Journal on Selected Topics in Quantum Electronics*, 15(4):1028–1040.

Cvetkovic, A., Mohedano, R., Dross, O., Hernandez, M., Benítez, P., Miñano, J. C., Vilaplana, J., and Chaves, J. (2012). Primary optics for efficient high-brightness led colour mixing. *Proc. of SPIE*, 8485:1–11.

Ding, Y. and Gu, P. (2007). Freeform reflector for uniform illumination. *Guangxue Xuebao/Acta Optica Sinica*, 27(3):540–544.

Dross, O. (2012). Investigation of the design space for low aspect ratio led collimators. *Proc. SPIE*, 8550:85502M.

D'Zmura, M. and Lennie, P. (1986). Mechanisms of color constancy. *Journal of the Optical Society of America A*, 3(10):1662–1672.

Fairchild, M. D. (2005). *Color Appearance Model*. John Wiley & Sons Ltd. The Atrium, Southern Gate, Chichester, England.

Farnsworth, D. (1943). The farnsworth-munsell 100-hue and dichotomous test for color vision. *Journal of the Optical Society of America*, 33(10):568–574.

Fotios, S. and Houser, K. (2009). Experiencing light - international conference on the effects of light on wellbeing. In de Kort, Y. A. W., Ijsselsteijn, W. A., Vogels, I. M. L. C., Aarts, M. P. J., Tenner, A. D., and Smolders, K. C. H. J., editors, *Tuning the Spectrum of Lighting to enhance Spatial Brightness: Investigations of Research Methods*.

Ghose, T. and Palmer, S. E. (2010). Extremal edges versus other principles of figure-ground organization. *Journal of Vision*, 10(8):3:1–17.

Gorkom, R. P. V., As, M. A. V., Verbeek, G. M., Hoelen, C. G. A., Alferink, R. G., Mutsaers, C. A., and Cooijmans, H. (2007). Etendue conserved color mixing. *Proceedings of SPIE - The International Society for Optical Engineering*, 6670:66700E.

Grand, J. L. and Hage, S. G. E. (1980). *Physiological Optics*, volume 13. Springer Verlag, Berlin, Heidelberg, New York.

Green, D. G. (1968). The contrast sensitivity of the colour mechanisms of the human eye. *Journal of Physiology*, 196:415–429.

Guild, J. (1931). The colorimetric properties of the spectrum. *Philosophical Transactions fo the Royla Society A*, 230:149–187.

Hansen, T., Pracejus, L., and Gegenfurtner, K. R. (2009). Color perception in the intermediate periphery of the visual field. *Journal of Vision*, 9(4):1–12.

Hellström, A. (2003). Comparison is not just subtraction: Effects of time- and space-order on subjectiv stimulus difference. *Perception and Psychophysics*, 65(7):1161–1177.

Hita, E., Romero, J., del Barco, L. J., and Martínez, R. (1982). Temporal aspects of color discrimination. *Journal of the Optical Society of America*, 72(5):578–582.

Hurvich, L. M. and Jameson, D. (1957). An opponent-process theory of color vision. *Psychological Review*, 64:384–404.

Jennings, B. J. and Barbur, J. L. (2010). Colour detection thresholds as a function of chromatic adaptation and light level. *Ophthalmic and Physiological Optics*, 30:560–567.

Jähne, B. (2005). *Digital Image Processing*. Springer - Verlag Berlin Heidelberg NewYork.

Johnson, G. M., Song, X., Montag, E. D., and Fairchild, M. D. (2010). Derivation of a color space for image color difference measurement. *Color Research and Application*, 35(6):387–400.

Katkov, M., Tsodyks, M., and Sagi, D. (2006). Analysis of a two-alternative force-choice signal detection theory model. *Journal of Mathematical Psychology*, 50:411–420.

Kelly, D. H. (1979). Motion and vision. ii. stabilized spatio-temporal threshold surface. *Journal of the Optical Society of America*, 69(10):1340–1349.

Krauskopf, J. (2001). A journey in color space. *COLOR Research and Application*, 26:S2–S11.

Krauskopf, J. and Gegenfurtner, K. (1992). Color discrimination and adaptation. *Vision Research*, 32(11):2165–2175.

Kruskal, W. H. and Wallis, W. A. (1952). Use of ranks in one-criterion variance analysis. *Journal of the American Statistical Association*, 47(260):583–621.

Kunzer, M. (2014). Led-lampen: Noch heller und stromsparender. *FORSCHUNG KOMPAKT der Fraunhofer-Gesellschaft*, 03:11–12.

Kurtenbach, W., Sternheim, C. E., and Spillmann, L. (1984). Change in hue of spectral colors by dilution with white light (abney effect). *Journal of the Optical Society of America A*, 1(4):365–372.

Kvam, P. H. and Vidakovic, B. (2007). *Nonparametric Statistics with Applications to Science and Engineering*. John Wiley & Sons.

Le Grand, Y. (1968). *Light, Colour and Vision*. Chapmann and Hall LTD, 2. edition.

LightTools (2013). User manual lighttools (64) 8.1.0. *Synopsys, Inc*.

Lindsey, D. T., Brown, A. M., Reijnen, E., Rich, A. N., Kuzmova, Y. I., and Wolfe, J. M. (2010). Color channels, not color appearance or color categories, guide visual search for desaturated color targets. *Psychological Science*, 21:1208–1214.

Loomis, J. M. and Berger, T. (1979). Effects of chromatic adaptation on color discrimination and color apperance. *Vision Research*, 19:891–901.

Loy, G. and Zelinsky, A. (2003). Fast radial symmetry for detecting points of interest. *IEEE Transactions on Pattern Analysis and Machine Intelligence*, 25(8):959–973.

MacAdam, D. L. (1942). Visual sensitivities to color differences in daylight. *Journal of the Optical Society of America*, 32:247–274.

McKee, S. P., Klein, S. A., and Teller, D. Y. (1985). Statistical properties of forced-choice psychometric functions: Implications of probit anlysis. *Perception and Psychophysics*, 37(4):286–298.

Monaci, G., Menegaz, G., Süsstrunk, S., and Knoblauch, K. (2004). Chromatic contrast detection in spatial chromatic noise. *Visual Neuroscience*, 21(3):291–294.

Moreno, I. (2010). Illumination uniformity assessment based on human vision. *Optics Letter*, 35:4030–4032.

Moreno, I. and Contreras, U. (2007). Color distribution from multicolor led array. *Optics Express*, 15(6):3607–3618.

Mullen, K. T. (1985). The contrast sensitivity of human colour vision to red-green and blue-yellow chromatic gratings. *Journal of Physiology*, 359:381–400.

Nachmias, J. (2006). The role of virtual standards in visual discrimination. *Vision Research*, 46(15):2456–2464.

Nagy, A. L. (1999). Interactions between achromatic and chromatic mechanisms in visual search. *Vision Research*, 39:3253–3266.

Norcia, A. M., Candy, T. R., Pettet, M. W., Vildavski, V., and Tyler, C. W. (2002). Temporal dynamics of the human response to symmetry. *Journal of Vision*, 2(2):132–139.

Ohno, Y. (2005). Spectral design conciderations for white led color rendering. *Optical Engineering*, 44(11):111302:1–9.

Osram GmbH (2013). Osr ct ri lmo. Internal.

Patching, G. R., Englund, M. P., and Hellström, A. (2008). Time- and space- oder effects in timed brightness discrimination of paired visual stimuli. In *Fechner Day 2008. Proceedings of the 24th Annual Meeting of the International Society for Psychohysics*.

Pointer, M. R. (1973). Color discrimination as a function of observer adaptation. *Journal of the Optical Society of America*, 64(6):750–759.

Poirson, A. B. and Wandell, B. A. (1993). Appearance of colored pattern: pattern-color separability. *Journal of the Optical Society of America A*, 10(12):2458–2470.

Pérez-Carpinell, J., Baldoví, R., de Fez, M. D., and Castro, J. (1998). Color memory matching: Time effect and other factors. *COLOR Research and Application*, 23(4):234–247.

Pridmore, R. W. and Melgosa, M. (2005). Effect of luminance of samples on color discrimination ellipses: Analysis and prediction of data. *COLOR Research and Application*, 30(3):186–197.

Roorda, A. and Williams, D. R. (1999). The arrangement of the three cone classes in the living human eye. *Nature*, 397(6719):520–522.

Rovamo, J. M., Kankaanpää, M. I., and Kukkonen, H. (1999). Modelling spatial constrast sensitivity functions for chromatic luminace-modulated gratings. *Vision Research*, 39:2387–2398.

Schab, F. R. and Crowder, R. G. (1988). The role of succession in temporal cognition: Is the time- order error a recency effect of memory? *Perception and Psychophysics*, 44(3):233–242.

Schanda, J. (2007). *Colorimetry; Unterstanding the CIE System*. John Wiley & Sons, Inc., Hoboken, New Jersey.

Shevell, S. K., editor (2003). *The science of color, second edition*. Elsevier Ltd, Oxford.

Smith, V. C. and Pokorny, J. (1975). Spectral sensitivity of the foveal cone photopigments between 400 and 500 nm. *Vision Research*, 15:161–171.

Smith, V. C. and Pokorny, J. (2003). *The Science of Color*, chapter Color Matching and Color Discrimination, pages 103–148. Elsevier Ltd.

Steigerwald, D. A., Bhat, J. C., Collins, C., Fletcher, R. M., Holcomb, M. O., Ludowise, M. J., Maritn, P. S., and Rudaz, S. L. (2002). Illumination with solid state lighting technology. *IEEE international journal on selected topics in quantum electronics*, 8(2):310–320.

Stockman, A., MacLeod, D. I. A., and Johnson, N. E. (1993). Spectral sensitivities of the human cones. *Journal of the Optical Society of America A*, 10(12):2491–2521.

Stockman, A. and Sharpe, L. T. (2000). The spectral sensitivities of the middle- and long-wavelength-sensitive cones derived from measurements in observers of known genotype. *Vision Research*, 40:1711–1731.

Sun, C.-C., Moreno, I., Lo, Y.-C., Chiu, B.-C., and Chien, W.-T. (2012). Collimating lamp with well color mixing of red/green/blue leds. *Optics Express*, 20:A75–A84.

Thurstone, L. L. (1927). A law of comparative judgment. *Psychological Review*, 34(4):273–286.

Uchida, Y. and Taguchi, T. (2005). Lighting theory and luminous characteristics of white light-emitting diodes. *Optics Engineering*, 44:1240031–1240039.

Uchikawa, H., Uchikawa, K., and Boynton, R. M. (1989). Influence of achromatic surrounds on categorical perception of surface colors. *Vision Research*, 29(7):881–890.

Uchikawa, K. and Shinoda, H. (1996). Influence of basic color categories on color memory discrimination. *COLOR Research and Application*, 21(6):430–439.

Wagemans, J. (1995). Detection of visual symmetries. *Spatial Vision*, 9(1):9–32.

Wang, H., Cui, G., Luo, M. R., and Xu, H. (2012). Evaluation of colour-difference formulae for different colour-difference magnitudes. *COLOR Research and Application*, 37(5):316–325.

Watson, A. B. and Ahumada, A. J. (2005). A standard model for foveal detection of spatial contrast. *Journal of Vision*, 5:717–740.

Webster, M. A. (1996). Human colour perception and its adaptation. *Network: Computation in Neural Systems*, 7:587–634.

Webster, M. A. and Mollon, J. D. (1994). The influence of contrast adaptation on color appearance. *Vision Research*, 34:1993–2020.

Wilcoxon, F. (1945). Individual comparisons by ranking methods. *Biometrics Bulletin*, 1(6):80–83.

Winston, R., Miñano, J. C., and Benítez, P. (2005). *Nonimaging optics*. Elsevier Academic Press, Burlington, San Diegeo, London.

Wright, W. D. (1929). A re-determination of the mixture curves of the spectrum. *Transactions of the Optical Society*, 31:201–218.

Wurm, L. H., Legge, G. E., Isenberg, L. M., and Luebker, A. (1993). Color improves object recognition in normal and low vision. *Journal of Experimental Psychology: Human Perception and Performance*, 19(4):899–911.

Wyszecki, G. and Stiles, W. S. (1967). *Color Sciene: Concepts and Methods, Quantitative Data and Formulas*. John Wiley & Sons Inc., New York, London, Sydney.

Yebra, A., García, J. A., Nieves, J. L., and Romero, J. (2001). Chromatic discrimination in relation to luminance level. *COLOR Research and Application*, 26(2):123–131.

Zhang, X. and Wandell, B. A. (1997). A spatial extension of cielab for digital color image reproduction. http://white.stanford.edu/ brian/scielab/scielab3/.

Appendix A

Overview of spotlight slides with parameter Hue, Pattern, Chroma, and Symmetry as well as $\bar{z}$ and calculated dab, $Grad_{ab}$, S_{lin}, S_{rad}, and U_{sl} values.

Nr.	Hue	Pattern	Sym.	Chroma	$\bar{z}$	dab	$Grad_{ab}$	S_{lin}	S_{rad}	U_{sl}
				Spotlights of 1st human factor experiment						
1	0	0	0	0	-0.94	3.21	2.54	1.08	1.99	33.59
2	2	1	0	1	-1.05	3.82	2.52	0.94	2.16	34.70
3	4	5	0	1	-0.50	3.74	2.78	1.19	2.22	37.38
4	3	3	0	1	-0.68	3.80	2.77	1.19	2.27	37.52
5	3	1	1	1	0.04	3.70	2.75	1.35	2.49	37.77
6	5	5	0	1	-0.62	3.48	2.56	1.21	2.22	35.04
7	1	2	0	1	0.09	4.10	2.77	1.17	2.75	38.67
8	3	3	1	1	-0.78	3.67	2.64	1.18	2.24	36.05
9	3	5	0	1	-0.49	3.40	2.76	1.24	2.08	36.43
10	3	3	0	1	-1.02	3.70	2.72	1.26	2.05	36.85
11	4	3	0	1	-0.91	3.61	2.63	1.25	2.17	36.02
12	1	1	0	1	-0.58	3.63	2.72	1.14	2.36	36.66
13	5	3	1	1	-0.37	3.68	2.60	1.61	2.69	37.54
14	3	3	0	1	-0.15	3.88	2.83	1.20	2.32	38.26
15	5	3	1	2	-0.47	3.69	2.74	1.18	2.32	36.99
16	1	4	1	1	-0.30	4.53	2.83	1.26	2.96	40.73
17	1	4	1	1	0.44	4.22	2.87	1.69	2.68	41.23
18	5	5	0	2	0.19	3.82	3.22	1.20	2.47	41.40
19	3	3	1	2	0.47	4.08	3.45	1.64	2.44	45.15
20	3	3	0	2	0.01	3.77	3.12	1.20	2.08	40.07
21	3	3	0	2	-0.52	3.57	2.68	1.20	2.20	36.22
22	4	5	0	2	-0.43	4.00	2.90	1.24	2.37	39.28

Nr.	Hue	Pattern	Sym.	Chroma	$\bar{z}$	dab	$Grad_{ab}$	S_{lin}	S_{rad}	U_{sl}
23	1	2	0	2	0.08	4.39	2.98	0.98	2.61	40.33
24	4	3	0	2	0.04	3.30	2.93	1.14	1.79	36.85
25	3	1	1	2	0.46	4.22	2.99	1.86	2.72	42.81
26	3	3	0	2	-0.08	3.75	2.81	1.22	2.11	37.64
27	2	1	0	2	-0.38	4.08	3.11	1.23	2.14	40.94
28	1	2	0	2	0.27	4.46	2.94	1.25	3.01	41.46
29	1	4	1	2	0.70	4.93	3.08	1.86	3.50	46.06
30	1	2	0	3	0.46	4.69	2.94	1.25	3.15	42.14
31	3	3	0	3	0.26	3.86	3.33	1.17	2.14	41.97
32	4	3	0	3	0.26	4.01	3.68	1.26	2.40	45.70
33	1	1	0	3	0.53	4.40	3.50	1.09	2.69	44.94
34	2	1	0	3	0.06	4.28	3.25	1.44	2.34	43.38
35	3	5	0	2	-0.08	3.97	2.92	1.40	2.36	39.80
36	4	5	0	3	-0.45	3.78	2.93	1.21	2.10	38.66
37	3	3	0	3	0.55	4.15	3.98	1.27	2.32	48.37
38	3	3	1	3	0.71	4.06	3.23	2.49	2.50	45.96
39	1	4	1	3	0.76	4.70	3.41	2.88	3.94	51.63
40	5	3	1	3	0.57	4.38	3.21	2.11	2.93	45.89
41	3	3	1	3	0.86	4.33	4.34	2.88	2.65	56.86
42	5	5	0	3	0.35	3.92	4.63	1.82	2.90	55.20
43	3	5	0	3	0.58	4.40	4.15	1.39	2.69	51.07
44	1	4	1	3	0.82	5.41	3.93	3.53	4.39	59.99
45	1	4	1	3	0.72	5.44	3.46	2.41	4.01	52.50
46	3	3	0	3	0.49	4.15	4.04	1.46	2.34	49.39
	Additional spotlights of 2nd human factor experiment									
47	3	3	1	1	-	3.44	3.35	1.23	2.10	41.17
48	3	3	1	2	-	3.41	3.63	1.44	2.10	44.02
49	3	3	1	3	-	3.27	3.58	1.75	2.08	44.19
50	5	4	1	1	-	3.35	3.27	2.48	2.47	44.44
51	5	4	1	2	-	3.90	3.48	3.07	2.99	49.81
52	5	4	1	3	-	4.18	3.76	3.55	3.50	54.69
53	6	2	0	1	-	3.02	2.97	1.17	1.96	36.79
54	6	2	0	2	-	3.01	3.41	1.08	2.09	40.14

Nr.	Hue	Pattern	Sym.	Chroma	$\overline{z}$	dab	$Grad_{ab}$	S_{lin}	S_{rad}	U_{sl}
55	6	2	0	3	-	3.71	4.47	1.39	3.02	52.25
56	4	1	0	1	-	3.51	2.99	1.31	2.62	39.26
57	4	1	0	2	-	3.33	3.67	1.45	2.60	44.61
58	4	1	0	3	-	4.02	4.08	1.56	3.14	50.49
59	5	3	1	1	-	3.31	3.41	1.24	2.44	41.66
60	5	3	1	2	-	3.19	3.57	1.31	2.33	42.79
61	5	3	1	3	-	3.31	4.40	1.69	2.49	51.04
62	6	1	0	1	-	3.41	2.89	1.35	2.34	38.07
63	6	1	0	2	-	3.77	3.28	1.34	2.82	42.49
64	6	1	0	3	-	3.75	3.69	1.63	2.86	46.62
65	0	0	0	0	-	3.90	2.71	1.43	2.13	37.86

Hue: 1: red, 2: blue, 3: red-blue, 4: yellow:blue, 5: RGB, 6:green
Pattern: 1: ring, 2: dot, 3: rings, 4: dots, 5: combination
Symmetry: 0: symmetrical, 1: asymmetrical
Chroma: 1: chroma 1, 2: chroma 2, 3: chroma 3

Publications

Journal Papers

1. A. Teupner, K. Bergenek, R. Wirth, P. Benítez, J.C. Miñano (2015). Optimization of a merit function for the visual perception of color uniformity in spot lights. *Color Research and Applications*, 40(3):287-296, doi: 10.1002/col.21888, first published online 18th of April 2014
2. A. Teupner, K. Bergenek, R. Wirth, P. Benítez, J.C. Miñano (2015). Color uniformity in spotlights optimized with reflectors and TIR lenses. *Optics Express*, 23(3):A118-A123, doi: 10.1364/OE.23.00A118.

Conference Papers

1. European Conference on Visual Perception: A. Teupner, K. Bergenek, R. Wirth, P. Benítez, J.C. Miñano (2013). Visual Perception of Color Blending in Spotlights. *Poster presentation*
2. Fontiers in Optics 2013, Orlando: A. Teupner, K. Bergenek, R. Wirth, P. Benítez, J.C. Miñano (2013). Visual Recognition of Color Blending Levels in Light Spots and Related Merit Function. *OSA Technical Digest*, FTu2B.2.
3. SPIE Photonics West 2014, San Francisco: A. Teupner, K. Bergenek, R. Wirth, P. Benítez, J.C. Miñano (2014). Merit function for the evaluation of color uniformity in the far field of LED spot lights. *Proc. SPIE*, 9003:900303 (invited paper).
4. SPIE Optics + Photonics 2014, San Diego: A. Teupner, K. Bergenek, R. Wirth, P. Benítez, J.C. Miñano (2014). Optimization of optical systems for LED spot lights concerning the color uniformity. *Proc. SPIE*, 9190:91900J.